TriDurLE

National Center for Transportation Infrastructure Durability & Life-Extension

Project ID: 2021-UU-01

DEVELOPMENT OF A STORMWATER DETENTION/INFILTRATION SYSTEM FOR URBAN HIGHWAYS USING PERMEABLE LIGHTWEIGHT CELLULAR CONCRETE, PHASE I

Steven F. Bartlett

Tatiana Camargo Gontscharow

Yaqi Huang

University National Transportation Center TriDurLE

Department of Civil and Environmental Engineering

405 Spokane Street PO Box 642910

Washington State University Pullman, WA 99164-2910

June 2024

ACKNOWLEDGEMENTS

The authors acknowledge the grant provided by TriDurLe National Transportation Center. The authors would also like to recognize that AERIX Industries, the University of Utah Asian Campus (UAC), and IGES Inc. provided in-kind matching contributions, project technical support, and advice. In addition, we thank Dr. Jongsoo Choi of the Land and Housing Corporation of Korea. He helped guide some of the application concepts developed in this research.

DISCLAIMER

The authors alone are responsible for the preparation and accuracy of the information, data, analysis, discussions, recommendations, and conclusions presented. The contents do not necessarily reflect the views, opinions, endorsements, or policies of The TriDurLe National Transportation Center makes no representation or warranty of any kind and assumes no liability, therefore.

TABLE OF CONTENTS

LIST OF FIGURES

LIST OF TABLES

EXECUTIVE SUMMARY

This phase I study examines permeable low-density cellular concrete's hydraulic and mechanical properties (PLDCC) within a controlled laboratory environment for pavement, drainage, and water storage systems. We also explore how these properties might be applied to sustainable and resilient infrastructure systems. The increasing potential for urban flooding, aggravated by global warming and urban hardscape, gives impetus to develop these applications. However, the potential use of PLDCC as subterraneous detention/retention basins for decentralized stormwater management systems (DSWMS) and for roadway, building, and retaining wall drains and water filters is still developing.

The permeability testing completed for this research involved conducting laboratory tests on 53 PLDCC samples varying between 25.0 to 32.6 pcf to determine the resilient modulus, hydraulic conductivity, dry and partially saturated unit weight, water storage capacity, buoyant unit weight, and potential compatibility with geotextile materials. Our laboratory findings indicate that PLDCC exhibited a hydraulic conductivity ranging from 2.2E-03 to 2.7E-01 cm/s, comparable to clean sand or sand and gravel mixtures. This relatively high permeability for a cementitious material suggests that PLDCC will efficiently drain surface water or allow groundwater flow when placed below the surface. Also, the high void ratio or porosity of PLDCC produces a partially saturated water storage capacity of up to 60% by volume, which is significantly higher than compacted earthen materials (e.g., sand and gravel). In addition, the partially saturated unit weight of PLDCC is similar to that of water, resulting in minimal to zero buoyance uplift when subject to groundwater inundation or rise.

Additionally, laboratory assessments involving the integration of geotextile with PLDCC reveal negligible or no occurrence of clogging while preserving its infiltration ability. This initial finding suggests that nonwoven geotextile filter fabric can be integrated with PLDCC to reduce its plugging potential when placed in contact with fine-grained soils.

One uncertainty not addressed for roadway systems is PLDCC's structural response in pavement systems as a subbase or base material. Specifically, pavement design inputs (e.g., Resilient Modulus) are

missing from the engineering literature. We subjected PLDCC samples to low-strain cyclic axle loads to obtain their Resilient Modulus (RM) values. Those samples were subsequently tested in uniaxial compression, and the unconfined compression (UC) results were compared with the corresponding RM values. This comparison indicates that RM values are acceptable for use as a pavement subbase. In addition, the results were used to evaluate how substituting a typical granular subbase material with PLDCC could affect long-term pavement performance. This evaluation utilized the Guide for Mechanistic-Empirical Design of Pavement Structures approach. Our research suggests PLDCC's mechanical properties make it a viable alternative to granular subbases for traditional pavement systems. However, we did not evaluate the effect of the degree of saturation on the mechanical properties of PLDCC and recommend this topic for future research.

CHAPTER 1. INTRODUCTION

This worldwide flooding scenario will increase in the following years due to the consequences of global warming, which will trigger an increased frequency of sudden heavy rain events. Such events are 7% more probable for each degree augmented in the overall planet's temperature (IPCC 2022). Furthermore, these rain events are happening with a higher frequency and intensity, which frequently contributes to a decline in water quality. This trend has been reported in South America since the early 20th century and in North America since the mid-20th century (IPCC 2022). Revising this trend is one of the biggest challenges for the continued development of many Asian countries.

In the US, it is estimated that flood losses were about $200 million per year from 2004 to 2014. However, the actual loss amount is much higher since these estimates do not include uninsured property losses, indirect losses, or other essential factors. In addition, flooding is considered a natural hazard with higher social and economic impacts on the American population (National Academies of Sciences and Medicine 2019).

The same situation is observed on a global scale. Asian countries like China and South Korea have experienced fast urban development over the past decades, reflected in the rampant installation of hardscaping or impervious surfaces. As a result of the extensive hardscaping, the urban flooding phenomenon intensified even more. For example, in Hohhot, a city in China, the increase in impervious surfaces contributes two to four times more to the flooding risk than the action of climate change. In addition, the current flood protection infrastructure in South Korea is expected to comport only about 30% of future flood levels by 2100 (IPCC 2022).

Thus, it is unsurprising that the reduction in flooding risks with land planning systems has been intensely discussed worldwide. In the Northeast Asian region, the concept of "Sponge Cities" is often discussed (Xia et al., 2017). This concept was first proposed in China in 2012 and can be defined as low-impact construction concentrated on runoff management, augmenting the resilience of urban environments concerning water-related challenges (Guan et al. 2021, Song 2022). For that, the development of a sponge

city is based on four main principles: to safeguard urban water resources, to promote ecological water management, to promote the installation of green infrastructure, and to install permeable pavement (Nguyen et al., 2019).

Traditional pavement materials and construction methods using conventional materials face challenges in meeting the rising need for sustainable infrastructures that effectively incorporate environmental considerations. For instance, while commonly used concrete and asphalt exhibit strong load-bearing capabilities suitable for heavy traffic, their lack of hydraulic conductivity (permeability) often leads to increased surface water runoff and a heightened risk of flooding (Du et al. 2015). Additionally, water accumulation on impermeable surfaces can cause pavement cracking and deterioration (Zhang et al., 2008). Furthermore, rainwater runoff from paved surfaces can transport pollutants, sediments, and petrochemicals into nearby bodies of water, thereby causing damage to ecosystems (Kamali, Delkash, et al. 2017).

Permeable pavement technology has been suggested as a subsystem in the Sponge City concept. However, permeable pavements have relatively low water storage capacity to prevent roadway flooding. This system typically contains a top layer of permeable concrete, pavers, or porous asphalt, followed by a coarse aggregate layer (base) and subgrade soil (Kia et al., 2017). Also, adding a second base, the subbase layer, is a standard procedure to reduce the stress over the subgrade (Su et al., 2017). In addition, the potential for reduced pavement life resulting from an increased deterioration rate of "permeable" pavements must be considered. Shackel (2006) also points out that permeable bases and subbases generally comprise granular materials. These unbound layers are constructed using similar placement and compaction procedures. However, Shackel (2006) draws attention to the necessity of developing materials and techniques that improve the permeability and resistance of the base coarse or granular layers placed beneath permeable pavements. These layers have considerable influence over the response of the pavement to traffic loads (Kumar et al., 2006) and offer structural support for the pavement. They are also vital for the design of the volume of water accepted by permeable pavement systems (Shackel, 2006).

1.1. PROBLEM STATEMENT

To address these and other concerns, researchers have been investigating innovative materials and

techniques to mitigate these issues and develop new field applications. The Land and Housing Corporation (LH Korea) is developing an alternative to conventional permeable pavement technology in the Republic of Korea. They are researching ways to improve stormwater management technology for runoff-regulated urban areas. The Korean version of the "Sponge Cities" concept is a type of DSWMS (decentralized stormwater management system) that includes subsurface storage and infiltration galleries. The prototype DSWMS consists of traditional rigid or flexible pavement flanked on its sides with curb, gutter, and sidewalk areas capped with permeable pavers. Beneath the sidewalk, underlying granular detention/water basins are used as infiltration galleries to distribute the water into the underlying soil. Catch basins feed these galleries via pipes or lateral channels, allowing water to be distributed to the galleries, which consist of crushed bottom ash contained within geocells to provide extra strength to this layer. However, LH Korea is currently reconsidering the use of the bottom ash due to the potential for heavy metal contamination of the underlying groundwater.

We believe that PLDCC is an attractive alternative to bottom ash or other earthen aggregate material as a potential storage/infiltration material for DSWMS applications. PLDCC differs significantly in texture and hydraulic properties from the more commonly used closed-cell lightweight cellular concrete LCC. It is made by mixing Portland cement, water, and a preformed foam in various proportions to create a hardened material with an oven-dry density of 50 pcf or less. Lightweight versions of this material have dry densities between 25 to 30 pcf; thus, PLDCC is a lightweight material that can be placed under urban roadways. Also, PLDCC has a relatively high permeability with a hydraulic conductivity ranging between 2E-3 to 3E-1 cm/s, comparable to coarse, clean sand and gravel mixtures. This relatively high permeability and storage capacity, approximately 60 percent by volume, results from the distinctive internal interconnected bubble structure created by a specialized foaming agent. In addition, with a relatively high cation exchange capacity (CEC), it can used as a filter to sequester heavy metals and other contaminants (Kevern, 2018)

While the material properties of PLDCC will be explored (e.g., strength, stiffness, and durability), this research will also evaluate the hydraulic properties of PLDCC, which includes measuring (1) PLDCC

density in dry and partially saturated states, (2) hydraulic conductivity, (3) water storage capacity, and (4) buoyant unit weight. In addition, the behavior of PLDCC under different hydraulic conditions greatly influences its functionality and suitability for various geosystems. Additionally, assessing the compatibility between PLDCC and geotextiles offers opportunities to develop integrated filter systems that enhance filter effectiveness and contamination sequestration, reducing the potential for clogging or plugging of the PLDCC medium.

There has been no case where PLDCC has been implemented as a runoff storage/infiltration material for roadways. However, the Mission Rock Project in the Port of San Francisco used PLDCC as a lightweight fill to prevent loading and subsequent damaging consolidation settlement of the "Bay Mud" that underlies the site. The PLDCC allowed a 5-ft rise of grade across the development while creating a basal layer for the subsurface flow of groundwater/tidewater/stormwater throughout the project area. The project's pavement design included a PLDCC subbase overlain by an LCC base capped by a PCCP and an asphalt-wearing surface. Therefore, the Mission Rock Project's use of PLDCC as a subbase and drainage medium suggests that it may be a reasonable alternative for constructing new or retrofitted stormwater.

In addition, we believe that the stormwater infiltration gallery developed by LH Korea can be extended from the sidewalk zone to the area directly under the footprint of the roadway system. Because PLDCC has a compressive strength ranging from about 80 to 160 psi (0.55 to 1.1 MPa), it has sufficient strength and bearing capacity to act as a roadway subbase. In addition, it is also excavatable for new utility placement or repair of damaged buried systems.

1.2. OBJECTIVES

Additional research is needed before PLCC can be implemented in such systems. The specific objectives of this research project are:

1) Evaluate PLDCC as a highway construction material for potential subsurface use in stormwater management systems as an infiltration system.
    a) Perform applicable hydraulic testing of PLDCC

b) Complete hydraulic laboratory testing of properties, including hydraulic conductivity, storage capacity, dry and buoyant unit weights

   i) Evaluate potential countermeasures for system clogging.

c) Perform applicable material testing of PLDCC

   i) Complete material laboratory testing of properties, including dry unit weight, uniaxial compressive strength, and resilient modulus.

2) Make recommendations regarding design and construction considerations, draft specifications, and requisite construction and installation methods for implementing the technology

1.3. EXPECTED CONTRIBUTIONS

We will evaluate PLDCC as a viable alternative material for stormwater runoff transmission, infiltration, and storage. If successful, the research will provide additional alternatives to a complex problem. We believe the PLCC technology can be used in new construction and retrofitted situations. The case is probably most applicable for retrofitting and replacement in urban areas where there is limited right-of-way or where the presence of buried or nearby infrastructure is prohibitive to conventional systems. Also, we believe that additives or filters working in conjunction with the PLCC can improve water quality. Preliminary results show that PLCC can remove heavy metal contaminants. However, other additives and filters may be required for petroleum products.

1.4. REPORT OVERVIEW

The sequence of tasks to carry out the research is outlined in this report. In addition, the report provides information about the relevant research tools.

Chapter 1 provides an introduction and an overview of the problem statement, the objectives, and expected contributions.

Chapter 2 describes an overview of the literature on the state of practice of cellular concrete technology and the available hydraulic and material properties of PLDCC.

Chapter 3 describes the laboratory test methods and results of PLDCC testing.

Chapter 4 includes the findings of this report.

Chapter 5 includes a summary of this report and the authors' conclusions.

CHAPTER 2. LITERATURE REVIEW

2.1 PROPERTIES OF LDCC AND PLDCC

Low-Density Cellular Concrete (LDCC)

ACI 523 Guide (ACI 2014) defined Cast-in Place Low-Density Cellular Concrete (LDCC) as "concrete made with hydraulic cement, water, and preformed foam to form a hardened material having an over-dry density of 50 lb/ft^3 (800 kg/m^3) or less". Predetermined amounts of liquid foaming agent and water are mixed to make the foam used in the LDCC mix. The ratio of the foaming agent to water is typically 1:50. A foam generator is used to process this foaming agent into a foam that is subsequently mixed with water and cement to produce LDCC.

The LDCC is also commonly called Foam Concrete, Controlled Low-Strength Cellular Concrete, and Low-Density Cellular Concrete (LDCC) (Taylor and Halsted, 2021). Adding preformed foam creates the cellular structure in LDCC. However, other less efficient methods can be used to make these cavities, such as adding aerating agents. These agents produce chemical reactions during the mixing process, resulting in gas production that consequently includes the air cells or the addition of pre-foaming agents in the water (Raj et al., 2019).

Adding preformed foam has been the primary means of creating the air cells for the LDCC structure. The introduction of synthetic-based foam liquid concentrated in the 1990s as a substitute for the protein-based foam liquid concentrate has resulted in higher longevity and stability of the LDCC due to the better stability of the air bubbles inside the concrete structure (Sutmoller and Gomez, 2022). Synthetic foaming agents are amphiprotic and hydrophilic substances that, by reducing the surface tension of dilution, create a material with lower density. The introduction of the foaming agent creates a complex chemical environment in which the compatibility of the cement and the surfactant is critical in allowing the entrainment of air and the development of the cellular structure (Chica and Alzate, 2019).

When fresh, the LDCC is in a liquid state, which allows it to be easily pumped and makes it a self-

compacting material with good workability. Moreover, these characteristics can be altered by other factors such as mix design, temperature, and agitation time (ACI 2014). The consistency of the LDCC can also be strongly altered with the use of superplasticizers and other components, such as fly ash, which decreases the material viscosity by augmenting the presence of fines and water demand (Raj, et al., 2019).

The main physical properties influencing LDCC performance are dry shrinkage, the air-void system, and water absorption (Raj et al., 2019). As with any Portland cement product, the LDCC experiences drying shrinkage. This shrinkage can be up to ten times greater in LDCC than in regular concrete due to decreased water content in the cement paste. For most LDCC designs, especially for geotechnical fill environments in which the verification of this phenomenon is complex, the shrinkage can be assumed as 0.5 to 1% (Taylor and Halsted, 2021). In addition, the air-void system is strongly linked with the air-cell structure and formation and the addition of fines and other additives to the mix (Raj et al., 2019).

The foam content has important implications for fresh and hardened LDCC characteristics. For example, excess foam can cause a decrease in the flow rate in the fresh state. The foam content also influences the compressive strength of the hardened LDCC (Amran et al., 2015). The foaming agents should be tested before being used to ensure their properties. The commercially available ones must meet the requirements of ASTM C869, the Standard Specification for Foaming Agents Used in Making Preformed Foam for Cellular Concrete (Taylor and Halsted, 2021).

Also, the volume of water absorbed by the LDCC is nearly double that of regular concrete. This volume is not strongly influenced by the amount of air in the material, which suggests that some of the voids are filled with water (Kearsley and Wainwright, 2001). Besides being dependent on the material age, porosity, and density, the mechanical properties of the LDCC, such as compressive strength, tensile strength, and modulus of elasticity, are much less than those of regular concrete (Raj et al., 2019).

LDCC was introduced as a lightweight alternative to conventional building and fill materials in the 1940s. For some systems, the LDCC's low unit weight and excellent thermal properties make it advantageous in some building applications. It can be easily employed in building blocks and panels and

offers good results when used in roof insulation (Zahari et al., 2009). The uses of LDCC include, but are not limited to, the replacement of existing soil, soil stabilization, formation of raft foundations, stabilization of surplus structures, geotechnical rehabilitation, soil settlement, as well as prefabrication and installation of load-bearing or non-load-bearing walls and floor screeds in place of old sewer pipes and wells (Eskew et al., 2021). LDCC significantly reduces weight, with the potential for up to an 80% decrease compared to Portland Concrete Cement. Also, LDCC possesses good acoustic and thermal insulation properties and exhibits a high fire resistance level. In some cases, cellular concrete presents cost savings in raw materials and can be easier to place using placement via pumping. Also, LDCC material does not require compaction or vibration during installation, eliminating the need for leveling procedures (Chica and Alzate, 2019).

Permeable Low-Density Cellular Concrete (PLDCC)

PLDCC, Permeable Low-Density Cellular Concrete, emerged as a novel technology in the early 2000s to increase drainage capacity and buoyancy issues with LDCC when used at or below the groundwater table. While sharing many of the advantages of LDCC, PLDCC exhibits considerably higher hydraulic conductivity and partially saturated unit weight. PLDCC obtains this by a modified foaming agent that produces a more interconnected bubble structure and fabric (Figure 1). This disrupted fabric with connected void space enables better water transmission and higher retention and storage within PLDCC.

For optimal hydraulic conductivity and infiltration, the target density of PLDCC typically ranges between 25 pcf (400 kg/m^3) to 35 pcf (561 kg/m^3). Successfully constructed PLDCC in this density range usually has a void ratio between 86% and 90% and typically exhibits infiltration rates that attain about 4.2E-2 cm/s (150 cm/hr) to 4.7E-1 cm/s (1700 cm/hr). The hydraulic conductivity values of PLDCC can reach approximately 5.6E-2 cm/s (200 cm/hr) to 1.5E-1 cm/s (700 cm/hr) (Eskew et al. 2021). These authors conclude that hydraulic conductivity is generally inversely proportional to the density of PLDCC.

An example of the application of PLDCC for stormwater management is a detention system constructed at Tulane University (Aerix 2019). An underground storage reservoir consisting of PLDCC

was built beneath the floor slab of a pile-supported building foundation slab. This reservoir acted as a detention basin to contain stormwater discharge within the property's footprint and was installed to comply with the city's stormwater management regulations. Because of its favorable water storage capabilities, lightweight properties, and acceptable compressive strength, the PLDCC system has met performance expectations (Aerix 2019).

PLDCC has also effectively reduced roadway flooding and settlement, as evidenced by the project constructed underneath West Lake Eloise Drive in Florida. This pavement constructed atop this soft soil site suffered from seasonal flooding and settlement damage. These factors produced frequent road closures and significant maintenance and repair costs. To address these challenges, engineers proposed utilizing PLDCC as a subbase and backfill with a hydraulic conductivity of approximately 9E-01 cm/s. The PLDCC acted as a roadway underdrain and enabled surface and groundwater to flow beneath the roadway, maintaining uniform water levels on both sides without necessitating cross-drains. Additionally, PLDCC's high infiltration capacity diminished hydrostatic pressure and the potential for ground uplift (Eskew et al. 2021).

Similarly, the Mission Rock Project under construction in the Port and San Francisco faced settlement and flow issues associated with groundwater, tidal fluctuations, storm surge, and global sea level rise. This 16-acre site was raised approximately 5 feet using PLDCC and LDCC to accommodate commercial and residential buildings planned for the development. These lightweight materials were selected so as not to trigger damaging consolidation settlement in the Young Bay Mud that underlies the site. In addition, stone columns were installed in the upper part of the soil column to densify potentially liquefiable zones. The pavement design for the project included a PLDCC subbase, topped with an LCC base, Portland Concrete Cement Pavement (PCCP), and an asphalt-wearing surface. By utilizing PLDCC, it was possible to elevate the site's grade while establishing a permeable underlayment for landscaped areas and roadways for the subsurface flow of stormwater, tidewater, and groundwater (Bartlett et al., 2020).

Figure 2 compares the hydraulic conductivity, saturated unit weight, and water storage capacity derived from the PLDCC test samples to support the design of the Mission Rock Project. These tests show

that PLDCC has a hydraulic conductivity similar to clean coarse sand (1E-2 to 1 cm/s), obtains partially saturated unit weights that vary from 50 to 62 pcf when submerged, and has a water storage capacity ranging from 30 to 60 percent by volume of the test specimen. However, the design should consider a small potential for hydraulic uplift from buoyancy forces that could inundate the PLDCC during heavy rain events (Sutmoller and Gomez, 2022). However, this concern can be easily addressed by placing material atop the PLDCC (Bartlett et al., 2020).

PLDCC in Pavement and Stormwater Management Systems

The pavement's wearing surface distributes concentrated tire loads acting on it, thus providing a durable and functional surface for vehicles. This pavement system (bottom to top) usually comprises the following sublayers placed atop the subgrade: subbase, base, and pavement surface (usually concrete or asphalt). Furthermore, the material's strength and durability are generally higher for the upper layers and offer surface runoff and drainage for the pavement to promote a safer and longer roadway life span (Mallick and El-Korchi 2008).

Once the rainwater passes the wearing surface, the amount of additional water absorbed by the system depends on the permeability and depth of the granular layers (Shackel, 2006), which are the base and the subbase that effectively function as a reservoir. Shackel (2006) also points out that permeable eco-pavement base and subbase could be able to remove contaminants from the runoff while satisfying geotechnical filter criteria - which avoids the movement of fine particles between the different layers, besides offering adequate stiffness and water storage capacity.

In addition, these underlying layers are usually constructed using the same material utilized on conventional pavements (Shackel, 2006). Layers like crushed rock or coarse gravel have a maximum water storage capacity of 40% by volume (Sutmoller and Gomez, 2022). Porous bases and subbases are typically designed through the Moulton (1979) or the Casagrande and Shannon (1952) method. The Moulton method is based on the concept that the layer's thickness must be equal to or greater than the flow depth, while the

Casagrande and Shannon method is based on studies related to freeze-thaw-susceptible and considers the time to drain (Mallick and El-Korchi, 2008).

Shackel (2006) suggests introducing new materials with high permeability and good structural properties as substitutes for current granular materials. There are some new developments, but these have been restricted to parking lots and commercial applications with light traffic loads and low speeds (Weiss et al., 2019).

PLDCC is a new lightweight concrete product with properties consistent with those suggested by Shackel (2006). However, in some applications, issues have been expressed about the potential accumulation of fine-grained sediment in PLDCC, which could result in long-term clogging of the PLDCC matrix, thus negatively impacting its beneficial hydraulic properties. While field applications of PLDCC are just beginning, similar research has highlighted issues encountered by other permeable pavement materials (Sansalone et al., 2012). Researchers have conducted extensive studies regarding the hydraulic characteristics and potential for clogging in permeable pavement systems.

We note that it is essential to recognize that neither LDCC nor PLDCC should be exposed to the environment as a wearing surface. These lightweight materials are typically used as backfill or subbase materials; hence, they will be overlain by other layers, such as the pavement surface. These situations make the potential for clogging of PLDCC less acute (Sutmoller, 2020). In addition, a common countermeasure to inhibit clogging is using a geotextile separation layer. Studies indicate that integrating geotextiles with a permeable pavement system can yield significant benefits (Scholz, 2013). Geotextiles, such as nonwoven geotextiles, are essential in limiting sediment migration into the permeable medium. Also, geotextiles can reduce pollution levels by impeding the infiltration of fine particles and pollutants into underlying drainage layers if placed below the permeable pavement layer (Wu et al., 2020). Therefore, integrating a layer of nonwoven geotextile, as used in conjunction with porous or conventional pavement systems, may be an effective countermeasure, improve water quality, and mitigate blockage-related issues.

Summary

The available literature on the hydraulic behavior of PLDCC is limited, resulting in significant gaps in our knowledge. The hydraulic and material properties resulting from recent advancements in foaming agent technology for PLDCC mixes have not been thoroughly investigated. There is a lack of studies examining the hydraulic properties and the potential use of filters (i.e., geotextiles) with PLDCC to prevent or reduce long-term clogging. Furthermore, more exploration is needed regarding using PLDCC with other filtering materials to sequester contaminants and improve water quality.

Further, we see potential applications of PLDCC that will be placed under roadways as a permeable subbase or base material. These applications may entail four scenarios: (1) acting as an underdrain beneath the roadway system to allow horizontal flow to mitigate flooding, as was done for the West Lake Eloise Drive in Florida and the Mission Rock Project in California; (2) acting as a lightweight porous base/subbase material in conventional or permeable pavement system; (3) creating as an underground detention and infiltration basin for stormwater management along the margins or underneath the roadway system similar to the concepts developed by LH Korea, (4) acting as a component of a filtration system to sequester contaminants and improve surface runoff water quality.

Additional research is still needed, especially concerning PLDCC hydraulic and mechanical properties, durability, and response to cyclic (i.e., traffic) loads. We hope the research herein will guide the development of these and other applications.

Figure 1. Comparison of the fabric and texture of LDCC (left) and PLDCC (right).

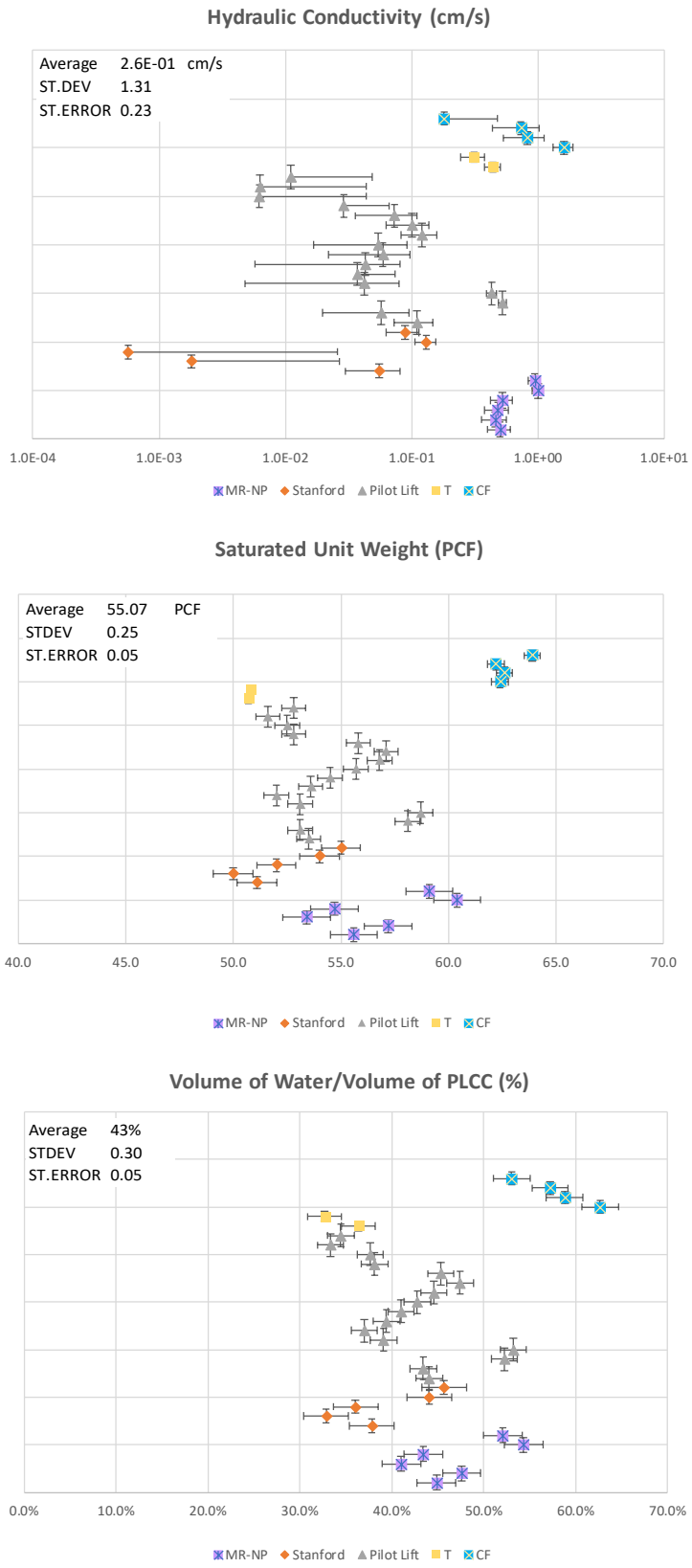

Figure 2. Comparison of PLDCC Hydraulic Properties from the Mission Rock Project.

CHAPTER 3. METHODOLOGIES

3.1 HYDRAULIC PROPERTIES

The study's objectives were accomplished through the implementation of a three-stage process. Firstly, PLDCC samples with densities varying from 25 to 32.6 pcf were created. Subsequently, laboratory tests were conducted to measure the hydraulic properties (e.g., hydraulic conductivity, saturated unit weight, water storage capacity, and buoyant unit weight) of the PLDCC specimens to compare them with existing data from the published literature. The results of this testing are found in Appendix A. Also, the hydraulic performance of combining PLDCC with filtering material (i.e., nonwoven geotextile) was evaluated.

Sample Preparation

As mentioned, PLDCC is a composite material of Portland cement, water, and a pre-foamed foaming agent. A total of six batches of PLDCC specimens were created for this research project. Table 1 below shows the samples' batch numbers, IDs, and corresponding wet-cast densities. Batches 1 to 3 were produced using AERIX INDUSTRIES™ foaming agents, namely AQUAERIX™ and AQUAERIX-LB™. The remaining three batches were cast at the soil laboratory of the University of Utah utilizing AQUAERIX-LB™ foam chemical provided by AERIX INDUSTRIES.

Table 1. PLDCC Batch Information

Batch #	Sample ID	Wet Cast PLDCC Density (PCF)		Foam Chemical	Cement	W/C Ratio	Produced By
		Target	Actual				
1	TY-5 to TY-14, TY-16 to TY-19	26	25.1	Aquaerix @ 1:50 Dilution	Quikrete Type I/II	0.55	Aerix Industries
2	TY-20 to TY-38	32.5	32.6	Aquaerix @ 1:50 Dilution	Quikrete Type I/II	0.55	Aerix Industries
3	A1 to A8	28	27.6	Aquaerix-LB @ 1:50 Dilution	Quikrete Type I/II	0.55	Aerix Industries
4	Y5, Y7,Y8, and Y10	25	25	Aquaerix-LB @ 1:50 Dilution	Quikrete Type I/II	0.55	Univeristy of Utah
5	Y14, Y16, Y17, and Y18	30	30	Aquaerix-LB @ 1:50 Dilution	Quikrete Type I/II	0.55	Univeristy of Utah
6	B1 to B4	25	25	Aquaerix-LB @ 1:50 Dilution	Quikrete Type I/II	0.55	Univeristy of Utah

The foaming chemical used in producing the PLDCC sample was first diluted with water

at a ratio of 1:50, then combined with a slurry consisting of Portland Cement Type I/II and water. The water-to-cement ratio was set at 0.55 while maintaining a foam density of 2.5 PCF according to the mix design recommended by AERIX INDUSTRIES. Figure 3 illustrates the production equipment and process for creating PLDCC specimens. Appendix B provides further details on the sample production procedure.

Figure 3. Sample Production of PLDCC

Constant Head Hydraulic Conductivity Testing of PLDCC

The hydraulic conductivity testing of PLDCC in this study followed the modified version of ASTM D2434-68, Standard Test Method for Permeability of Granular Soils. This modified procedure is consistent with the one used for the laboratory testing of PLDCC in the Mission Rock Project and was developed by Castle Rock Consulting, LLC as presented in Appendix C.1.

Appendix C.1. Castle Rock Consulting, LLC, Castle Rock, Colorado, describes the modified testing procedure.

A Mariotte bottle with a height of 4 ft was constructed to maintain a consistent head for the permeability test of PLDC. The construction process followed the guidelines by Bashyal et al. (2019). Using the Mariotte bottle, water is discharged at a steady pressure level, allowing for more accurate and reliable maintenance of a constant head compared to manual methods (Gregory et al. 2005). Refer to Figure 4 for an illustration of the completed Mariotte bottle and setup used in conducting the constant head permeability test of PLDCC.

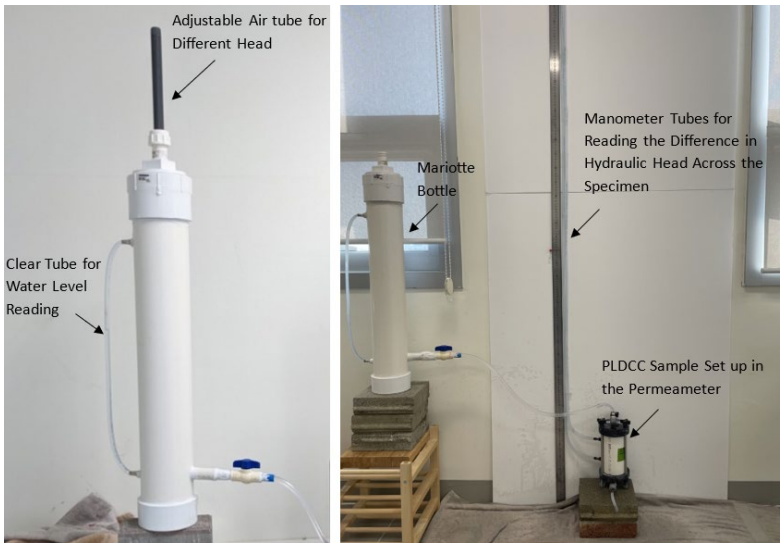

Figure 4. Constant Head Permeability Testing Device

Submerged Saturated Unit Weight and Storage Capacity of PLDCC

The approach for determining the submerged "saturated" unit weight of PLDCC also follows a modified procedure developed by Castle Rock Consulting, LLC. This procedure is included in Appendix C.2. A visual representation of the saturation process can be seen in Figure 5, depicting a PLDCC sample undergoing saturation. Once saturation is achieved, measurement parameters such as partially saturated unit weight, water storage capacity, and buoyancy unit weight can be determined.

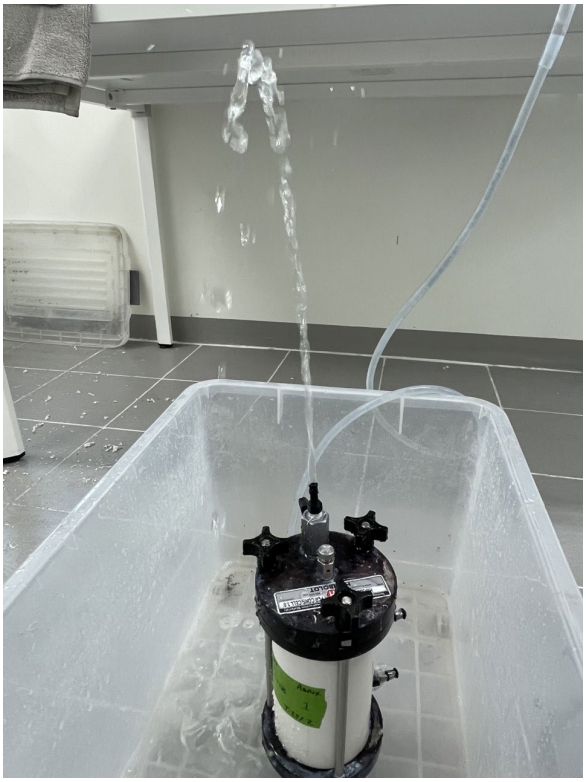

Figure 5. PLDCC Sample During Saturation

Evaluation of Combining a Filter Fabric with PLDCC

Geotextiles have numerous benefits across various applications. Nonwoven geotextiles demonstrate excellent filtration and separation properties for the applications we envision, making them ideal for applications that rely on water flow, filtration, and separation, such as permeable paving (Scholz, 2013). Therefore, this part of the study, which focuses on investigating the hydraulic behavior of PLDCC combined with a filtering material, used nonwoven geotextile as the target of interest. Figure 6 shows the nonwoven geotextile used in this study.

Four samples of PLDCC were produced in 6-inch diameter by 12-inch-tall cylinder concrete molds to evaluate the joint behavior of PLDCC acting in concert with a geotextile. For these specimens, a geotextile of exact dimensions was deliberately placed at the bottom of the mold, serving as a foundation for the wet cast placement of PLDCC.

Figure 6. Water Infiltrating a Nonwoven Geotextile

Before casting the samples, the plastic concrete molds were cut open on both ends, and their interior walls were roughened with sandpaper to ensure that the PLDCC would remain securely in place post-curing. A hole was drilled on each mold's side and fitted with a threaded 1/2-inch ID hose barb, and a cap with 6 inches of diameter was placed at the base of the concrete mold to maintain the slurry mixture within the mold during pouring. The cap may be detached for subsequent testing purposes.

The scheme of the setup constant head test device, as shown in Figure 7, is a modification of Sobolewski's (2005) testing approach. A 5-gallon bucket was used as the constant-head reservoir for the testing. A hole of equal size and dimensions was drilled on one side, and a hose barb measuring 1/2 inch in inner diameter was attached. After curing the PLDCC sample, remove the bottom cap and place the plastic mold inside a 5-gallon bucket. The bucket was filled with water to the level of a pre-drilled hole on its side and maintained at this level by continuously adding water during the test. The flow rate through the PLDCC specimens was measured at 1-minute intervals for one hour.

Each PLDCC sample underwent a set of three tests. The first series of tests (i.e., Test 1, Figure 8) assessed the infiltration rate (i.e., unsaturated flow behavior before reaching steady state flow) using a geotextile layer placed at the bottom of the sample during casting and curing. This configuration replicates downward flow through a PLDCC reservoir basin lined with a basal geotextile layer where PLDCC has been poured directly on the liner.

After this initial test, the samples were allowed to air dry for approximately two weeks and then outfitted with a new piece of geotextile secured at its base in preparation for another round of testing (i.e., Test 2, Figure 8). This configuration replicates cases where a filter fabric is added to the system after curing the PLDCC.

After this second evaluation, the sample was again dried through air exposure and subjected to a third round of testing without any accompanying geotextile layer (Test 3, Figure 8). This configuration provides the hydraulic conductivity of the PLDCC without the filter fabric layer. Ultimately, we compared the infiltration rate obtained from all three test configurations to determine whether changes had occurred in the system. These and other results are discussed in Chapter 4.

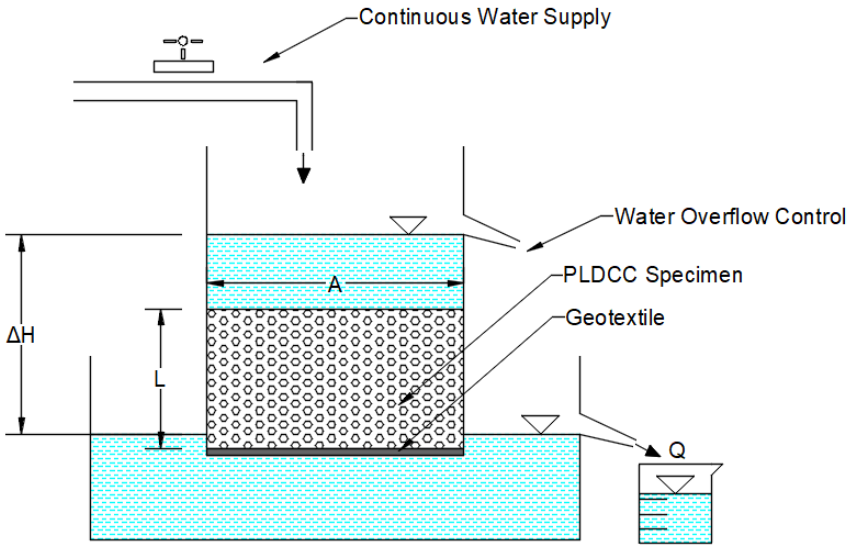

Figure 7. Constant Head Test Device

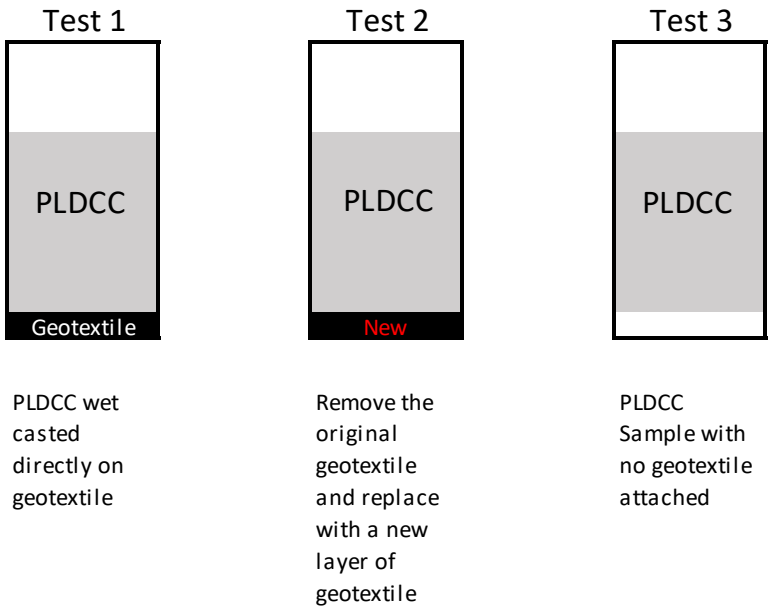

Figure 8. Sample Conditions for PLDCC and Nonwoven Geotextile Evaluations

3.2 LOW AND HIGH STRAIN MECHANICAL PROPERTIES

As discussed in Chapter 2, PLDCC has potential applications as a lightweight permeable base or subbases for roadway and stormwater management systems. As such, PLDCC must meet ultimate and serviceability limit state requirements. Some research has been done to address PLDCC hydraulic and ultimate limit state properties (i.e., hydraulic conductivity and unconfined compression testing); however, little is known regarding its low-strain behavior to support mechanistic pavement design. To this end, 12 PLDCC samples were cast, and resilient modulus and uniaxial compressive testing were evaluated using the following procedures.

Sample Preparation

Twelve samples of PLDCC were produced in cylindrical molds of 3 in diameter by 6 in height along three batches, described in Table 2. The PLDCC utilized in this study was created by the combination of slurry, composed of cement type I/II with water in a proportion of 1:0.55, with foam with a density of 2.5 pcf (approximately 0.393 kN/m^3). This foam was produced utilizing water, AQUAERiX-LB foaming agent, and adequate pump equipment, as shown in Figure 9. This foaming agent and the laboratory equipment used in this study were developed and donated by AERIX Industries.

Table 2. Permeable Low-Density Cellular Concrete (PLDCC) Batches Data

Batch	Production Date	Foam Density (PCF)		PLDCC Density (PCF)		
				Fresh		Dry
		Target	Actual	Target	Actual	
0	September 22, 2022	2.5	2.58	30	29.60	23.23
1	November 24, 2022	2.5	2.43	25	24.00	20.08
2	December 19, 2022	2.5	2.45	25	25.27	21.14

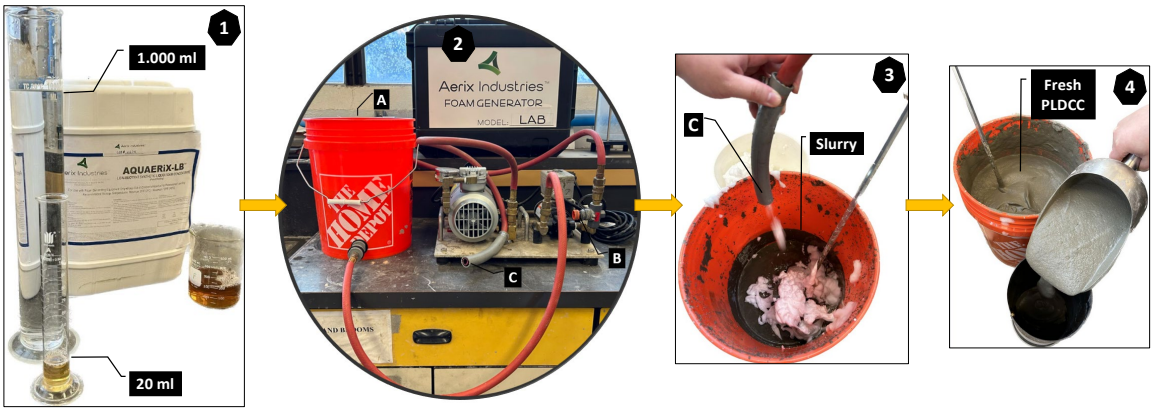

Figure 9. Laboratorial Permeable Low-Density Cellular Concrete (PLDCC) production

Figure 9-1 shows a beaker of AQUAERiX-LB (brown solution) and a graduated cylinder with the foaming agent with water. A mixture of 20 ml for each 1,000 ml of water) was used. This mixture was added to bucket A (Figure 9-2), which acted as the reservoir for the foam generator. The valve at B (Figure 9-2) controls the foam density intake to the generator, and the hose at C is the foam's exit point. In Figure 9-3, the foam is mixed with the concrete slurry to form PLDCC. The final mix is shown in Figure 9-4. The batch information has been previously presented in Table 1.

Resilient Modulus Testing

The resilient modulus (RM) is an effective way to characterize the stiffness of the various layers used in the pavement system (pavement, base, subbase, and subgrade materials) and is an essential input property to mechanistic pavement design. The RM is the ratio between the axial cyclic stress and the recoverable strain. This modulus is obtained through repeated cyclic stress-controlled triaxial tests that subject the testing samples to a fixed stress for 0.1 seconds, followed by a rest period of 0.9 seconds. During the cyclic loading, the specimens were subjected to relatively low confining pressures in the triaxial device, similar to a wide range of pressure that might be encountered in the in-situ condition under dead and live loads under a roadway (Table 3).

In addition, resilient modulus testing also allows the examination of samples over different ranges of moisture content, density, and temperature (Bennert and Maher, 2005). However, these variables were not explored during this study. In this study, the PLDCC samples of different densities were submitted to the resilient modulus testing using the testing sequence established by AASHTO TP46-94 in a dry state.

Uniaxial Compressive Strength

The uniaxial compression test is often used as an "index" of the mix quality and is routinely done for QC (quality control) testing for PLDCC and other cellular concrete products. The compressive strength tests were conducted on the samples previously tested for the resilient modulus following the ASTM C 495.

Table 3. Testing sequence for base/subbase materials (AASHTO TP46-94)

Sequence Number	Confining pressure (psi)	Deviator Stress (psi)	Number of Pulses
Conditioning	15.0	15.0	500
1	3.0	3.0	100
2	3.0	6.0	100
3	3.0	9.0	100
4	5.0	5.0	100
5	5.0	10.0	100
6	5.0	15.0	100
7	10.0	10.0	100
8	10.0	20.0	100
9	10.0	30.0	100
10	15.0	10.0	100
11	15.0	15.0	100
12	15.0	30.0	100
13	20.0	15.0	100
14	20.0	20.0	100
15	20.0	40.0	100

CHAPTER 4. RESULTS AND DISCUSSION

4.1 HYDRAULIC PROPERTIES

Hydraulic Conductivity, Submerged Saturated Unit Weight, and Storage Capacity

A total of 6 batches of samples were produced for this study. Batches 1 through 5 were used to evaluate the hydraulic properties of PLDCC, including dry unit weight, hydraulic conductivity, saturated unit weight, water storage capacity, and buoyant unit weight. The specimens from batch 6 were utilized to assess the hydraulic behavior when the PLDCC was combined with a nonwoven geotextile.

AERIX INDUSTRIES produced the first two batches of PLDCC specimens in their laboratory and later tested by us at the University of Utah. The initial batch consisted of 14 samples with a wet cast density measuring 25.1 PCF, while the second batch had a wet cast density of 32.6 PCF; both sets were manufactured using AQUAERIX™ foaming agent. Tables 4 and 5 summarize the results for Batchs 1 and 2, respectively.

The second batch of PLDCC samples demonstrates a decreased hydraulic conductivity range compared to the first, with a lower density. Upon comparing these results with those obtained from the Mission Rock Project (Figure 2 and Figure 10), it was clear that neither of these batches met the expected range of hydraulic conductivity for PLDCC.

After consulting with AERIX INDUSTRIES, it was decided that a new batch would be manufactured using their still-in-development foaming chemical known as AQUAERIX-LB™. The abbreviation "LB" denotes "low buoyancy," indicating the updated aim to produce PLDCC with reduced buoyancy force (i.e., higher submerged weight) while maintaining its high hydraulic conductivity. AERIX INDUSTRIES produced specimens for the third batch. The third batch consisted of eight specimens produced utilizing AQUAERIX-LB™ exhibited a wet cast density of 27.6 PCF (Table 6).

Table 4 summarizes the results of the tested hydraulic properties in this sample batch. Additionally, Figure 9 illustrates a comparison in hydraulic conductivity between the first and third batches.

Table 4 Hydraulic Properties on PLDCC Samples - Batch 1

Batch 1 - Wet Cast Density: 25.1 PCF					
Sample ID	Dry UW (PCF)	Hydraulic Conductivity (cm/s)	Saturated UW (PCF)	Vol.water/ Vol.PLDCC	Buoyant UW (PCF)
TY-5	22.4	3.0E-03	51.0	46%	-11.4
TY-6	22.8	8.6E-03	51.2	46%	-11.2
TY-7	22.9	7.5E-03	49.3	42%	-13.1
TY-8	21.0	4.1E-03	50.1	47%	-12.3
TY-9	22.3	3.6E-02	50.2	45%	-12.2
TY-10	22.7	1.7E-02	45.8	37%	-16.6
TY-11	22.6	1.4E-02	47.5	40%	-14.9
TY-12	21.0	1.3E-02	51.5	49%	-10.9
TY-13	22.1	1.3E-02	49.7	44%	-12.7
TY-14	22.1	1.9E-02	48.4	42%	-14.0
TY-16	20.7	7.9E-03	50.3	47%	-12.1
TY-17	20.6	7.6E-03	50.3	48%	-12.1
TY-18	22.2	2.9E-02	49.0	43%	-13.4
TY-19	22.6	1.1E-02	49.6	43%	-12.8
Average	22.0	1.4E-02	49.6	44%	-12.8
ST.DEV	0.03	0.66	0.03	0.07	0.12

Table 5. Hydraulic Properties on PLDCC Samples - Batch 2

Batch 2 - Wet Cast Density: 32.6 PCF					
Sample ID	Dry UW (PCF)	Hydraulic Conductivity (cm/s)	Saturated UW (PCF)	Vol.water/ Vol.PLDCC	Buoyant UW (PCF)
TY-20	29.0	1.4E-03	50.5	34%	-11.9
TY-21	28.4	8.3E-04	50.7	36%	-11.7
TY-22	28.8	1.7E-03	50.0	34%	-12.4
TY-23	28.5	1.6E-03	50.8	36%	-11.6
TY-24	28.4	1.3E-03	51.0	36%	-11.4
TY-25	28.0	2.1E-03	50.7	36%	-11.7
TY-26	28.5	1.5E-03	51.6	37%	-10.8
TY-27	28.7	2.6E-03	50.9	36%	-11.5
TY-28	29.1	2.1E-03	51.6	36%	-10.8
TY-29	28.3	1.6E-03	50.3	35%	-12.1
TY-30	27.7	9.1E-04	49.4	35%	-13.0
TY-31	29.2	1.3E-02	44.2	24%	-18.2
TY-32	28.0	2.1E-03	50.9	37%	-11.5
TY-33	28.8	1.4E-03	50.8	35%	-11.6
TY-34	28.9	2.0E-03	51.4	36%	-11.0
TY-35	28.1	1.2E-03	51.1	37%	-11.3
TY-36	28.2	2.1E-03	50.0	35%	-12.4
TY-37	27.7	1.0E-03	49.7	35%	-12.7
TY-38	29.6	1.1E-03	51.3	35%	-11.1
Average	28.5	2.2E-03	50.4	35%	-12.0
ST.DEV	0.02	1.15	0.03	0.08	0.13

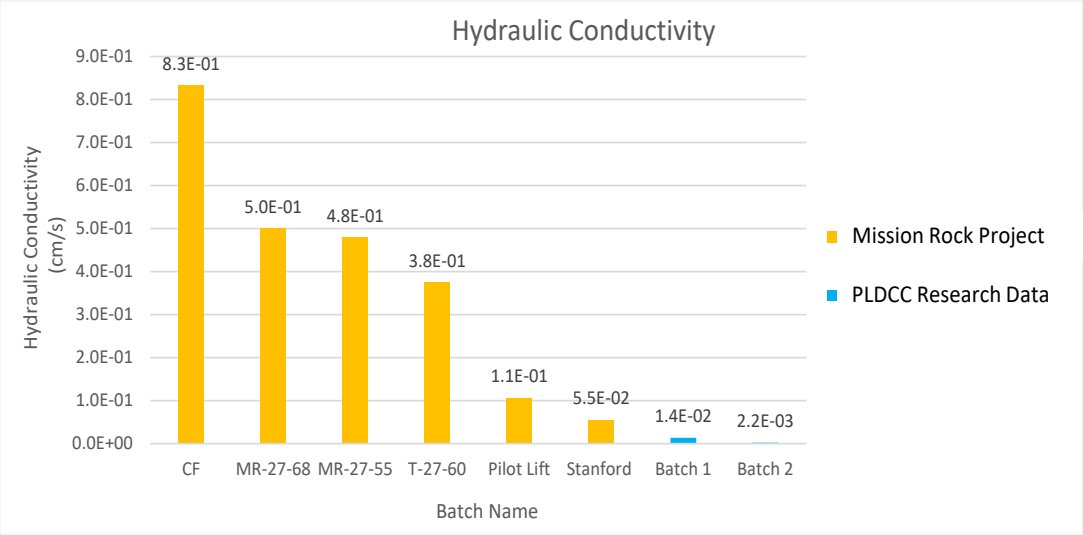

Figure 10. Comparison of Average Hydraulic Conductivity with Batch 1 and 2

Table 6. Hydraulic Properties on PLDCC Samples - Batch 3

Batch 3 - Wet Cast Density: 27.6 PCF					
Sample ID	Dry UW (PCF)	Hydraulic Conductivity (cm/s)	Saturated UW (PCF)	Vol.water/ Vol.PLDCC	Buoyant UW (PCF)
A1	26.2	2.3E-01	64.4	61%	2.0
A2	25.8	1.5E-01	63.6	61%	1.2
A3	25.5	3.6E-01	61.8	58%	-0.6
A4	26.1	2.9E-01	62.3	58%	-0.1
A5	26.8	3.5E-01	61.9	56%	-0.5
A6	25.7	3.1E-01	62.7	59%	0.3
A7	26.6	1.4E-01	61.7	56%	-0.7
A8	26.0	3.1E-01	61.3	57%	-1.1
Average	26.1	2.7E-01	62.5	58%	0.1
ST.DEV	0.02	0.32	0.02	0.03	16.21

After the evaluation of batch 3 samples, two more batches of samples were produced by the University of Utah using the foam generator and process shown in Figure 9. This batching was done to conduct a more comprehensive analysis of the PLDCC manufactured with AQUAERIX-LB™ foaming agent. Both batches 4 and 5 consisted of four specimens. Batch 4 targeted a lower density (25 PCF) than Batch 3, while Batch 5 was targeted for 30 PCF. The results of the tested hydraulic properties in the samples from batches 4 and 5 are summarized in Table 7.

Table 7. Hydraulic Properties on PLDCC Samples - Batch 4 and Batch 5

Batch 4 - Wet Cast Density: 25 PCF					
Sample ID	**Dry UW (PCF)**	**Hydraulic Conductivity (cm/s)**	**Saturated UW (PCF)**	**Vol.water/ Vol.PLDCC**	**Buoyant UW (PCF)**
Y5	23.4	4.6E-02	51.9	46%	-10.5
Y7	23.8	4.1E-02	51.4	44%	-11.0
Y8	24.0	4.8E-02	51.8	45%	-10.6
Y10	23.7	4.1E-02	50.3	43%	-12.1
Average	23.7	4.4E-02	51.3	44%	-11.1
ST.DEV	0.01	0.08	0.01	0.03	0.07
Batch 5 - Wet Cast Density: 30 PCF					
Sample ID	**Dry UW (PCF)**	**Hydraulic Conductivity (cm/s)**	**Saturated UW (PCF)**	**Vol.water/ Vol.PLDCC**	**Buoyant UW (PCF)**
Y14	26.0	1.1E-02	54.1	45%	-8.3
Y16	26.1	8.8E-03	52.9	43%	-9.5
Y17	25.9	1.7E-02	54.2	45%	-8.2
Y18	26.0	1.2E-02	53.6	44%	-8.8
Average	26.0	1.2E-02	53.7	44%	-8.7
ST.DEV	0.00	0.27	0.01	0.02	0.07

Table 8 presents an overview of test results conducted on five batches of PLDCC samples, which include hydraulic conductivity, saturated unit weight, and water storage capacity. The first two batches were created using the AQUAERIX™ foaming agent. They yielded average hydraulic conductivity values around 1.4E-02 cm/s for samples with densities close to 25 PCF. In contrast, the average hydraulic conductivity value for samples with densities of about 32.6 PCF was measured at approximately 2.2E-03 cm/s. When comparing these results to typical backfill materials such as clean sand or combinations of clean sand and gravel, which generally exhibit permeabilities ranging between 1.0E-03 cm/s and 1.0E-00 cm/s (Eskew et al., 2021), it is evident that the hydraulic conductivity of PLDCC specimens in batches 1 and 2 falls within this range, albeit towards the lower bound of the range.

Table 8. Summary of Test Results.

Batch #	Wet Cast Density (PCF)	Average Permeability (cm/s)	Sat - UW (PCF)	Vol. Water/Vol. PLDCC (%)	Foam Chemical	Produced By
1	25.1	1.4E-02	49.6	44%	Aquaerix	Aerix Industries
2	32.6	2.2E-03	50.4	35%	Aquaerix	Aerix Industries
3	27.6	2.7E-01	62.5	58%	Aquaerix-LB	Aerix Industries
4	25	4.4E-02	51.3	44%	Aquaerix-LB	Univeristy of Utah
5	30	1.2E-02	53.7	44%	Aquaerix-LB	Univeristy of Utah

Batch 3, which incorporated the usage of AQUAERIX-LB™, a recently introduced foaming agent, demonstrated an average hydraulic conductivity rate of 2.7E-01 cm/s among samples with densities measuring 27.6 PCF. The observed hydraulic conductivity value was notably higher by a factor of twenty compared to that measured for batch one despite having lesser density, as shown in Figure 11. For this batch of samples, the average saturated unit weight is approximately 62.5 PCF, about the unit weight of water at 62.4 PCF, indicating that this material would exhibit negligible buoyancy. (Due to its open-cell fabric that permits air pockets and excluded void space within the PLDCC, complete saturation of all voids is not likely for in-situ conditions.)

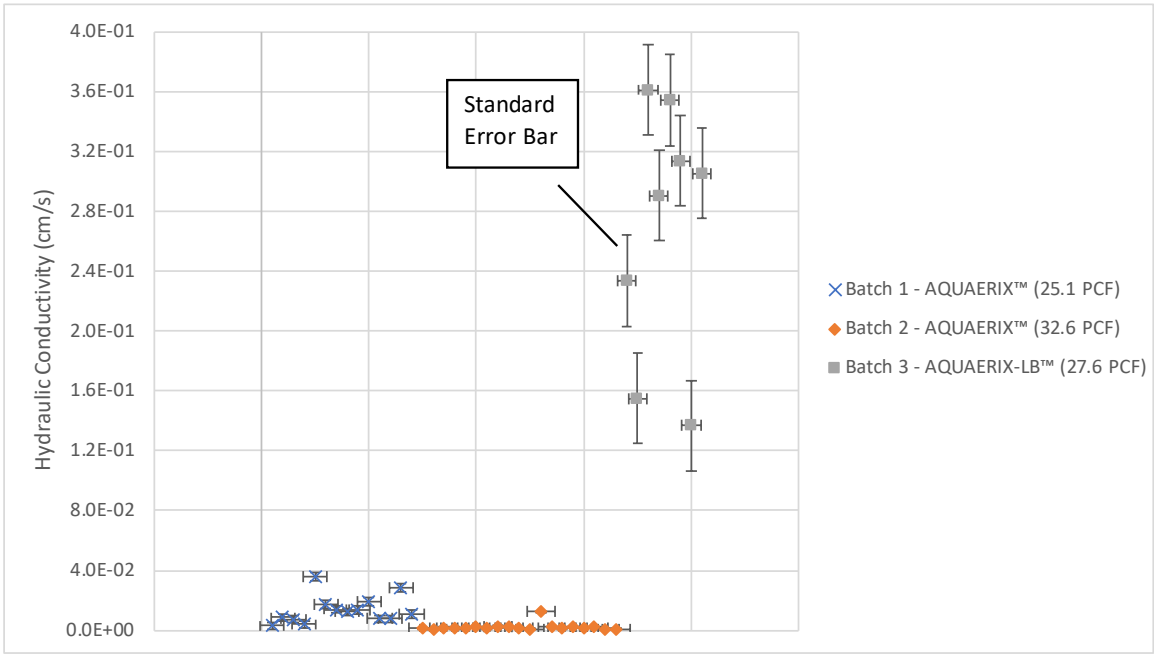

Figure 11. Hydraulic Conductivity of PLDCC with Different Foaming Agents

We conclude that utilization of AQUAERIX-LB™ produced a more open and connected air bubble structure when compared with AQUAERIX (Figure 12). As a result, the water storage capacity of the PLDCC samples from batch 3 attained an average value of 58%, which is higher than that obtained from batches 1 (44%) and 2 (35%). This finding also means that a 1 m^3 unit volume of placed PLDCC can accommodate about 0.6 m^3 of water in its pore space. This water storage capacity is comparable to or exceeds lightly compacted loam, clean sand, and aggregate/gravel, which have respective water storage capacities of 20%, 30%, and 40%, respectively (Marritz, 2013).

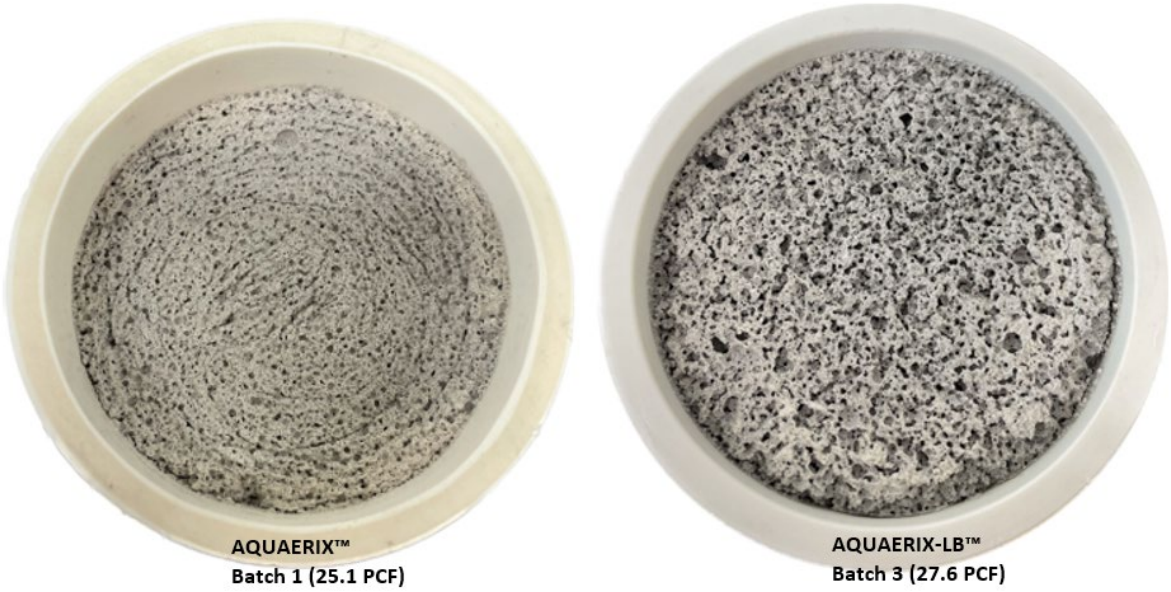

Figure 12. Comparison of Samples Produced by AQUAERIX and by AQUAERIX-LB

As anticipated, specimens with lower densities generally exhibited higher hydraulic conductivity values, as Averyanov (2018) found. However, the outcomes of batch 4 contradicted this tend. Specifically, the specimen with a wet cast unit weight of 25 PCF displayed an average hydraulic conductivity rate of 4.4E-02 cm/s, six times lower than that observed in batch 3, containing specimens with a density value of 27.6 PCF, as shown in Figure 13. In addition to

hydraulic conductivity, batch 3 demonstrated higher values for saturated unit weight, water storage capacity, and buoyant unit weight than batches 4 and 5.

Considering that batch 4 was made in the soil laboratory of the University of Utah, as opposed to being manufactured by AERIX INDUSTRIES, various batching and mixing factors may impact the cellular fabric and consequently affect its hydraulic characteristics.

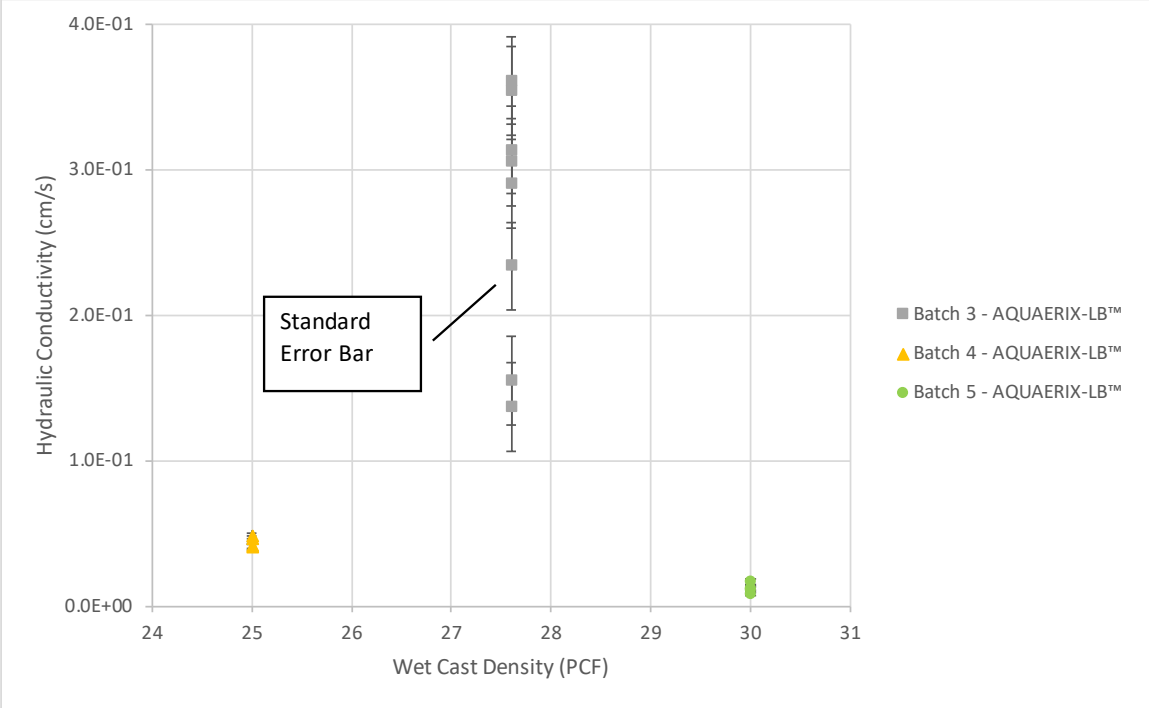

Figure 13. Hydraulic Conductivity of PLDCC Using Aquaerix-LB™ Foaming Agent.

Also, the foam generator utilized in the manufacturing process of PLDCC has the potential to influence the consistency of the foam density. The foam made by this generator, which resembles shaving cream with a dense consistency, should possess sufficient firmness and stability to withstand the pressure exerted by mortar until the cement sets, ultimately forming a robust concrete framework around air-filled voids, ensuring durability. While it is worth noting that AERIX INDUSTRIES provided the University of Utah with one of its laboratory-size foam generators, the equipment we used may differ from that employed in producing batch 3 samples by AERIX INDUSTRIES. Consequently, differences arising from variations in usage between different types or models of foam generators might give rise to differences in the overall mixture properties.

Additionally, the structure of PLDCC can be influenced by the mixing method or apparatus employed during its production. While foam concrete may be compatible with commonly used mixers such as tilt drums or pan mixers utilized for concrete or mortar, improper blending techniques or excessive agitation could reduce foam content throughout the process (Ramamurthy, et al., 2009).

Furthermore, the curing condition influences the hydraulic conductivity of PLDCC. While preliminary investigation indicated a 7-10 day cure duration for optimal readiness in conducting the permeability test, further exploration is essential to ascertain whether an extended cure period would be necessary for achieving ideal hydraulic features in AQUAERIX-LB™ created samples of PLDCC.

Table 9 presents the mean hydraulic conductivity, standard deviation, and standard error values for all batches of PLDCC samples. Although the U of Utah produced samples within the target density range, these specimens did not achieve hydraulic conductivity values comparable to those specimens made by AERIX INDUSTRIES. However, AQUAERIX-LB™ results were slightly higher than batches 1 and 2, which utilized an AQUAERIX™ foaming agent. These findings and the results from batch 3 support the more beneficial hydraulic characteristics obtained using the AQUAERIX-LB™ foaming agent in the PLDCC mix.

However, it is suggested that further exploration and improvements in the handling and production process might lead to more consistent hydraulic conductivity values from AQUAERIX-LB™ mixes. For example, the laboratory data indicate significant variability in the hydraulic conductivity values for PLDCC samples tested within the same batch (see Batch 3, Figure 14). These data suggest that hydraulic conductivity can vary by about one-half an order of magnitude. Similar variation is seen in the hydraulic conductivity values from previous laboratory results (Figure 2). For example, the "Pilot Lift" results from the Mission Rock Project (Figure 2) were tested by Castle Rock Consulting using the procedure given in Appendix C.1. These data also indicate significant variability in the hydraulic conductivity of PLDCC specimens. These results

imply that PLDCC samples with the same density can exhibit significantly different hydraulic conductivity. Therefore, it appears that the hydraulic conductivity of PLDCC depends on factors such as pore structure and size, void size distribution, and void connectivity within the specimen. Even if two PLDCC specimens have similar unit weights, these other factors appear to differ significantly enough to produce varying hydraulic conductivity values. .

However, the within-batch values for saturated unit weight and water storage capacity exhibit significantly less variability (Figures 15 and 16, respectively). This lesser variability is also be observed in the data from the Mission Rock project (Figure 2).

Table 9 Summary of Mean, Standard Deviation, and Standard Error of Each Batch

Hydraulic Conductivity (cm/s)					
Batch #	**1**	**2**	**3**	**4**	**5**
Average	1.4E-02	2.2E-03	2.7E-01	4.4E-02	1.2E-02
ST.DEV	0.66	1.15	0.32	0.08	0.27
ST.ERROR	0.18	0.26	0.11	0.04	0.14

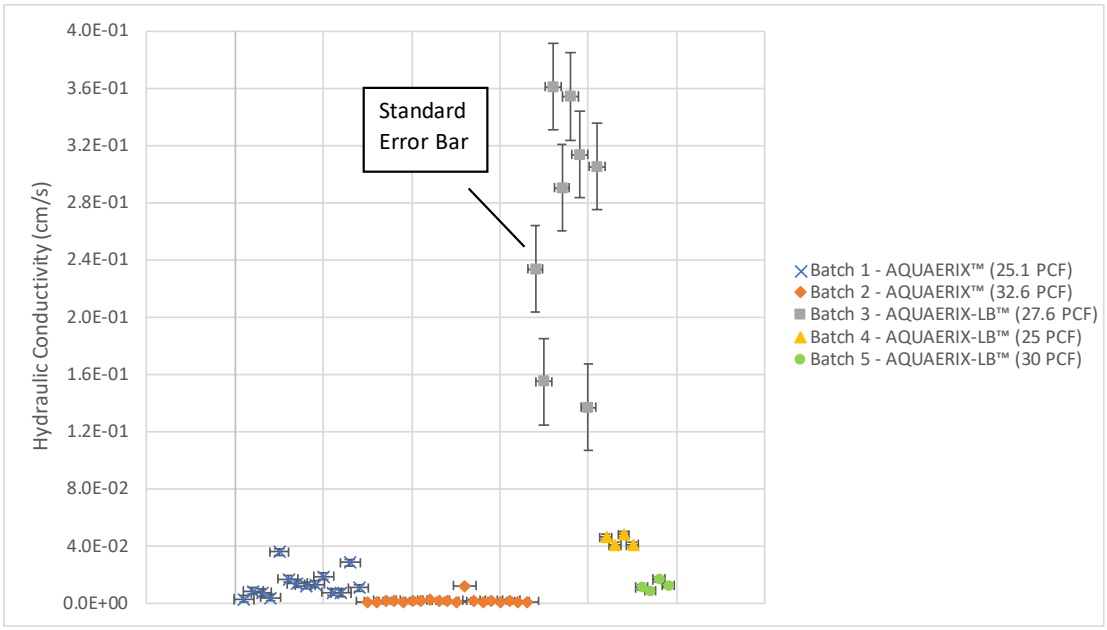

Figure 14. Within-Batch Sample Variability in Hydraulic Conductivity of PLDCC

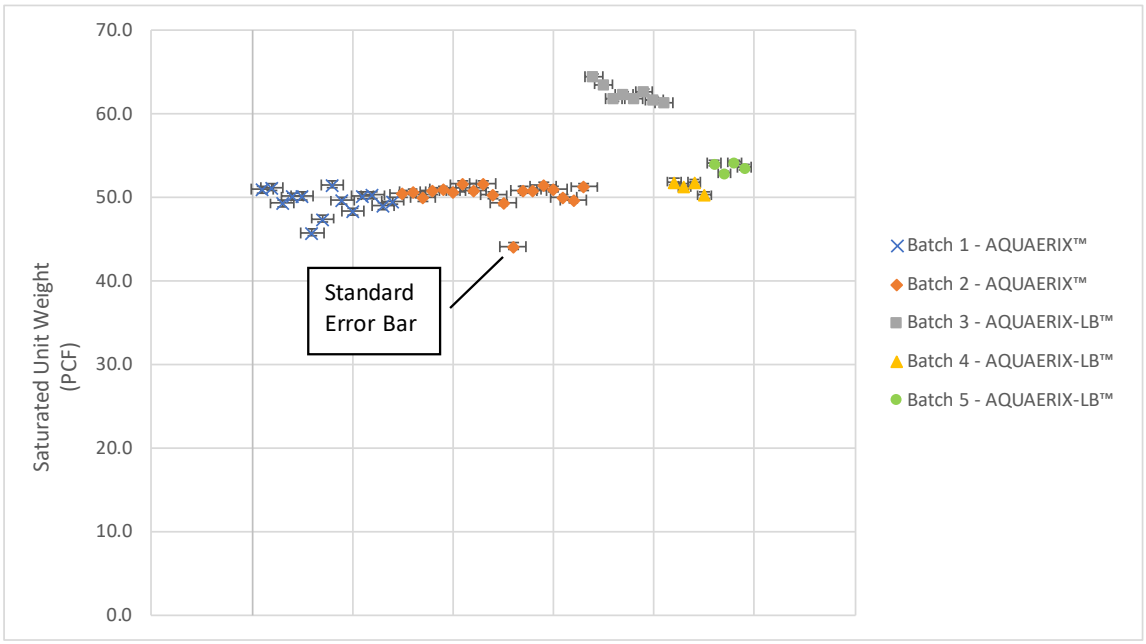

Figure 15. Within-Batch Sample Variability in The Saturated Unit Weight of PLDCC

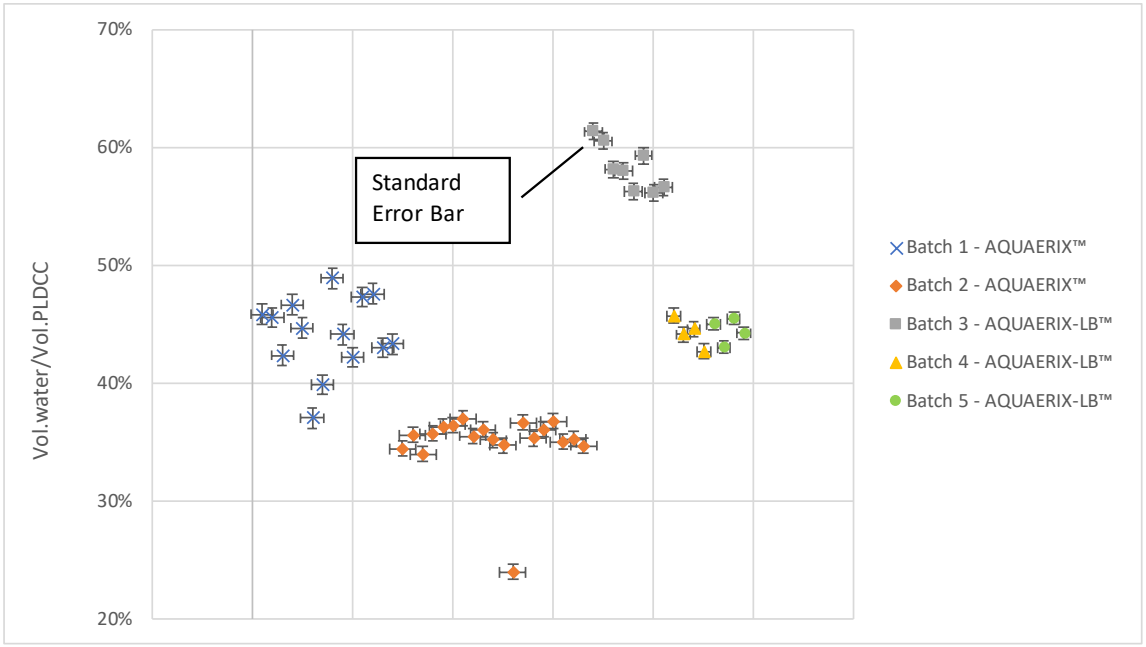

Figure 16. Within-Batch Sample Variability in The Water Storage Capacity of PLDC

Results from Combing a Filter Fabric with PLDCC

When a cement-based PLDCC mixture is applied to a permeable nonwoven geotextile fabric in its wet state, this application might obstruct the fabric's pores and impede the system's infiltration rate. To assess this possible effect, we evaluated the infiltration rate of PLDCC with a nonwoven geotextile following the procedure outlined in Section 3.1.

In summary, four specimens were used to test three potential variations of the possible system (Figure 8). The results of these four tests are shown in Figures 17 – 20. Each figure shows the three variations that were tested: (1) a wet cast directly onto geotextile and tested for infiltration rate after curing; (2) a second test with replacement of the original geotextile layer with a new geotextile layer; and (3) a third test without any geotextile layer present.

The infiltration testing commenced upon the PLDCC drying of the specimen, at which point the specimen showed a high, sponge-like absorbency. The water infiltration rate was rapid initially; however, after about 10 minutes, there was a notable change in the flow rate. The overall flow gradually diminished with time as the water began accumulating within the voids. After 30 minutes of testing, a slightly diminishing flow rate was observed for the duration of the experiment.

We noted that upon wet casting the PLDCC directly onto the geotextile, there was a strong adhesion between the two materials once fully cured. Some effort was necessary to remove the geotextile from this composite structure (Figure 21). The cement compound of PLDCC has established itself within the geotextile fabric during its casting and curing. Upon inspection, it was noted that water movement through the geotextile fabric was significantly disrupted due to portions of the fabric becoming obstructed by solidified cement.

Our data suggest only minor changes in infiltration rate among the three variations constructed. In the first few minutes of the test, the specimens with a wet-cast geotextile fabric had an infiltration rate of about 25 to 30 percent less than the PLDCC specimens without the filter fabric (Figures 17, 19, 20). At longer durations (i.e., 60 minutes), this difference diminished to about 0 to

10 percent. Therefore, the nonwoven geotextile plays a relatively minor role in impeding flow, especially as the flow approaches a steady state condition. However, additional examination may be warranted, including assessing whether these findings remain valid when utilizing geotextiles with differing permeabilities and over longer durations. Lastly, the geotextile component of the filtration system may experience long-term plugging caused by fine-grained soil particle accumulation at the separation layer or from biofouling. This research did not explore these mechanisms. However, we believe that by carefully selecting the geotextile, employing proper installation techniques, designing an effective filter system, and conducting regular maintenance, the plugging of nonwoven geotextiles and the PLDCC can be effectively prevented, ensuring their long-term performance in filtration applications.

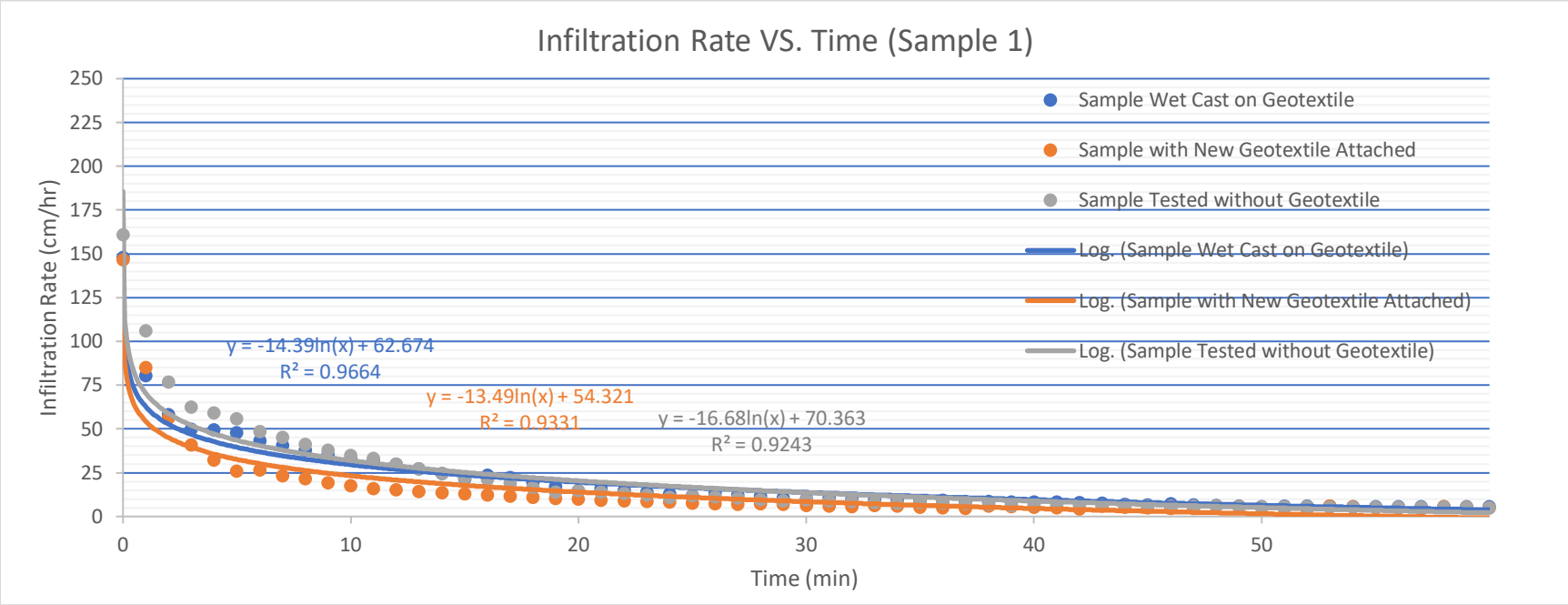

Figure 17. Infiltration Rates of PLDCC of Sample 1

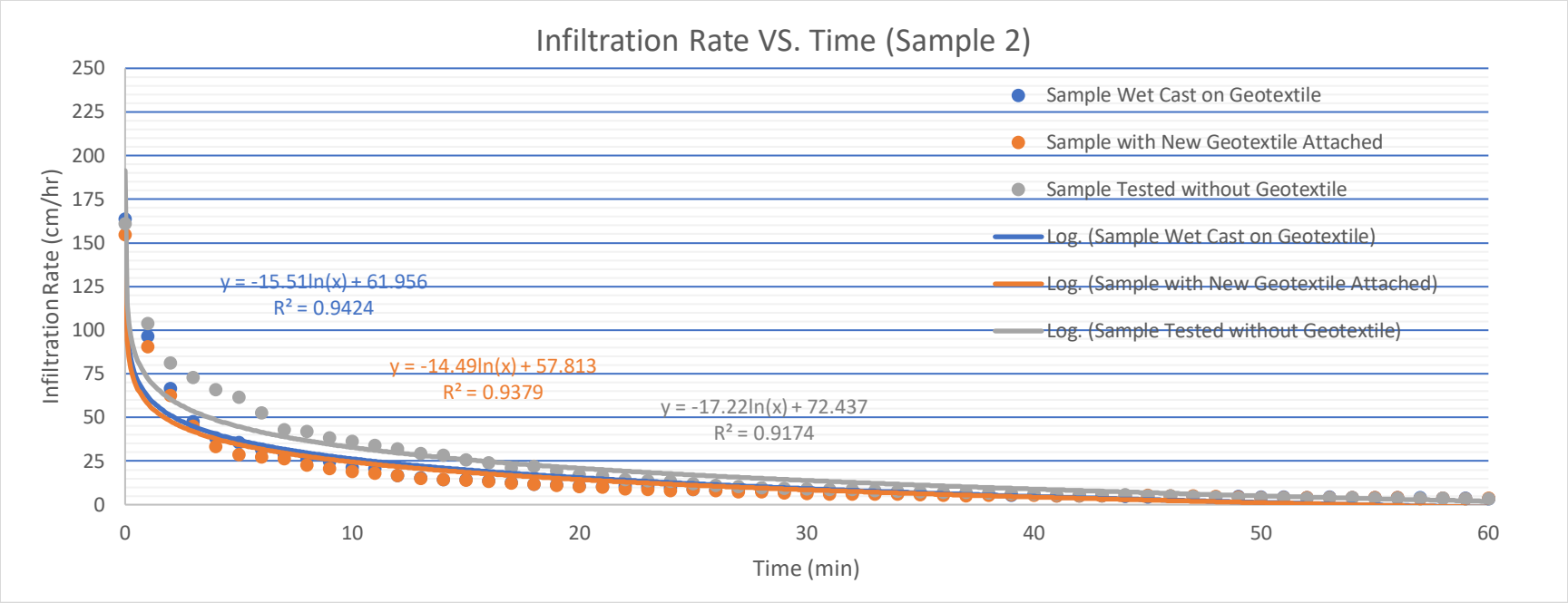

Figure 18. Infiltration Rates of PLDCC of Sample 2

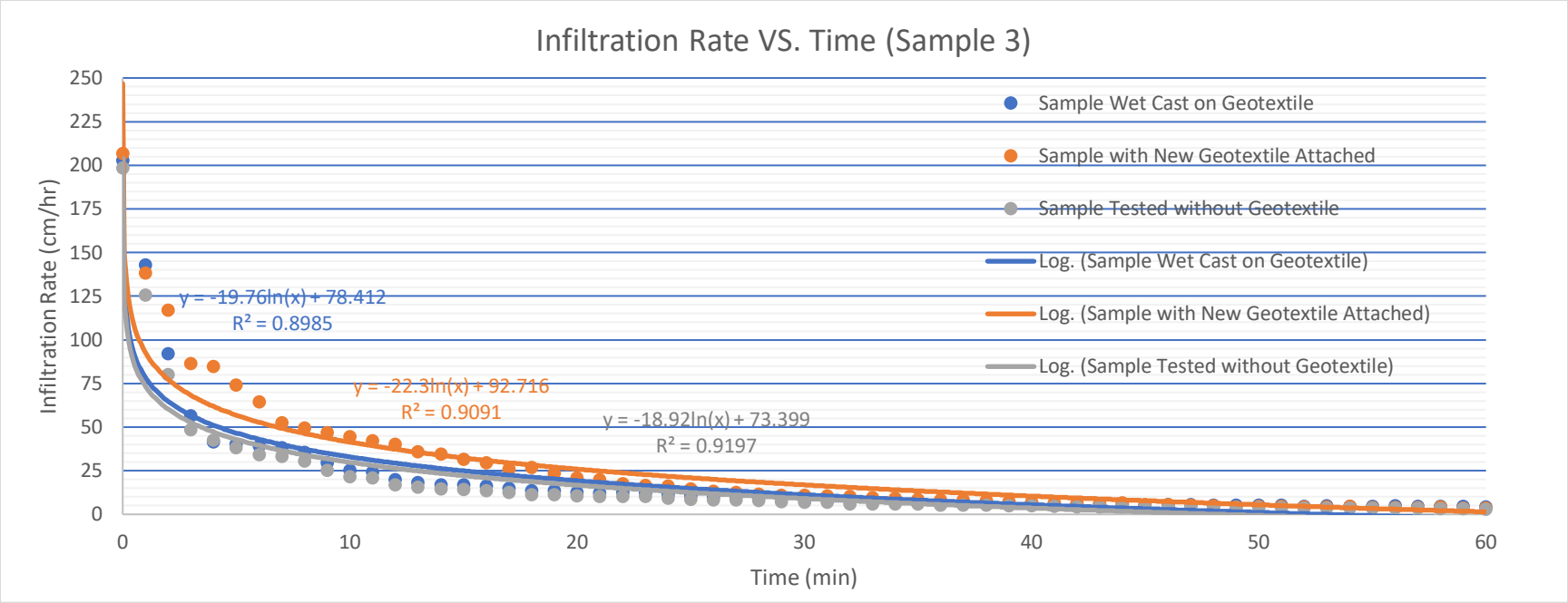

Figure 19. Infiltration Rates of PLDCC of Sample 3

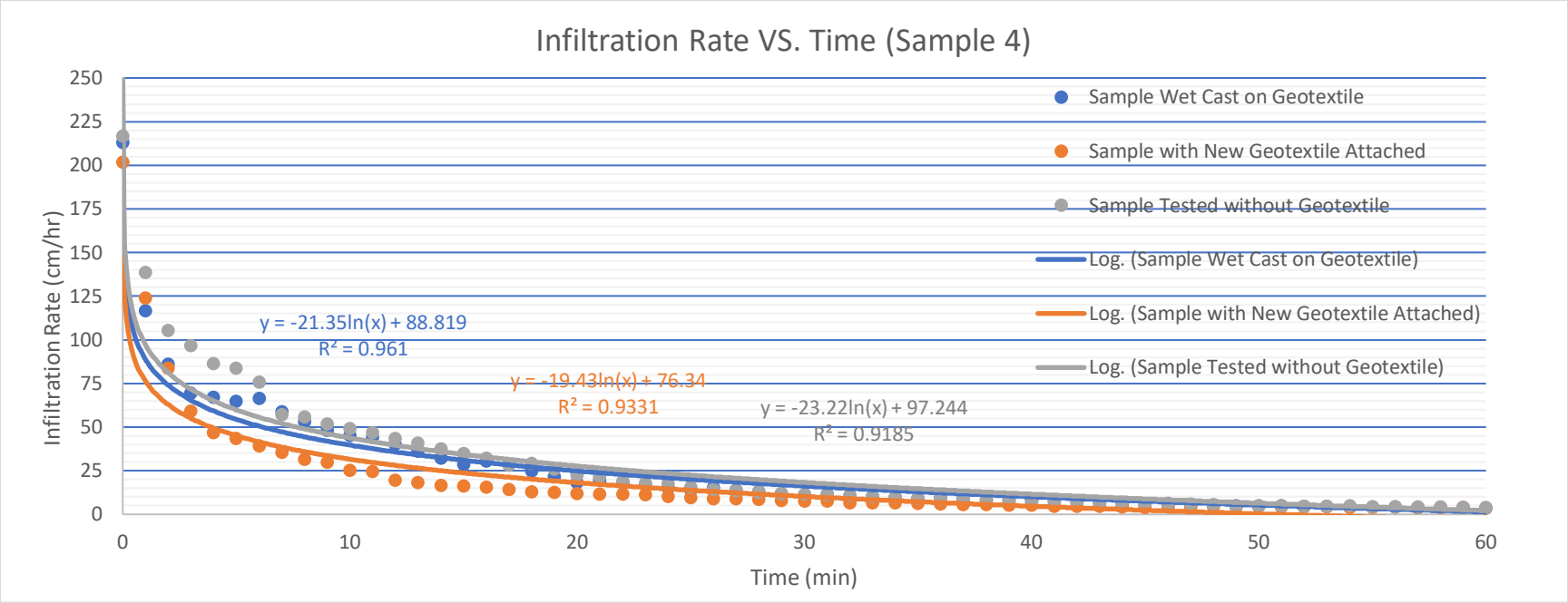

Figure 20. Infiltration Rates of PLDCC of Sample 4

Figure 21. Undamaged Geotextile and Geotextile Removed from PLDCC

4.2 MATERIAL PROPERTIES

Resilient Modulus

The PLDCC used in this study was made with AQUAERiX-LB foaming agent, which was mixed with water in a 1:50 proportion to produce a foam with a density between 2 to 2.1 pcf (32 to 33.6 kg/m^3) that was combined with slurry composed by water and cement in the ratio of 0.50. The resilient modulus test results of the twelve PLDCC samples, presented in graph format, are grouped by their respective batches in this chapter. These same data are also found in Appendix D. Figures 22-24 show the graphs obtained through the resilient modulus tests of batches 0, 1, and 2, respectively.

The Resilient Modulus can be represented in terms of Bulk Stress, which is obtained by dividing the vertical force acting on the sample by its area through the following equation:

$$MR = K_1 * \theta^{K_2} \qquad \text{[Eq. 4-1]}$$

where: MR = Resilient Modulus (MPa)
Θ = Bulk Stress (kPa) = $\sigma_1+\sigma_2+\sigma_3$
K_1 and K_2 = Material's Constant (-)

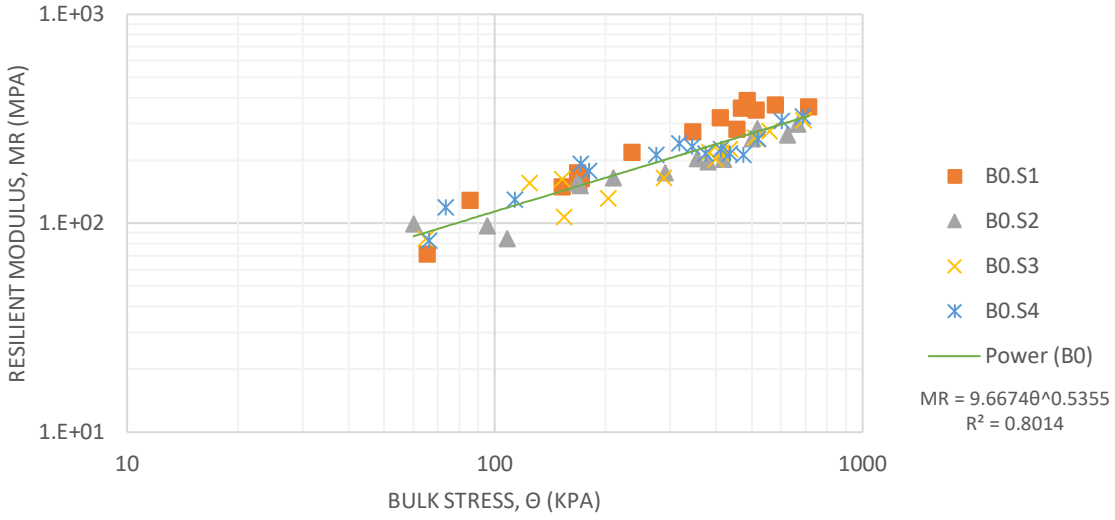

Figure 22. Graphical result of the resilient modulus test on samples of batch 0.

For Figure 22, the material's constant K1 and K2 equals 9.6674 and 0.5355. The coefficient of determination R^2 equals 0.8014, which suggests a relatively strong relationship.

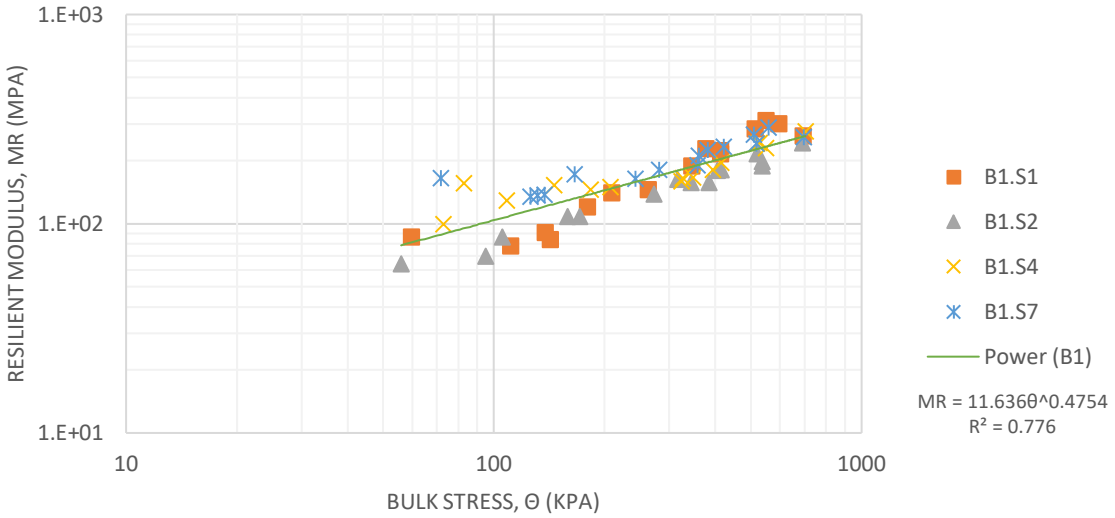

Figure 23. Graphical result of the resilient modulus test on samples of batch 1.

For Figure 23, the material's constant K1 and K2 equals 11.636 and 0.4754, and R^2 is 0.776.

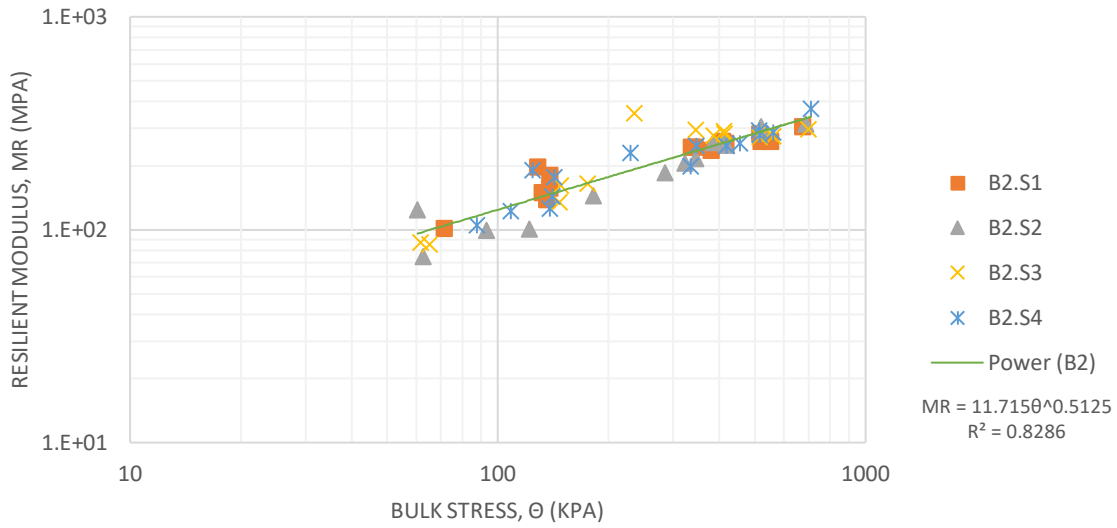

Figure 24 Graphical result of the resilient modulus test on samples of batch 2.

For Figure 24, the material's constant K1 and K2 are equal to 11.715 and 0.5125 and R^2 is 0.8286.

Table 3 summarizes the results obtained from the tests discussed in the previous chapters, which are analyzed and compared with other materials described in the literature. This table also tabulates the wet/fresh density of the different batches because density is usually used as a quality index property of Permeable Low-Density Cellular Concrete (PLDCC) attributes.

Table 10 Summary of resilient modulus test results for PLDCC.

Batch	Average Fresh Density		Resilient Modulus Equation		Uniaxial Compressive Strength (MPa)
	(pcf)	(kN/m^2)			
0	29.60	4.65	$MR=9.6674*\theta^{0.5355}$	[Eq.4- 2]	0.85
1	24.00	3.77	$MR=11.636*\theta^{0.4754}$	[Eq.4- 3]	0.40
2	25.27	3.97	$MR=11.715*\theta^{0.5125}$	[Eq. 4-4]	0.73

MR = Resilient Modulus (MPa)

Θ = Bulk Stress (kPa)

Kumar et al. (2006) analyzed the resilient modulus of subbase materials and identified the materials' constants, allowing the relationship between resilient Modulus and Bulk Stress. These relationships for PLDCC and other base materials are presented in Tables 11 and 12 and shown in Figure 25.

Table 11 Resilient Modulus equation of different subbase materials (Kumar et al. 2006)

Subbase Material	Resilient Modulus Equation	
Stone dust	$MR=57.566*\theta^{0.0911}$	[Eq. 4-5]
Fly Ash	$MR=61.011*\theta^{0.1169}$	[Eq. 4-6]
Coarse sand	$MR=86.338*\theta^{0.0919}$	[Eq. 4-7]
Riverbed material (RBM)	$MR=29.515*\theta^{0.3369}$	[Eq. 4-8]

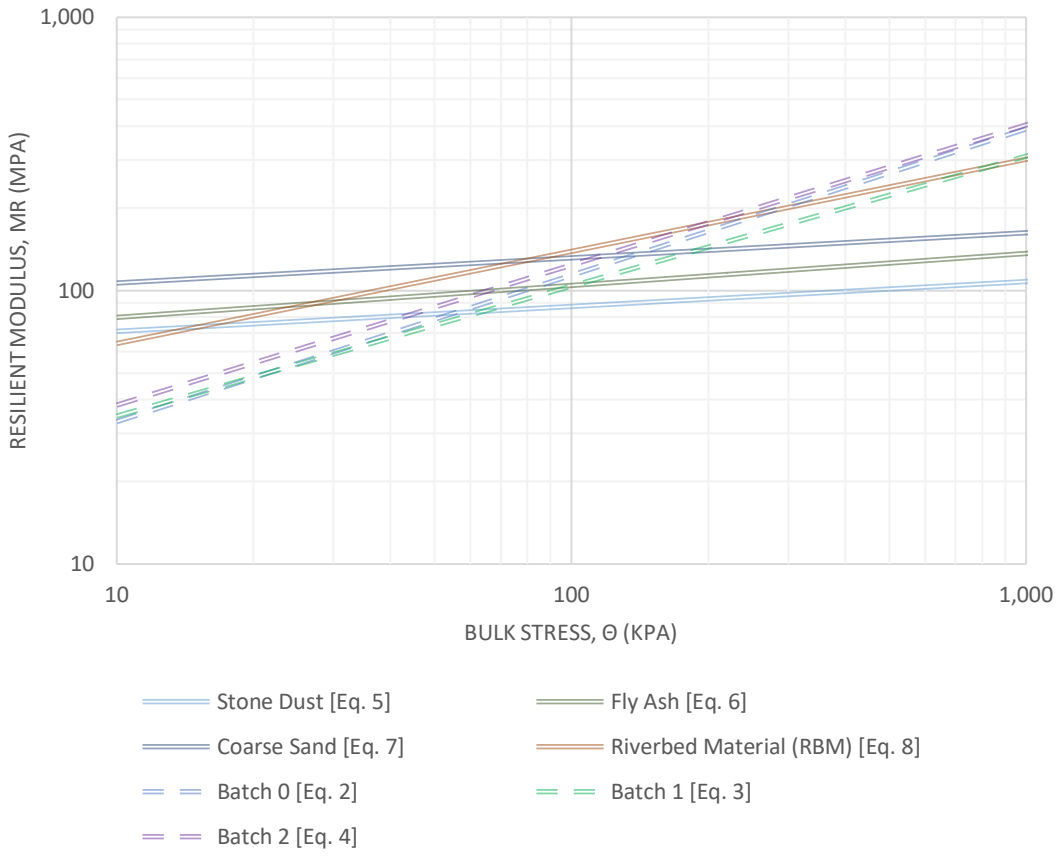

Figure 25. Bulk stress versus the Resilient Modulus of subbase materials and the PLDCC batches.

For values lower than 100 kPa of the Bulk Stress, the Resilient Modulus of PLDCC is 30 to 40 MPa, which is lower than other subgrade materials. However, when the Bulk Stress is between 100 to 200 kPa, a usual range for road bases undergoing dead and heavy truck live tire loads, the resilient modulus of PLDCC is comparable to or higher than the other subgrade materials reported by Kumar et al. (2006).

Bennert and Maher (2005) analyzed the resilient modulus of Dense Graded Aggregate Base Course (DGABC) from samples of varying gradations to develop a performance specification for the granular base and subbase material. The resilient module of these extreme DGABC samples and the bulk stress associated with these moduli are given in Table 12. This table shows the average resilient moduli expected for the PLDCC batches and the subbase materials analyzed by Kumar et al. (2006).

Over the range of bulk stresses tabulated in Table 12, the PLDCC of batches 0 and 2 have resilient modulus values close to RBM, as shown in Figure 25. Also, the PLDCC values are 11 and 19% higher

than the largest resilient modulus of the DGABC samples (158.88 MPa) analyzed by Bennert and Maher (2005). Additionally, the resilient modulus referring to the PLDCC batch 1 on Table 12 is reasonable for subbase applications, only slightly lower (3.4%) than the modulus obtained at the top DGABC sample.

Therefore, all the PLDCC batches we tested have comparable resilient modulus values with other base materials in the stress range of interest. However, these values are for unsaturated specimens, and the influence of the saturation degree of the PLDCC samples was not explored in this study.

Table 12. Comparison of the resilient moduli of subbase materials exposed to field bulk stresses.

Material	Bulk Stress, θ (kPa)	Resilient Modulus, MR (MPa)	Bulk Stress, θ (kPa)	Resilient Modulus, MR (MPa)
DGABC, Natural Gradation	227	158.88	254	-
DGABC, Low End		-		126.53
Stone Dust		94.37		95.32
Fly Ash		115.04		116.53
Coarse Sand		142.15		143.59
RBM		183.58		190.53
Batch 0		176.62		187.36
Batch 1		153.43		161.69
Batch 2		188.92		199.90

Uniaxial Compressive Strength

The PLDCC specimens were subjected to uniaxial compression (UC) tests after it was verified that the samples did not show any detectable fractures from the RM testing. In the end caps, durometers (DURO 50) were utilized. Thus, the software reports were adjusted for dorometer effects. The testing results are shown below. The results of this testing are found in Appendix E.

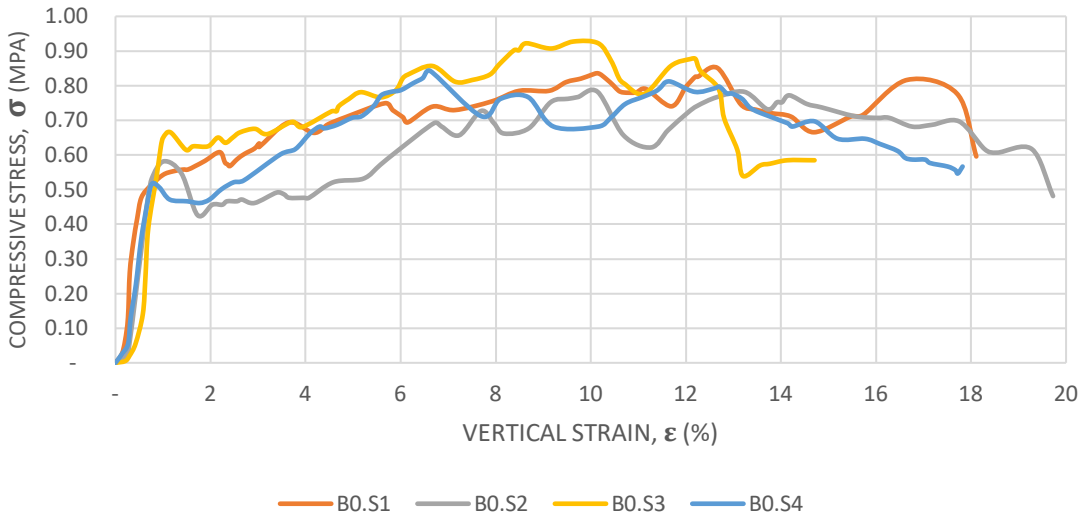

Figure 26. Unconfined compression test graph of batch 0.

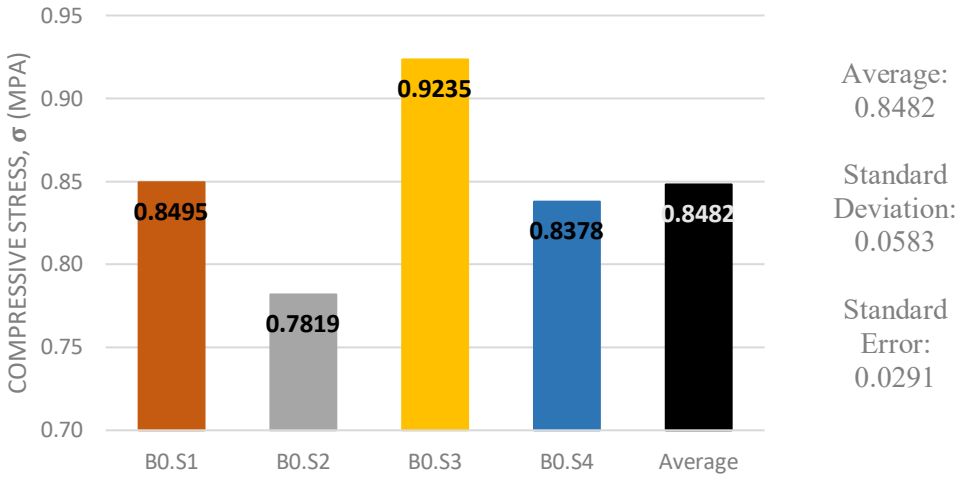

Figure 27. Unconfined compression of samples of batch 0.

On average, the samples of batch 0 (with an average fresh density of 29.6 pcf (4.65 kN/m^3)) have an average uniaxial compressive stress of approximately 0.85 MPa (123 psi).

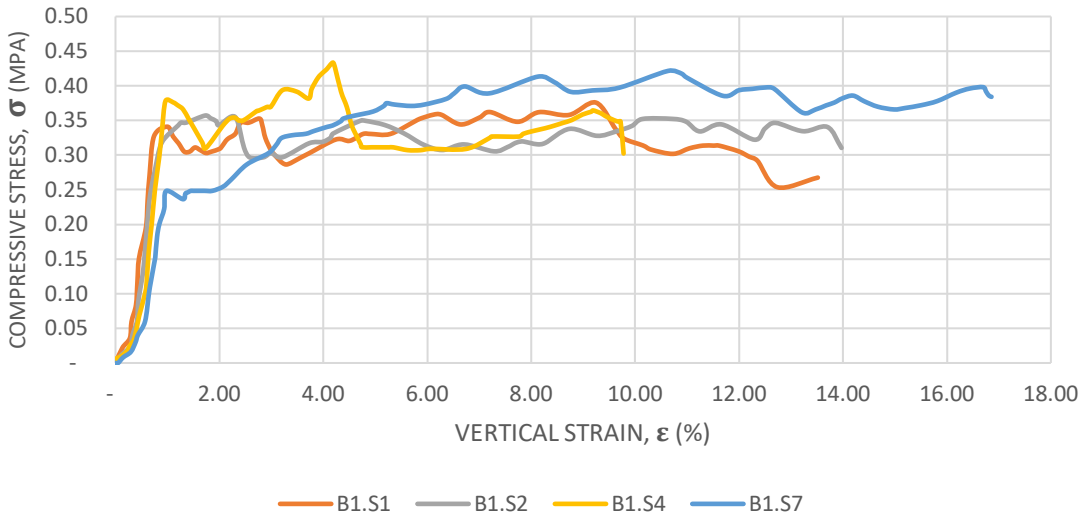

Figure 28. Unconfined compression test graph of batch 1.

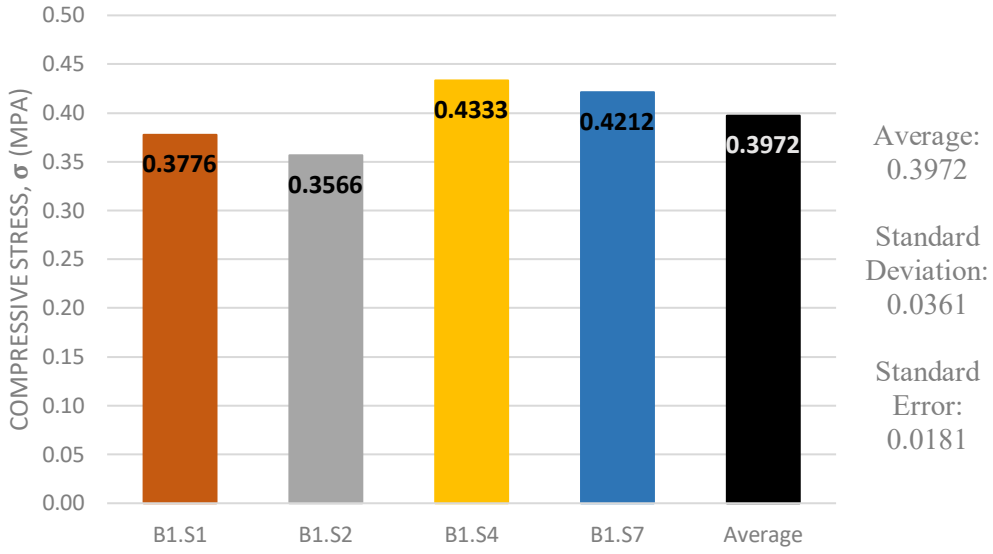

Figure 29. Unconfined compression of samples of batch 1.

On average, the samples of batch 1 (with an average fresh density of 24 pcf (3.77 kN/m^3)) have an average uniaxial compressive stress of 0.40 MPa (58 psi).

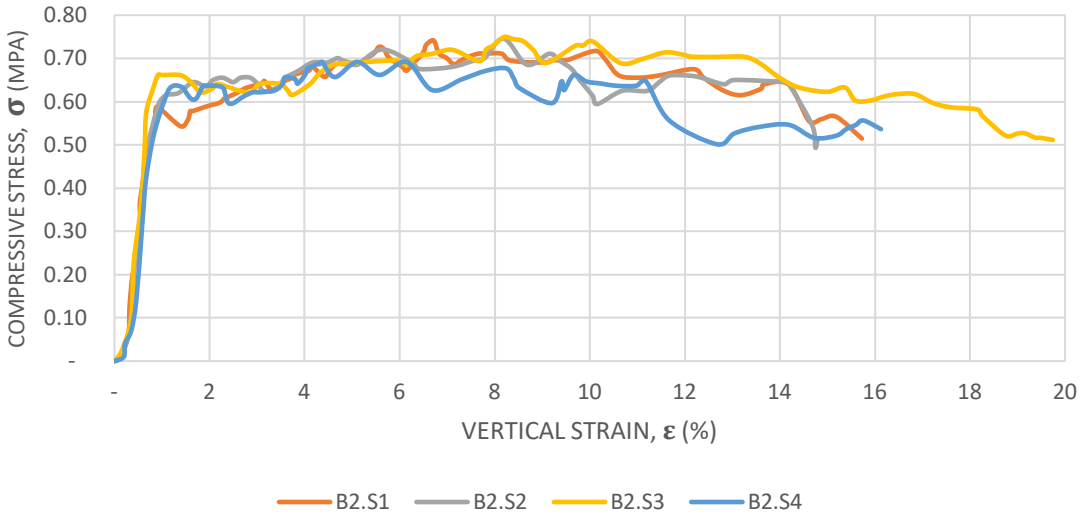

Figure 30. Unconfined compression test graph of batch 2.

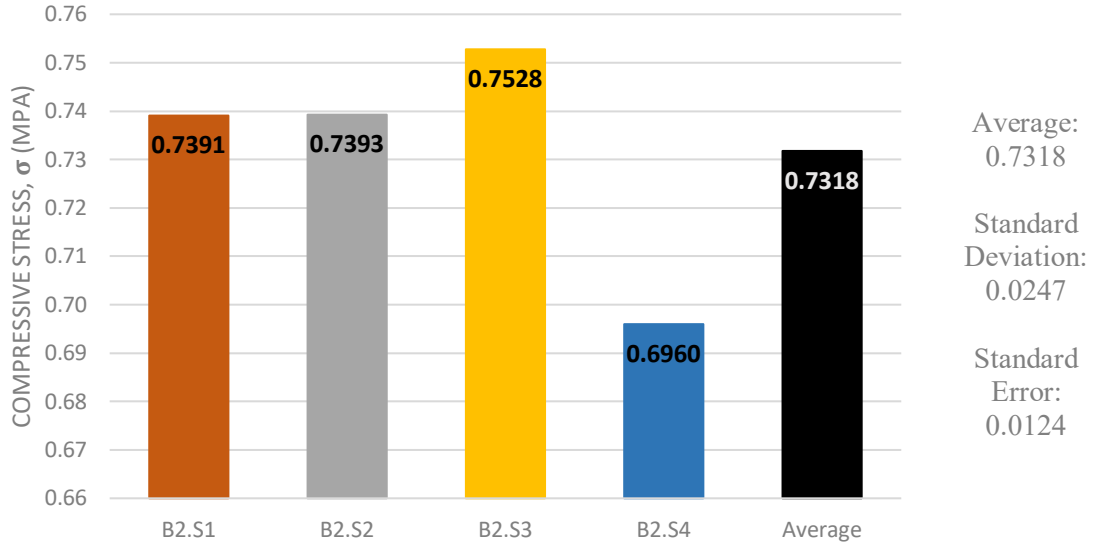

Figure 31. Unconfined compression of samples of batch 2.

On average, the samples of batch 2 (which have an average fresh density of 25.27 pcf (3.97 kN/m^3)) have an average uniaxial compressive stress of approximately 0.73 MPa (106 psi).

In a study submitted to Aerix Industries by Kevern (2018) PLDCC, the compressive strength of dry specimens with a fresh density equal to 25 and 30 pcf (400.46 and 480.55 kg/m^3) was reduced by 30 and 23%, respectively, when saturated. Meanwhile, samples with a fresh density of 35 pcf (560.65 kg/m^3) showed no reduced compressive strength when saturated (Kevern 2018).

The compressive strength of the dry PLDCC samples analyzed by Kevern (2018) and those examined in this study can be observed in Figure 32. This figure shows that Kevern's samples (K25, K30, K35) had higher results than the average PLDCC samples of all three batches in this study. This difference appears to be due to minor fractures in batches B0, B1, and B2 samples, which probably originated from the resilient modulus test. However, there is the possibility that this reduction is related to the difference in foam density used in each study.

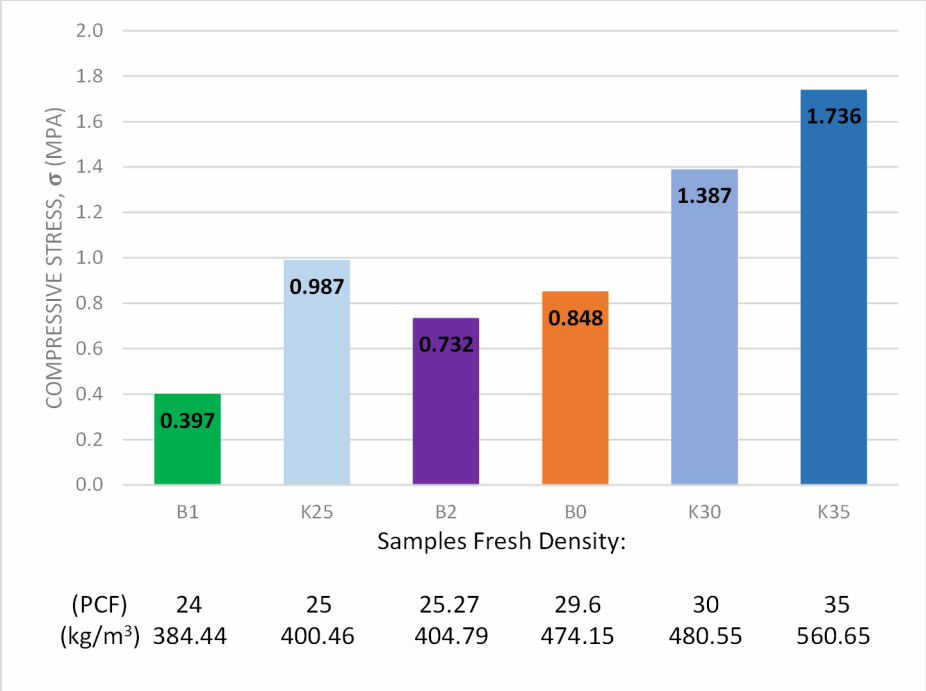

Figure 32 Compressive strength of dry PLDCC samples of different fresh densities.

We observed that the rupture of all the samples of batches 0, 1, and 2 started with the fracturing and crushing of the sample's bottom, followed by the development of fissures in the upward direction

(Figure 33). This behavior was observed in all PLDCC specimens, and the potential nonuniformity may be linked to the production process of the samples.

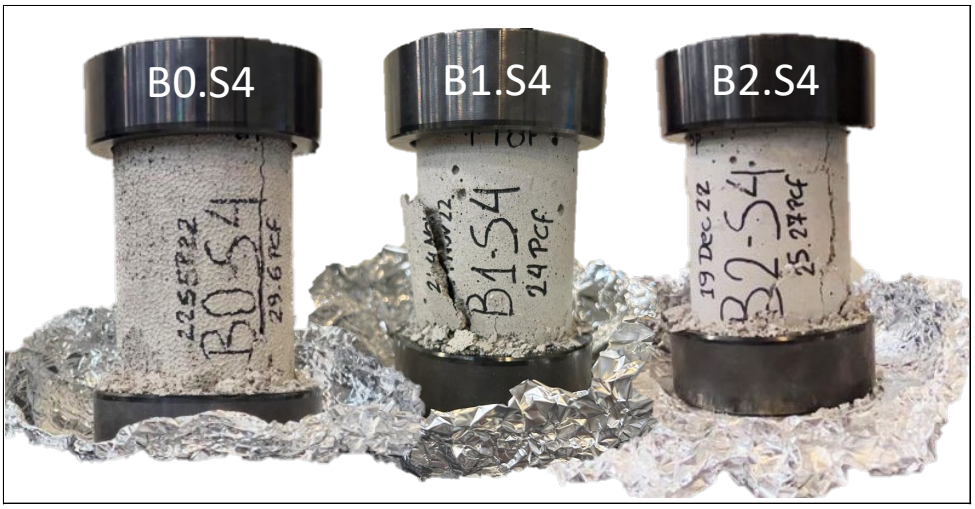

Figure 33. Samples of each batch immediately after the uniaxial compressive strength test.

Pavement Design Evaluations

This section compares the design of regular pavement with one using PLDCC (Permeable Low-Density Cellular Concrete) as a subbase instead of the typical granular material. Both designs consider the Utah Department of Transportation's (UDOT) official traffic count data for Redwood Road between MP 52.401 and MP 53.99, found on this department's website.

Traffic analysis

Redwood Road's annual average daily traffic (AADT) in 2019 was assumed as a current value for this analysis. This choice was made to avoid historical traffic data conflict due to the global pandemic of 2020. Thus, an amount equal to 52,000 vehicles per day was used to determine the design equivalent single axle load (ESAL), which can be verified in Figure 18.

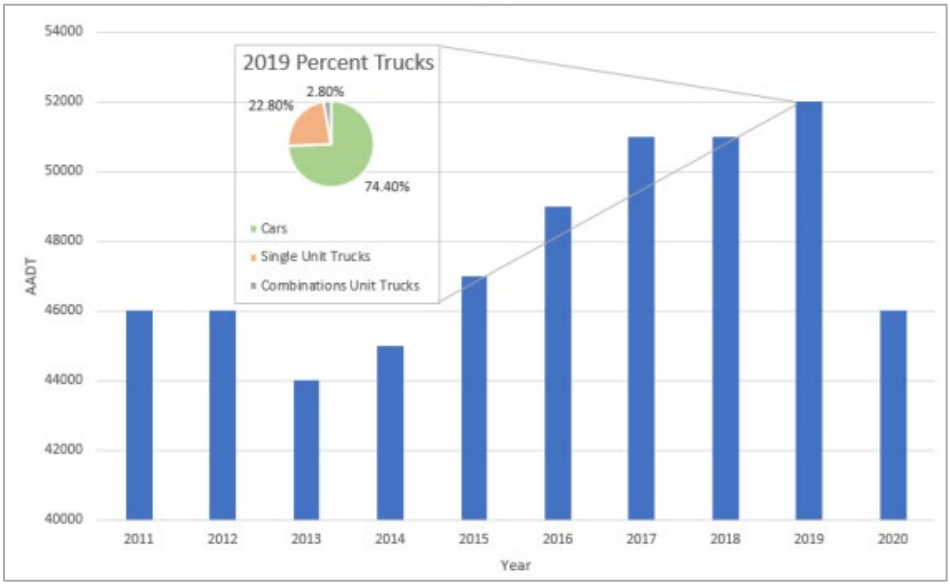

Figure 34. Historic AADT on Redwood Road registered on UDOT.

The pandemic strongly influenced the AADT of this region. The AADT is greatly different between 2019 and 2020. The pavement evaluatios for this roadway were projected for a design life (t) of 20 years, and their overall design parameters as shown in Table 13. Thus, to predict the traffic growth during this time, the UDOT AADT database was used to determine the growth rate (r)

through a trend line (Figure 35).

Table 13 Pavement designs layer's information.

Pavement:	Regular			w/ PLDCC		
Layer:	Height, h (in):	Resilient Modulus, RM (psi):	Poisson ratio, v:	Height, h (in):	Resilient Modulus, RM (psi):	Poisson's ratio, v:
Asphalt Concrete	8	405,000	0.35	8	405,000	0,35
Granular Base	8	37,500	0.4	8	37,500	0.4
Granular Subbase	6	9,000	0.4		-	
PLDCC Subbase		-		6	25,000	0.3
Subgrade	∞	4,500	0,45	∞	4,500	0,45

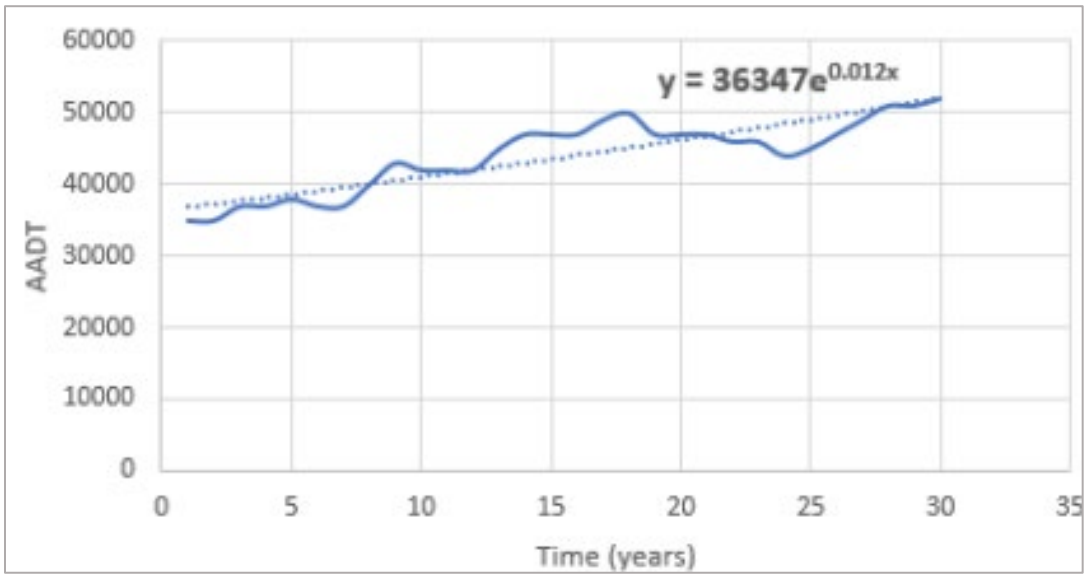

Figure 35 Redwood Road's annual average daily traffic (AADT) between 1990 and 2019.

The trendline equation in the figure shows a growth rate (r) equal to 0.012. This value is approximately 1% for the analysis made in this section. Then, the value of r was used to determine the growth factor (GY) in Equation 4-9, and Equations 4-10 – 4-13 determined

the truck factor (T_f). The summary of the calculation of this factor can be observed in Table 14, where the microstrain values were determined through the Weslea software. Finally, considering all the elements in Table 15, Equation 4-14 determines each pavement design's ESAL (Nf). This value is also presented in Table 15.

$$GY = \frac{(1+r)^t - 1}{r} \quad \text{[Eq. 4-9]}$$

$$Trucks = AADT * percent\ trucks_{Su\ or\ CU} * percentFHWA_{class} \quad \text{[Eq. 4-10]}$$

$$ELF = (\frac{\varepsilon}{\varepsilon_{18\ kip}})^{3.9492} \quad \text{[Eq.4- 11]}$$

$$ESAL\ Count = \sum trucks * \text{ELF} \quad \text{[Eq.4- 12]}$$

$$T_f = \frac{Total\ ESALs}{Total\ Trucks} \quad \text{[Eq.4-13]}$$

$$\text{Nf} = AADT * 365 * D * L * GY * T * \text{Tf} \quad \text{[Eq. 4-14]}$$

Table 14. Truck factor (T_f) calculation.

Pavement	FHWA Class	Trucks	Microstrain Steer Axle	Steer Axle ELF	Microstrain Single Axle	Single Axle ELF	Microstrain Tandem Axle	Tandem Axle ELF	ESAL Count	Truck Factor
Regular	4	2,962.97	93.17	0.15	120.82	0.42	-	-	1,677.59	0.75
	5	3,555.56	93.17	0.15	150.79	1.00	-	-	4,086.63	
	6	5,333.35	93.17	0.15	-	-	90.00	0.13	1,491.40	
	8	877.70	93.17	0.15	185.52	2.27	91.84	0.14	2,244.91	
	9	585.12	93.17	0.15	-	-	111.66	0.31	444.68	
Total:		13,314.71							9,945.21	
w/ PLDCC	4	2,962.97	88.61	0.16	110.73	0.39	-	-	1,630.91	0.76
	5	3,555.56	88.61	0.16	140.63	1.00	-	-	4,129.31	
	6	5,333.35	88.61	0.16	-	-	85.36	0.14	1,603.16	
	8	877.70	88.61	0.16	172.42	2.24	87.10	0.15	2,236.82	
	9	585.12	88.61	0.16	-	-	105.77	0.32	474.35	
Total:		13,314.71							10,074.54	

Table 15. Design equivalent single axle load (ESAL) calculation.

Pavement:	Regular	w/ PLDCC
Average Annual Daily Traffic (AADT)	52,053	
Lane Factor (L)	0.8	
Direction Factor (D)	0.5	
Percent of Trucks (T)	25.6%	
Growth Rate (r)	1%	
Project Life, years (t)	20	
Growth Factor (GY)	20.02	
Truck Factor (T_f)	0.75	0.76
Design ESAL (Nf)	31,997,684	32,413,794

Distress Modeling

The distress of the pavement designs here analyzed was made using the Pavement Damage Equations for Fatigue Bottom-Up Cracking and Permanent Deformation, which can be found in the Guide for Mechanistic-Empirical Design of Pavement Structures.

Fatigue

Equations 4-15 – 4-17 were used to determine the number of load repetitions that result in bottom-up fatigue cracking (Nfc) failure. The result of such equations, and the Miner's relationship between Nf and Nfc, are presented in Table 16.

$$M = 4.84 * (\frac{V_b}{V_a + V_b} - 0.69) \quad \text{[Eq. 4-15]}$$

$$k'_1 = \frac{1}{0.01 + {}^{12}/_{1 + e^{(15.676 - 2.8186 * h_{AC})}}} \quad \text{[Eq. 4-16]}$$

$$Nfc = 0.00432 * k'_1 * C * \left(\frac{1}{\varepsilon_t}\right)^{3.9492} * \left(\frac{1}{E}\right)^{1.281} \quad \text{[Eq. 4-17]}$$

Table 16. Design equivalent single axle load (ESAL) calculation.

Pavement:	Regular	w/ PLDCC
V_a	6	
V_b	12	
K'$_1$	250	
Elastic Modulus of the First Layer (E)	405,000	
Strain Under the First Layer (ε_t)	$150.79 * 10^{-6}$	$140.63 * 10^{-6}$
M	-0.113	
C	0.771	
Nfc	67,563,431	88,992,005
Nf/Nfc	0.47	0.36

Rutting

Rutting (PD) is a permanent deformation that occurs due to pavement structural failure due to the repetition of loads exceeding the pavement's bearing capacity. This deformation, which occurs cumulative over time, can be calculated following two methods depending on the bound present on each layer's material.

Unbound Material

Pavement's unbound materials are the granular layer's material of the base and subbase. These layers were subdivided into two to obtain a more accurate PD result. Equations 4-18 – 4-21 were used for these calculations; the results are presented in Table 17.

$$\log \rho = 0.622685 + 0.541524 * W_c \quad \text{[Eq. 4-18]}$$

$$\log \beta = -0.61119 - 0.017638 * W_c \quad \text{[Eq. 4-19]}$$

$$\log(\frac{\varepsilon_0}{\varepsilon_r}) = 0.74168 + 0.08109 * W_c - 0.000012157 * E \quad \text{[Eq. 4-20]}$$

$$PD = 1.673 * 1.04 * \frac{\varepsilon_0}{\varepsilon_r} * e^{-(\rho/N_f)^{0.7*\beta}} * \varepsilon_v * h_{sub} \quad \text{[Eq. 4-21]}$$

Table 17. Summary of values and calculation of the rutting in granular layers.

Pavement	Regular				w/ PLDCC	
Granular Sublayer	Base 1	Base 2	Subbase 1	Subbase 2	Base 1	Base 2
Nf	31,997,684				32,413,794	
Wc (%)	12				12	
E (psi)	37,500		9,000		37,500	
h (in)	4		3		4	
β_{GB}	1.673				1.673	
$\log(\frac{\varepsilon_0}{\varepsilon_r})$	1.2589		1.6053		1.2589	
$M_r/1000$	37.50		9.00		37.50	
Adj. Strain Ratio	1.0421		0.3753		1.0421	
Adj. Ratio $*(\frac{\varepsilon_0}{\varepsilon_r})$	18.9137		15.1247		18.9137	
Log(β)	-0.8228				-0.8228	
Corrected β	0.1053				0.1053	
Log(ρ)	7.1210				7.1210	
ρ	$1.32*10^7$				$1.32*10^7$	
$(\rho/N)^{\beta}$	0.911				0.911	
$e^{-(\rho/N)\beta}$	0.402				0.402	
$\frac{\varepsilon_\rho}{\varepsilon_v}$	12.72		10.17		12.74	
ε_ρ	0.00311	0.00284	0.00352	0.00324	0.00179	0.00153
ε_r	244.58	223.47	346.20	318.25	140.25	120.06
PD (in)	0.0124	0.0114	0.0106	0.0097	0.0071	0.0061

Bound Material

The material that adheres together, such as the asphalt concrete (mix PG 70-28) used in the pavement designs analyzed in this section, is classified as a bound material. The PLDCC subbase was also considered a bound material. Equations 4-22 to 4-25 were used to calculate the PD of these pavement layers; the results are presented in Table 18.

$$C_1 = -0.1039 * {h_{ac}}^2 + 2.4868 * h_{ac} - 17.342 \quad \text{[Eq. 4-22]}$$

$$C_2 = 0.0172 * {h_{ac}}^2 - 1.7331 * h_{ac} + 27.428 \quad \text{[Eq. 4-23]}$$

$$k_1 = (C_1 + C_2 * depth) * 0.328196^{depth} \quad \text{[Eq. 4-24]}$$

$$PD = k_1 * 10^{-3.4488} * T^{1.5606} * {N_f}^{0.479244} * h_{ac} * \varepsilon_r \quad \text{[Eq. 4-25]}$$

Table 18. Summary of values and calculation of the rutting in bounded layers.

Pavement	**Regular**	**w/ PLDCC**	
Layer	Asphalt Concrete	Asphalt Concrete	PLDCC Subbase
Microstrain, ε_r	112.86	105.47	65.82
h_{ac} (in)	8	8	6
Depth (in)	4	4	4
C_1	14.66	14.66	17.65
C_2	-4.10	-4.10	-6.16
Nf	31,997,684	32,413,794	32,413,794
T	45	45	45
k_1	0.63	0.63	0.75
ε_p	0.04	0.04	0.03
$\varepsilon_p/\varepsilon_r$	338.36	340.47	402.08
PD (in)	0.3055	0.2873	0.1588

Total Rutting

Following this analysis, the regular pavement's total rutting (PD) equals 0.34 in., a value 26.1% less than the one in the pavement design that uses PLDCC as a subbase. However, because the maximum PD allowed in this case was 0.5, both pavement designs are acceptable, with an estimatedproject life of 20 years. The total rutting for these pavement designs is given in Table 19.

Table 19. Estimated total rutting of the analyzed pavements.

Pavement	Regular	w/ PLDCC
Layers:		
Asphalt Concrete	0.3055	0.2873
Granular Base	0.0238	0.0132
Granular Subbase	0.0203	-
PLDCC Subbase	-	0.1588
Total (in):	0.34	0.46

Designs Comparison

Both pavement designs can be applied on Redwood Road since the Miner's relationship (Nf/Nfc given in Table 16) in both cases is smaller than 1, indicating that the pavement will not suffer from fatigue cracking along its use. And that the total rutting of both pavements, after 20 years of service, will be smaller than 0.5 inches. However, we note that the pavement with PLDCC as a subbase material has a rutting close to the limit value in this case.

Other Considerations

The tests and analysis in the study suggest that the Permeable Low-Density Cellular Concrete (PLDCC) has structural characteristics that allow its use as a pavement subbase or base. However, addressing other considerations this study has not evaluated may be necessary. First, all the PLDCC samples analyzed were tested in a dry state. However, actual pavement systems will undoubtedly vary from this condition. Increasing moisture content in the PLDCC may influence its low and high-strain mechanical properties. Secondly, a statistical evaluation of the 12 samples we evaluated suggests that PLDCC has relatively high variability. This variability can be observed not only in comparing specimens of different batches but also in comparing samples within the same batch. We believe some of this variability could be reduced in the sample batching and preparation process; nonetheless, aleatoric uncertainty remains and should be considered in the design process. For example, the specimen preparation followed the methods recommended by AERIX Industries. During this process, we observed that lighter PLDCC tends to

concentrate at the top of the container. This separation contributed to the fracture behavior shown in Figure 33 and failure initiation in the bottom part of the specimens. Finally, this work did not evaluate the influence of environmental factors (e.g., temperature oscillation, freeze-thaw cycles, and other sources of physical and chemical reactions that could reduce PLDCC's mechanical properties. These factors could be explored more deeply through controlled laboratory and construction-scale prototypes.

CHAPTER 5. SUMMARY AND CONCLUSIONS

5.1 SUMMARY

Hydraulic Properties

This report investigated the hydraulic characteristics of permeable low-density cellular concrete (PLDCC) and its potential role in sustainable infrastructure development. Valuable information has been obtained through laboratory experiments conducted on six batches of PLDCC samples, providing insights into the material's hydraulic conductivity, dry and saturated unit weight, water storage capacity, and buoyant unit weight. Furthermore, this research has also assessed the hydraulic performance of PLDCC when combined with geotextile by examining the infiltration rate of the combined system.

Mechanical Properties

This research also evaluated the mechanical properties of PLDCC to determine the viability of using PLDCC as a pavement subbase or base material. We conducted Resilient Modulus (RM) and uniaxial compressive (UC) strength tests using samples of PLDCC at different densities to fulfill this objective.

5.2 CONCLUSIONS

Hydraulic Properties

1. The relatively permeable, interconnected pores and open fabric of PLDCC lend to its use in surface and in-situ applications requiring transmission and storage of water. Findings from our laboratory-based hydraulic conductivity tests show that the hydraulic conductivity of PLDCC is comparable to clean sand or sand and gravel mixtures. This finding indicates the potential for PLDCC to serve as an efficient, lightweight drain in geosystems.

2. The open and connected fabric of PLDCC produces a lightweight material (weighing nearly four to five times less than conventional earthen materials) yet still achieves a partially saturated unit weight under laboratory conditions comparable to water. This finding implies that PLDCC will have a small to negligible buoyancy force for applications where the PLDCC is placed below or within the water table.

3. The water storage capacity of PLDCC is more significant than other types of compacted granular soil, with a value of about 45 to 60% by volume. Compared to compacted loam or clear sand, PLDCC has three times more storage capacity and exceeds that of aggregate or gravel by approximately 1.5 to 2 times. This high storage capacity of PLDCC can potentially contribute to water storage for use in near-surface stormwater detention and retention facilities and cisterns, especially where lightweight material is required or desirable.

4. Laboratory experiments on utilizing PLDCC with a nonwoven geotextile beneath exhibited a relatively small influence on the system's infiltration performance. This result suggests the feasibility of integrating PLDCC with a geotextile in a drain or infiltration system. Enhancing the overall filtration capacity and performance of the drainage-storage functions is possible.

5. For design, accounting for the variability in hydraulic conductivity observed in the tested samples is vital. This variation can be attributed to several factors, including disparities in foaming agent quality, mixture proportions, and mixing methods. These factors can impact the pores' size and distribution within PLDCC material. Therefore, technology development endeavors should focus on identifying and optimizing key factors that influence the hydraulic conductivity of PLDCC, such as foam generation techniques, foam stability, and foam distribution within the concrete matrix. Moreover, conducting comprehensive investigations into the repercussions of various curing conditions, mixing protocols, and foam-to-cement ratios on the hydraulic characteristics of PLDCC would yield invaluable perspectives.

6. The long-term behavior and durability of PLDCC should be initiated, particularly for field or construction-scale applications. These studies could explore potential differences that arise between controlled laboratory conditions and field conditions in terms of production techniques and environmental conditions. By conducting such studies, valuable information can be gained that would inform design

guidelines, optimize construction methodologies, and strengthen the dependability and efficiency of PLDCC as a solution for future infrastructure development. These include but are not limited to investigating PLDCC structural and bearing capacity performance, filtration capacity, contaminate and pollution removal, thermal and sound properties, air permeability, and fire resistance.

Mechanical Properties

1. The results of the RM and UC tests indicate acceptable ranges for this application for subbase materials for conventional flexible pavement systems. This conclusion was tested by comparing evaluations from mechanistic-empirical pavement design that implemented PLCC and other subbase materials. Our results show that the PLDCC's mechanical properties make it a viable alternative to granular subbases of traditional flexible pavement systems. The properties we evaluated suggest the feasibility of using PLDCC as an alternative subbase material, especially where drainage and water storage capabilities are desired in the roadway system.

2. The RM behavior of PLDCC is stress-dependent; this modulus increases significantly with increasing bulk stress. We found that when PLDCC is subjected to levels of bulk stress typically found in pavement subbases (i.e., in situ bulk stress levels greater than 100 kPa), the RM is equal to or higher than the RM of other subbase materials, such as stone dust, coarse sand, fly ash. At higher stress levels, only riverbed materials produce comparable RM values.

3. When PLDCC samples were subjected to uniaxial compression, the uniaxial compressive strength (UCS) showed smaller values than those obtained by Kevern (2018). Kevern results ranged from 201 to 252 psi for 30 and 35 psf densities, respectively. The average of our batch values ranged from 58 to 123 psi for PLDCC densities between 24 and 29 pcf. Nonetheless, this latter range is acceptable for subbase materials.

REFERENCES

ACI (2014). American Concrete Institute 523.3 R-14 Guide for Cellular Concretes above 50 lb/ft 3 (800 kg/m3), American Concrete Institute Farmington Hills, MI, USA.

Aerix (2019). Aerix Industries "2424 Tulane Project Spotlight" in https://aerixindustries.com/2424-tulane-project-spotlight/

Amran Y. H. M and Farzadnia N., Ali A. A. A. (2015). "Properties and applications of foamed concrete; a review." Construction and Building Materials 101: 990-1005.

Averyanov, S. (2018). Analysis of construction experience of using lightweight cellular concrete as a subbase material, University of Waterloo.

Bartlett, S. F., Peters, S., Arulmoli, A. (2020). Mission Rock Lightweight Cellular Concrete Technical Advisory Panel Technical Review Report. Volume 1 – Main TAP Report, Prepared for Parsons – RJSD Joint Venture Team: 121.

Bashyal, M., Mulvaney, M.J., Bean, E. Z., and Singh, H. (2019). "Design and Construction of a Constant Head Infiltrometer: SS-AGR-433/AG433, 6/2019." EDIS 2019(3).

Bennert, T. and A. Maher (2005). The development of a performance specification for granular base and subbase material, New Jersey. Dept. of Transportation.

Casagrande, A., and Shannon, W.L., (1952). Base Course Drainage for Airport Pavements. Transactions: American Society of Civil Engineering, 792-814.

Chica, L. and A. Alzate (2019). "Cellular concrete review: New trends for application in construction." Construction and Building Materials 200: 637-647.

Du, S., Shi, P., Rompaey V. (2015)., A. "Quantifying the impact of impervious surface location on flood peak discharge in urban areas." Nat Hazards 76, 1457–1471 (2015

Eskew J., Hill K., Madrid L., Sutmoller N. (2021) "Soft Soil Settlement Remediation and Roadway Elevation Increase with Permeable Low-Density Cellular Concrete (PLDCC)." Geo-Extreme 2021: 90-100.

Guan X, Wang J., Xiao F. (2021). "Sponge city strategy and application of pavement materials in sponge city," Journal of Cleaner Production, Volume 303, 20 June 2021, 127022.

Gregory J. H., Dukes M. D., Miller G. L., Jones, P. H. (2005). "Analysis of Double-Ring Infiltration Techniques and Development of a Simple Automatic Water Delivery System," Applied Turfgrass Science 2(1): 1-7.

IPCC (2022). Global Warming of 1.5° C: IPCC Special Report on Impacts of Global Warming of 1.5° C above Pre-industrial Levels in Context of Strengthening Response to Climate Change, Sustainable Development, and Efforts to Eradicate Poverty, Cambridge University Press.

Kamali M., Delkash M, Tajrishy M. (2017). "Evaluation of permeable pavement responses to urban surface runoff." Journal of Environmental Management 187: 43-53.

Kearsley, E. and P. Wainwright (2001). "Porosity and permeability of foamed concrete." Cement and concrete research 31(5): 805-812.

Kevern, J. T. (2018). "Permeable Low Density Cellular Concrete (PLDCC): Summary of Basic Research for Characterization and Performance," Aerix Industries Webinar Series, Feb. 6, 2019.

Kia A., Wong H. S., Cheeseman, C. R. (2017). "Clogging in permeable concrete: A review." Journal of Environmental Management 193: 221-233.

Kumar P., Chandra, S. and Kumar R. (2006). "Comparative study of different subbase materials." Journal of Materials in Civil Engineering 18(4): 576-580.

Mallick, R. B. and El-Korchi, T. (2008). Pavement engineering: principles and practice, CRC Press.

Marritz, L. (2013). "Pros and Cons of Using Aggregate to Store Stormwater." In https://www.deeproot.com/blog/blog-entries/the-pros-and-cons-of-using-aggregate-to-store-stormwater/

Moulton, L.K., Seals, K.R., (1979). " Determination of the In-Situ Permeability of Base and Subbase Courses." Final Report No. FHWA-RD-79-88, Department of Civil Engineering, West Virginia University, Morgantown, West Virginia.

National Academies of Sciences, E., and Medicine (2019). Framing the challenge of urban flooding in the

United States, National Academies Press.

Nguyen T. T, Ngo H. H., Guo W., Wang X.C., Ren N., Li G., Ding J., Nguyen H., Liang H. (2019). "Implementation of a specific urban water management-Sponge City." Science of the Total Environment 652: 147-162.

Raj, A., Sathyan D., Mini K. M (2019). "Physical and functional characteristics of foam concrete: A review." Construction and Building Materials 221: 787-799.

Ramamurthy K., Kunhanandan Nambiar E. K., Ranjani G. I. S. (2009). "A classification of studies on properties of foam concrete." Cement and concrete composites 31(6): 388-396.

Sansalone J., Kuang X., Ying G., Ranieri, V. (2012). "Filtration and clogging of permeable pavement loaded by urban drainage." Water research 46(20): 6763-6774.

Scholz, M. (2013). "Water quality improvement performance of geotextiles within permeable pavement systems: A critical review." Water 5(2): 462-479.

Shackel, B. (2006). Design of permeable paving subject to traffic. 8th International Conference on Concrete Block Paving.

Song, C. (2022). "Application of nature-based measures in China's sponge city initiative: Current trends and perspectives." Nature-Based Solutions 2: 100010.

Su N., Xiao F., Wang J., Amirkhanian S. (2017). "Characterizations of base and subbase layers for Mechanistic-Empirical Pavement Design." Construction and Building Materials 152: 731-745.

Sutmoller, N. and M. Gomez (2022). "An introduction to low-density cellular concrete and advanced engineered foam technology." North American Tunneling 2022 Proceedings.

Taylor S. and Halsted G. (2021) "Guide to Lightweight Cellular Concrete for Geotechnical Applications," Portland Cement Association, Washington, D. C. https://intrans.iastate.edu/app/uploads/2021/01/guide_to_LCC_for_geotech_apps.pdf

Weiss, P. T., Kayhanian M, Gulliver, J.S., Khazanovich, L. (2019). "Permeable pavement in northern North American urban areas: research review and knowledge gaps." International journal of pavement

engineering 20(2): 143-162.

Wu H., Yao C., Li C., Miao I., Zhong Y., Lu Y., Liu T. (2020). "Review of application and innovation of geotextiles in geotechnical engineering." Materials 13(7): 1774.

Xia, J., Zhang Y. Y, Xiong L, He S., Wang L, and Yu Z. (2017). "Opportunities and challenges of the Sponge City construction related to urban water issues in China." Science China Earth Sciences **60**(4): 652-658.

Zhang Z., Wu Z., Martinez M. , Gaspard K. (2008). "Pavement structures damage caused by Hurricane Katrina flooding." Journal of geotechnical and geoenvironmental engineering 134(5): 633-643.

Zahari N. M., Rahman I. A., Ahmad Mujahid Ahmad Zaidi A. M. A. (2009). Foamed concrete: potential application in thermal insulation. Malaysian Technical Universities Conference on Engineering and Technology.

APPENDIX A - LABORATORY HYDRAULIC CONDUCTIVITY TEST DATA

LABORATORY CONSTANT HEAD PERMEABILITY TEST

Specimen ID:

Y5

PVC Cell Height, h_m	154.94	mm	Height of PVC cell
PVC Cell Weight,w	235.61	g	Weight of PVC cell
PVC Internal Diameter, D	76.63	mm	Internal Diameter of PVC cell
Top Gap Height, d_T	14.19	mm	Depth of the top surface of the PLDCC specimen to the cell rim (average)
Botton Gap Height, d_B	10.34	mm	Depth of the bottom surface of the PLDCC specimen to the cell rim (average)
Equipment Weight, W_E	1546.92	g	Weight of Permeameter with monometer plugs
Equipment + Dry sample, W_{dry}	2007.88	g	Weight of Permeameter cantained in un-saturated PLDCC sample
Equipment + Sat sample, W_{sat}	2444.08	g	Weight of Permeameter cantained in saturated PLDCC sample
Assembly Excess Water, EW	48.14	g	Weight of excess water contained in the Permeameter assembly
PLDCC Sample Height, Hs	13.04	cm	
PLDCC Cross-sectional Area, A	46.12	cm^2	
Unsat. PLDCC Weight	225.25	g	
PLDCC Vol, V	601.45	cm3	
Unsat. PLDCC Unit Weight, W_{unsat}	0.37	g/cm^3	
	23.37	lb/ft^3	
Total Weight of Water, W_w	436.20	g	
Weight of Excess Cell Water, E_{wc}	113.12	g	
Weight of Saturated PLDCC, W_{sat}	500.19	g	
Saturated PLDCC Unit Weight, Uw_{sat}	**0.83**	**g/cm^3**	
	51.89	**lb/ft^3**	
Vol. Water in PLDCC	274941.603	mm^3	
Vol. PLDCC	601448.6	mm^3	
Vol. Water/Vol. PLDCC	**45.71%**		%Water contained in PLDCC when saturated (water storage capacity)

Constant Head Permeability Test

Tare Weight, W_A	213.31	g
Tare Weight, W_B	213.14	g
Tare Weight, W_C	211.98	g
Manometer H1	254.00	mm
Manometer H2	717.55	mm
Δh	46.36	cm
Vol. of Water + Tare A	610.20	cm^3
Vol. of Water + Tare B	600.78	cm^3
Vol. of Water + Tare C	592.96	cm^3
Average Flow, Q	388.50	cm^3
Length of Specimen Along Path of Flow	7.62	cm
Interval of Time, t	30.00	sec
Hydraulic Conductivity, K	**4.62E-02**	**cm/sec**

Permeability Test Report of Specimen Y5

LABORATORY CONSTANT HEAD PERMEABILITY TEST

Specimen ID:

Y7

PVC Cell Height, h_m	152.19	mm	Height of PVC cell
PVC Cell Weight,w	231.15	g	Weight of PVC cell
PVC Internal Diameter, D	76.70	mm	Internal Diameter of PVC cell
Top Gap Height, d_T	14.89	mm	Depth of the top surface of the PLDCC specimen to the cell rim (average)
Botton Gap Height, d_B	11.48	mm	Depth of the bottom surface of the PLDCC specimen to the cell rim (average)
Equipment Weight, W_E	1547.20	g	Weight of Permeameter with monometer plugs
Equipment + Dry sample, W_{dry}	2000.15	g	Weight of Permeameter cantained in un-saturated PLDCC sample
Equipment + Sat sample, W_{sat}	2426.79	g	Weight of Permeameter cantained in saturated PLDCC sample
Assembly Excess Water, EW	48.14	g	Weight of excess water contained in the Permeameter assembly
PLDCC Sample Height, Hs	12.58	cm	
PLDCC Cross-sectional Area, A	46.21	cm^2	
Unsat. PLDCC Weight	221.83	g	
PLDCC Vol, V	581.39	cm3	
Unsat. PLDCC Unit Weight, W_{unsat}	0.38	g/cm^3	
	23.81	lb/ft^3	
Total Weight of Water, W_w	426.64	g	
Weight of Excess Cell Water, E_{wc}	121.88	g	
Weight of Saturated PLDCC, W_{sat}	478.45	g	
Saturated PLDCC Unit Weight, Uw_{si}	**0.82**	**g/cm^3**	
	51.35	**lb/ft^3**	
Vol. Water in PLDCC	256624.9503	mm^3	
Vol. PLDCC	581393.5	mm^3	
Vol. Water/Vol. PLDCC	**44.14%**		%Water contained in PLDCC when saturated (water storage capacity)

Constant Head Permeability Test

Tare Weight, W_A	213.31	g
Tare Weight, W_B	213.14	g
Tare Weight, W_C	211.98	g
Manometer H1	292.10	mm
Manometer H2	762.00	mm
Δh	46.99	cm
Vol. of Water + Tare A	573.02	cm^3
Vol. of Water + Tare B	564.27	cm^3
Vol. of Water + Tare C	555.53	cm^3
Average Flow, Q	351.46	cm^3
Length of Specimen Along Path of Flow	7.62	cm
Interval of Time, t	30.00	sec
Hydraulic Conductivity, K	**4.11E-02**	**cm/sec**

Permeability Test Report of Specimen Y7

LABORATORY CONSTANT HEAD PERMEABILITY TEST

Specimen ID:

Y8

PVC Cell Height, h_m	155.27	mm	Height of PVC cell
PVC Cell Weight,w	235.55	g	Weight of PVC cell
PVC Internal Diameter, D	76.30	mm	Internal Diameter of PVC cell
Top Gap Height, d_T	16.79	mm	Depth of the top surface of the PLDCC specimen to the cell rim (average)
Botton Gap Height, d_B	10.44	mm	Depth of the bottom surface of the PLDCC specimen to the cell rim (average)
Equipment Weight, W_E	1548.17	g	Weight of Permeameter with monometer plugs
Equipment + Dry sample, W_{dry}	2008.50	g	Weight of Permeameter cantained in un-saturated PLDCC sample
Equipment + Sat sample, W_{sat}	2442.21	g	Weight of Permeameter cantained in saturated PLDCC sample
Assembly Excess Water, EW	48.14	g	Weight of excess water contained in the Permeameter assembly
PLDCC Sample Height, Hs	12.80	cm	
PLDCC Cross-sectional Area, A	45.72	cm^2	
Unsat. PLDCC Weight	224.97	g	
PLDCC Vol, V	585.33	cm3	
Unsat. PLDCC Unit Weight, W_{unsat}	0.38	g/cm^3	
	23.98	lb/ft^3	
Total Weight of Water, W_w	433.71	g	
Weight of Excess Cell Water, E_{wc}	124.52	g	
Weight of Saturated PLDCC, W_{sat}	486.02	g	
Saturated PLDCC Unit Weight, Uw_{si}	**0.83**	**g/cm^3**	
	51.81	**lb/ft^3**	
Vol. Water in PLDCC	261052.1	mm^3	
Vol. PLDCC	585325.7	mm^3	
Vol. Water/Vol. PLDCC	**44.60%**		%Water contained in PLDCC when saturated (water storage capacity)

Constant Head Permeability Test

Tare Weight, W_A	213.31	g
Tare Weight, W_B	213.14	g
Tare Weight, W_C	211.98	g
Manometer H1	273.05	mm
Manometer H2	666.75	mm
Δh	39.37	cm
Vol. of Water + Tare A	563.92	cm^3
Vol. of Water + Tare B	553.77	cm^3
Vol. of Water + Tare C	542.21	cm^3
Average Flow, Q	340.49	cm^3
Length of Specimen Along Path of Flow	7.62	cm
Interval of Time, t	30.00	sec
Hydraulic Conductivity, K	**4.80E-02**	**cm/sec**

Permeability Test Report of Specimen Y8

LABORATORY CONSTANT HEAD PERMEABILITY TEST

Specimen ID:

Y10

PVC Cell Height, h_m	153.94	mm	Height of PVC cell
PVC Cell Weight,w	234.09	g	Weight of PVC cell
PVC Internal Diameter, D	76.69	mm	Internal Diameter of PVC cell
Top Gap Height, d_T	11.20	mm	Depth of the top surface of the PLDCC specimen to the cell rim (average)
Botton Gap Height, d_B	12.83	mm	Depth of the bottom surface of the PLDCC specimen to the cell rim (average)
Equipment Weight, W_E	1548.17	g	Weight of Permeameter with monometer plugs
Equipment + Dry sample, W_{dry}	2010.59	g	Weight of Permeameter cantained in un-saturated PLDCC sample
Equipment + Sat sample, W_{sat}	2425.82	g	Weight of Permeameter cantained in saturated PLDCC sample
Assembly Excess Water, EW	48.14	g	Weight of excess water contained in the Permeameter assembly
PLDCC Sample Height, Hs	12.99	cm	
PLDCC Cross-sectional Area, A	46.19	cm^2	
Unsat. PLDCC Weight	227.74	g	
PLDCC Vol, V	600.11	cm3	
Unsat. PLDCC Unit Weight, W_{unsat}	0.38	g/cm^3	
	23.68	lb/ft^3	
Total Weight of Water, W_w	415.23	g	
Weight of Excess Cell Water, E_{wc}	110.97	g	
Weight of Saturated PLDCC, W_{sat}	483.87	g	
Saturated PLDCC Unit Weight, Uw_s	**0.81**	**g/cm^3**	
	50.31	**lb/ft^3**	
Vol. Water in PLDCC	256125.3	mm^3	
Vol. PLDCC	600108.1	mm^3	
Vol. Water/Vol. PLDCC	**42.68%**		%Water contained in PLDCC when saturated (water storage capacity)

Constant Head Permeability Test

Tare Weight, W_A	213.31	g
Tare Weight, W_B	213.14	g
Tare Weight, W_C	211.98	g
Manometer H1	292.10	mm
Manometer H2	723.90	mm
Δh	43.18	cm
Vol. of Water + Tare A	540.26	cm^3
Vol. of Water + Tare B	532.18	cm^3
Vol. of Water + Tare C	530.46	cm^3
Average Flow, Q	321.49	cm^3
Length of Specimen Along Path of Flow	7.62	cm
Interval of Time, t	30.00	sec
Hydraulic Conductivity, K	**4.09E-02**	**cm/sec**

Permeability Test Report of Specimen Y10

LABORATORY CONSTANT HEAD PERMEABILITY TEST

Specimen ID:

Y14

PVC Cell Height, h_m	154.53	mm	Height of PVC cell
PVC Cell Weight,w	234.71	g	Weight of PVC cell
PVC Internal Diameter, D	76.55	mm	Internal Diameter of PVC cell
Top Gap Height, d_T	18.39	mm	Depth of the top surface of the PLDCC specimen to the cell rim (average)
Botton Gap Height, d_B	16.05	mm	Depth of the bottom surface of the PLDCC specimen to the cell rim (average)
Equipment Weight, W_E	1548.17	g	Weight of Permeameter with monometer plugs
Equipment + Dry sample, W_{dry}	2003.52	g	Weight of Permeameter cantained in un-saturated PLDCC sample
Equipment + Sat sample, W_{sat}	2458.92	g	Weight of Permeameter cantained in saturated PLDCC sample
Assembly Excess Water, EW	48.14	g	Weight of excess water contained in the Permeameter assembly
PLDCC Sample Height, Hs	12.01	cm	
PLDCC Cross-sectional Area, A	46.02	cm^2	
Unsat. PLDCC Weight	230.50	g	
PLDCC Vol, V	552.70	cm3	
Unsat. PLDCC Unit Weight, W_{unsat}	0.42	g/cm^3	
	26.02	lb/ft^3	
Total Weight of Water, W_w	455.40	g	
Weight of Excess Cell Water, E_{wc}	158.51	g	
Weight of Saturated PLDCC, W_{sat}	479.26	g	
Saturated PLDCC Unit Weight, Uw_{si}	**0.87**	**g/cm^3**	
	54.11	**lb/ft^3**	
Vol. Water in PLDCC	248756.6	mm^3	
Vol. PLDCC	552699.0	mm^3	
Vol. Water/Vol. PLDCC	**45.01%**		%Water contained in PLDCC when saturated (water storage capacity)

Constant Head Permeability Test

Tare Weight, W_A	213.31	g
Tare Weight, W_B	213.14	g
Tare Weight, W_C	211.98	g
Manometer H1	254.00	mm
Manometer H2	781.05	mm
Δh	52.71	cm
Vol. of Water + Tare A	331.36	cm^3
Vol. of Water + Tare B	319.08	cm^3
Vol. of Water + Tare C	311.56	cm^3
Average Flow, Q	107.86	cm^3
Length of Specimen Along Path of Flow	7.62	cm
Interval of Time, t	30.00	sec
Hydraulic Conductivity, K	**1.13E-02**	**cm/sec**

Permeability Test Report of Specimen Y14

LABORATORY CONSTANT HEAD PERMEABILITY TEST

Specimen ID:

Y16

PVC Cell Height, h_m	152.48	mm	Height of PVC cell
PVC Cell Weight,w	232.38	g	Weight of PVC cell
PVC Internal Diameter, D	76.58	mm	Internal Diameter of PVC cell
Top Gap Height, d_T	20.29	mm	Depth of the top surface of the PLDCC specimen to the cell rim (average)
Botton Gap Height, d_B	14.79	mm	Depth of the bottom surface of the PLDCC specimen to the cell rim (average)
Equipment Weight, W_E	1548.17	g	Weight of Permeameter with monometer plugs
Equipment + Dry sample, W_{dry}	2006.85	g	Weight of Permeameter cantained in un-saturated PLDCC sample
Equipment + Sat sample, W_{sat}	2449.32	g	Weight of Permeameter cantained in saturated PLDCC sample
Assembly Excess Water, EW	48.14	g	Weight of excess water contained in the Permeameter assembly
PLDCC Sample Height, Hs	11.74	cm	
PLDCC Cross-sectional Area, A	46.06	cm^2	
Unsat. PLDCC Weight	226.00	g	
PLDCC Vol, V	540.76	cm3	
Unsat. PLDCC Unit Weight, W_{unsat}	0.42	g/cm^3	
	26.08	lb/ft^3	
Total Weight of Water, W_w	442.47	g	
Weight of Excess Cell Water, E_{wc}	161.58	g	
Weight of Saturated PLDCC, W_{sat}	458.75	g	
Saturated PLDCC Unit Weight, Uw_s	**0.85**	**g/cm^3**	
	52.94	**lb/ft^3**	
Vol. Water in PLDCC	232748.2	mm^3	
Vol. PLDCC	540763.5	mm^3	
Vol. Water/Vol. PLDCC	**43.04%**		%Water contained in PLDCC when saturated (water storage capacity)

Constant Head Permeability Test

Tare Weight, W_A	213.31	g
Tare Weight, W_B	213.14	g
Tare Weight, W_C	211.98	g
Manometer H1	215.90	mm
Manometer H2	885.19	mm
Δh	66.93	cm
Vol. of Water + Tare A	325.53	cm^3
Vol. of Water + Tare B	320.26	cm^3
Vol. of Water + Tare C	314.34	cm^3
Average Flow, Q	107.23	cm^3
Length of Specimen Along Path of Flow	7.62	cm
Interval of Time, t	30.00	sec
Hydraulic Conductivity, K	**8.84E-03**	**cm/sec**

Permeability Test Report of Specimen Y16

LABORATORY CONSTANT HEAD PERMEABILITY TEST

Specimen ID:

Y17

PVC Cell Height, h_m	154.20	mm	Height of PVC cell
PVC Cell Weight,w	234.67	g	Weight of PVC cell
PVC Internal Diameter, D	76.60	mm	Internal Diameter of PVC cell
Top Gap Height, d_T	20.93	mm	Depth of the top surface of the PLDCC specimen to the cell rim (average)
Botton Gap Height, d_B	18.24	mm	Depth of the bottom surface of the PLDCC specimen to the cell rim (average)
Equipment Weight, W_E	1548.17	g	Weight of Permeameter with monometer plugs
Equipment + Dry sample, W_{dry}	2002.19	g	Weight of Permeameter cantained in un-saturated PLDCC sample
Equipment + Sat sample, W_{sat}	2471.84	g	Weight of Permeameter cantained in saturated PLDCC sample
Assembly Excess Water, EW	48.14	g	Weight of excess water contained in the Permeameter assembly
PLDCC Sample Height, Hs	11.50	cm	
PLDCC Cross-sectional Area, A	46.08	cm^2	
Unsat. PLDCC Weight	219.75	g	
PLDCC Vol, V	530.09	cm3	
Unsat. PLDCC Unit Weight, W_{unsat}	0.41	g/cm^3	
	25.87	lb/ft^3	
Total Weight of Water, W_w	469.65	g	
Weight of Excess Cell Water, E_{wc}	180.51	g	
Weight of Saturated PLDCC, W_{sat}	460.75	g	
Saturated PLDCC Unit Weight, Uw_s	**0.87**	**g/cm^3**	
	54.24	**lb/ft^3**	
Vol. Water in PLDCC	241002.3	mm^3	
Vol. PLDCC	530088.1	mm^3	
Vol. Water/Vol. PLDCC	**45.46%**		%Water contained in PLDCC when saturated (water storage capacity)

Constant Head Permeability Test

Tare Weight, W_A	213.31	g
Tare Weight, W_B	213.14	g
Tare Weight, W_C	211.98	g
Manometer H1	180.98	mm
Manometer H2	762.00	mm
Δh	58.10	cm
Vol. of Water + Tare A	397.74	cm^3
Vol. of Water + Tare B	391.99	cm^3
Vol. of Water + Tare C	383.88	cm^3
Average Flow, Q	178.39	cm^3
Length of Specimen Along Path of Flow	7.62	cm
Interval of Time, t	30.00	sec
Hydraulic Conductivity, K	**1.69E-02**	**cm/sec**

Permeability Test Report of Specimen Y17

LABORATORY CONSTANT HEAD PERMEABILITY TEST

Specimen ID:

Y18

PVC Cell Height, h_m	153.77	mm	Height of PVC cell
PVC Cell Weight,w	233.98	g	Weight of PVC cell
PVC Internal Diameter, D	76.78	mm	Internal Diameter of PVC cell
Top Gap Height, d_T	22.59	mm	Depth of the top surface of the PLDCC specimen to the cell rim (average)
Botton Gap Height, d_B	17.76	mm	Depth of the bottom surface of the PLDCC specimen to the cell rim (average)
Equipment Weight, W_E	1546.64	g	Weight of Permeameter with monometer plugs
Equipment + Dry sample, W_{dry}	1999.76	g	Weight of Permeameter cantained in un-saturated PLDCC sample
Equipment + Sat sample, W_{sat}	2467.21	g	Weight of Permeameter cantained in saturated PLDCC sample
Assembly Excess Water, EW	48.14	g	Weight of excess water contained in the Permeameter assembly
PLDCC Sample Height, Hs	11.34	cm	
PLDCC Cross-sectional Area, A	46.31	cm^2	
Unsat. PLDCC Weight	219.03	g	
PLDCC Vol, V	525.21	cm3	
Unsat. PLDCC Unit Weight, W_{unsat}	0.42	g/cm^3	
	26.02	lb/ft^3	
Total Weight of Water, W_w	467.45	g	
Weight of Excess Cell Water, E_{wc}	186.84	g	
Weight of Saturated PLDCC, W_{sat}	451.50	g	
Saturated PLDCC Unit Weight, Uw_{si}	**0.86**	**g/cm^3**	
	53.64	**lb/ft^3**	
Vol. Water in PLDCC	232471.6	mm^3	
Vol. PLDCC	525208.0	mm^3	
Vol. Water/Vol. PLDCC	**44.26%**		%Water contained in PLDCC when saturated (water storage capacity)

Constant Head Permeability Test

Tare Weight, W_A	213.31	g
Tare Weight, W_B	213.14	g
Tare Weight, W_C	211.98	g
Manometer H1	298.45	mm
Manometer H2	908.81	mm
Δh	61.04	cm
Vol. of Water + Tare A	356.71	cm^3
Vol. of Water + Tare B	353.08	cm^3
Vol. of Water + Tare C	345.87	cm^3
Average Flow, Q	139.08	cm^3
Length of Specimen Along Path of Flow	7.62	cm
Interval of Time, t	30.00	sec
Hydraulic Conductivity, K	**1.25E-02**	**cm/sec**

Permeability Test Report of Specimen Y18

LABORATORY CONSTANT HEAD PERMEABILITY TEST
Specimen ID:
TY-5

PVC Cell Height, h_m	150.50	mm	Height of PVC cell
PVC Cell Weight,w	221.05	g	Weight of PVC cell
PVC Internal Diameter, D	77.29	mm	Internal Diameter of PVC cell
Top Gap Height, d_T	6.93	mm	Depth of the top surface of the PLDCC specimen to the cell rim (average)
Botton Gap Height, d_B	21.11	mm	Depth of the bottom surface of the PLDCC specimen to the cell rim (average)
Equipment Weight, W_E	1545.90	g	Weight of Permeameter with monometer plugs
Equipment + Dry sample, W_{dry}	1972.70	g	Weight of Permeameter cantained in un-saturated PLDCC sample
Equipment + Sat sample, W_{sat}	2415.80	g	Weight of Permeameter cantained in saturated PLDCC sample
Assembly Excess Water, EW	48.14	g	Weight of excess water contained in the Permeameter assembly
PLDCC Sample Height, Hs	12.25	cm	
PLDCC Cross-sectional Area, A	46.91	cm^2	
Unsat. PLDCC Weight	206.25	g	
PLDCC Vol, V	574.47	cm3	
Unsat. PLDCC Unit Weight, W_{unsat}	0.36	g/cm^3	
	22.40	lb/ft^3	
Total Weight of Water, W_w	443.10	g	
Weight of Excess Cell Water, E_{wc}	131.54	g	
Weight of Saturated PLDCC, W_{sat}	469.67	g	
Saturated PLDCC Unit Weight, Uw_{sa}	**0.82**	**g/cm^3**	
	51.02	**lb/ft^3**	
Vol. Water in PLDCC	263424.5274	mm^3	
Vol. PLDCC	574473.9	mm^3	
Vol. Water/Vol. PLDCC	**45.85%**		%Water contained in PLDCC when saturated (water storage capacity)

Constant Head Permeability Test

Tare Weight, W_A	104.10	g
Tare Weight, W_B	95.50	g
Tare Weight, W_C	102.90	g
Manometer H1	530.00	mm
Manometer H2	1420.00	mm
Δh	89.00	cm
Vol. of Water + Tare A	154.30	cm^3
Vol. of Water + Tare B	145.10	cm^3
Vol. of Water + Tare C	152.10	cm^3
Average Flow, Q	49.67	cm^3
Length of Specimen Along Path (	7.62	cm
Interval of Time, t	30.00	sec
Hydraulic Conductivity, K	**3.02E-03**	**cm/sec**

Permeability Test Report of Specimen TY-5

LABORATORY CONSTANT HEAD PERMEABILITY TEST
Specimen ID:
TY-6

PVC Cell Height, h_m	149.28	mm	Height of PVC cell
PVC Cell Weight,w	219.49	g	Weight of PVC cell
PVC Internal Diameter, D	77.27	mm	Internal Diameter of PVC cell
Top Gap Height, d_T	9.71	mm	Depth of the top surface of the PLDCC specimen to the cell rim (average)
Botton Gap Height, d_B	18.01	mm	Depth of the bottom surface of the PLDCC specimen to the cell rim (average)
Equipment Weight, W_E	1557.80	g	Weight of Permeameter with monometer plugs
Equipment + Dry sample, W_{dry}	1984.50	g	Weight of Permeameter cantained in un-saturated PLDCC sample
Equipment + Sat sample, W_{sat}	2422.40	g	Weight of Permeameter cantained in saturated PLDCC sample
Assembly Excess Water, EW	48.14	g	Weight of excess water contained in the Permeameter assembly
PLDCC Sample Height, Hs	12.16	cm	
PLDCC Cross-sectional Area, A	46.89	cm^2	
Unsat. PLDCC Weight	207.91	g	
PLDCC Vol, V	570.03	cm3	
Unsat. PLDCC Unit Weight, W_{unsat}	0.36	g/cm^3	
	22.76	lb/ft^3	
Total Weight of Water, W_w	437.90	g	
Weight of Excess Cell Water, E_{wc}	129.95	g	
Weight of Saturated PLDCC, W_{sat}	467.72	g	
Saturated PLDCC Unit Weight, Uw_{sat}	**0.82**	**g/cm^3**	
	51.20	**lb/ft^3**	
Vol. Water in PLDCC	259810.67	mm^3	
Vol. PLDCC	570025.1	mm^3	
Vol. Water/Vol. PLDCC	**45.58%**		%Water contained in PLDCC when saturated (water storage capacity)

Constant Head Permeability Test

Tare Weight, W_A	104.10	g
Tare Weight, W_B	95.50	g
Tare Weight, W_C	102.90	g
Manometer H1	520.00	mm
Manometer H2	1220.00	mm
Δh	70.00	cm
Vol. of Water + Tare A	217.90	cm^3
Vol. of Water + Tare B	206.30	cm^3
Vol. of Water + Tare C	210.50	cm^3
Average Flow, Q	110.73	cm^3
Length of Specimen Along Path (	7.62	cm
Interval of Time, t	30.00	sec
Hydraulic Conductivity, K	**8.57E-03**	**cm/sec**

Permeability Test Report of Specimen TY-6

LABORATORY CONSTANT HEAD PERMEABILITY TEST

Specimen ID:

TY-7

PVC Cell Height, h_m	149.61	mm	Height of PVC cell
PVC Cell Weight,w	219.66	g	Weight of PVC cell
PVC Internal Diameter, D	77.39	mm	Internal Diameter of PVC cell
Top Gap Height, d_T	9.55	mm	Depth of the top surface of the PLDCC specimen to the cell rim (average)
Botton Gap Height, d_B	13.34	mm	Depth of the bottom surface of the PLDCC specimen to the cell rim (average)
Equipment Weight, W_E	1542.39	g	Weight of Permeameter with monometer plugs
Equipment + Dry sample, W_{dry}	1982.49	g	Weight of Permeameter cantained in un-saturated PLDCC sample
Equipment + Sat sample, W_{sat}	2390.88	g	Weight of Permeameter cantained in saturated PLDCC sample
Assembly Excess Water, EW	48.14	g	Weight of excess water contained in the Permeameter assembly
PLDCC Sample Height, Hs	12.67	cm	
PLDCC Cross-sectional Area, A	47.04	cm^2	
Unsat. PLDCC Weight	218.44	g	
PLDCC Vol, V	596.13	cm3	
Unsat. PLDCC Unit Weight, W_{unsat}	0.37	g/cm^3	
	22.87	lb/ft^3	
Total Weight of Water, W_w	408.39	g	
Weight of Excess Cell Water, E_{wc}	107.68	g	
Weight of Saturated PLDCC, W_{sat}	471.02	g	
Saturated PLDCC Unit Weight, Uw_{sat}	**0.79**	**g/cm^3**	
	49.30	**lb/ft^3**	
Vol. Water in PLDCC	252576.98	mm^3	
Vol. PLDCC	596127.8	mm^3	
Vol. Water/Vol. PLDCC	**42.37%**		%Water contained in PLDCC when saturated (water storage capacity)

Constant Head Permeability Test

Tare Weight, W_A	0.00	g
Tare Weight, W_B	0.00	g
Tare Weight, W_C	0.00	g
Manometer H1	20.00	mm
Manometer H2	795.00	mm
Δh	77.50	cm
Vol. of Water + Tare A	221.70	cm^3
Vol. of Water + Tare B	208.80	cm^3
Vol. of Water + Tare C	212.30	cm^3
Average Flow, Q	214.27	cm^3
Length of Specimen Along Pa	7.62	cm
Interval of Time, t	60.00	sec
Hydraulic Conductivity, K	**7.46E-03**	**cm/sec**

Permeability Test Report of Specimen TY-7

LABORATORY CONSTANT HEAD PERMEABILITY TEST

Specimen ID:

TY-8

PVC Cell Height, h_m	150.23	mm	Height of PVC cell
PVC Cell Weight,w	220.46	g	Weight of PVC cell
PVC Internal Diameter, D	77.38	mm	Internal Diameter of PVC cell
Top Gap Height, d_T	12.76	mm	Depth of the top surface of the PLDCC specimen to the cell rim (average)
Botton Gap Height, d_B	15.11	mm	Depth of the bottom surface of the PLDCC specimen to the cell rim (average)
Equipment Weight, W_E	1545.90	g	Weight of Permeameter with monometer plugs
Equipment + Dry sample, W_{dry}	1960.30	g	Weight of Permeameter cantained in un-saturated PLDCC sample
Equipment + Sat sample, W_{sat}	2408.00	g	Weight of Permeameter cantained in saturated PLDCC sample
Assembly Excess Water, EW	48.14	g	Weight of excess water contained in the Permeameter assembly
PLDCC Sample Height, Hs	12.24	cm	
PLDCC Cross-sectional Area, A	47.03	cm^2	
Unsat. PLDCC Weight	193.94	g	
PLDCC Vol, V	575.47	cm3	
Unsat. PLDCC Unit Weight, W_{unsat}	0.34	g/cm^3	
	21.03	lb/ft^3	
Total Weight of Water, W_w	447.70	g	
Weight of Excess Cell Water, E_{wc}	131.06	g	
Weight of Saturated PLDCC, W_{sat}	462.44	g	
Saturated PLDCC Unit Weight, Uw_{sat}	**0.80**	**g/cm^3**	
	50.14	**lb/ft^3**	
Vol. Water in PLDCC	268504.81	mm^3	
Vol. PLDCC	575471.1	mm^3	
Vol. Water/Vol. PLDCC	**46.66%**		%Water contained in PLDCC when saturated (water storage capacity)

Constant Head Permeability Test

Tare Weight, W_A	104.10	g
Tare Weight, W_B	95.70	g
Tare Weight, W_C	103.00	g
Manometer H1	310.00	mm
Manometer H2	975.00	mm
Δh	66.50	cm
Vol. of Water + Tare A	156.70	cm^3
Vol. of Water + Tare B	145.80	cm^3
Vol. of Water + Tare C	150.40	cm^3
Average Flow, Q	50.03	cm^3
Length of Specimen Along Path (	7.62	cm
Interval of Time, t	30.00	sec
Hydraulic Conductivity, K	**4.06E-03**	**cm/sec**

Permeability Test Report of Specimen TY-8

LABORATORY CONSTANT HEAD PERMEABILITY TEST

Specimen ID:

TY-9

PVC Cell Height, h_m	150.13	mm	Height of PVC cell
PVC Cell Weight,w	220.06	g	Weight of PVC cell
PVC Internal Diameter, D	77.27	mm	Internal Diameter of PVC cell
Top Gap Height, d_T	12.16	mm	Depth of the top surface of the PLDCC specimen to the cell rim (average)
Botton Gap Height, d_B	12.16	mm	Depth of the bottom surface of the PLDCC specimen to the cell rim (average)
Equipment Weight, W_E	1546.60	g	Weight of Permeameter with monometer plugs
Equipment + Dry sample, W_{dry}	1976.10	g	Weight of Permeameter cantained in un-saturated PLDCC sample
Equipment + Sat sample, W_{sat}	2402.00	g	Weight of Permeameter cantained in saturated PLDCC sample
Assembly Excess Water, EW	48.14	g	Weight of excess water contained in the Permeameter assembly
PLDCC Sample Height, Hs	12.58	cm	
PLDCC Cross-sectional Area, A	46.90	cm^2	
Unsat. PLDCC Weight	210.94	g	
PLDCC Vol, V	590.00	cm3	
Unsat. PLDCC Unit Weight, W_{unsat}	0.36	g/cm^3	
	22.31	lb/ft^3	
Total Weight of Water, W_w	425.90	g	
Weight of Excess Cell Water, E_{wc}	114.05	g	
Weight of Saturated PLDCC, W_{sat}	474.65	g	
Saturated PLDCC Unit Weight, Uw_{sat}	**0.80**	**g/cm^3**	
	50.20	**lb/ft^3**	
Vol. Water in PLDCC	263708.31	mm^3	
Vol. PLDCC	589998.5	mm^3	
Vol. Water/Vol. PLDCC	**44.70%**		%Water contained in PLDCC when saturated (water storage capacity)

Constant Head Permeability Test

Tare Weight, W_A	0.00	g
Tare Weight, W_B	0.00	g
Tare Weight, W_C	0.00	g
Manometer H1	550.00	mm
Manometer H2	900.00	mm
Δh	35.00	cm
Vol. of Water + Tare A	232.50	cm^3
Vol. of Water + Tare B	232.31	cm^3
Vol. of Water + Tare C	232.31	cm^3
Average Flow, Q	232.37	cm^3
Length of Specimen Along Pa	7.62	cm
Interval of Time, t	30.00	sec
Hydraulic Conductivity, K	**3.60E-02**	**cm/sec**

Permeability Test Report of Specimen TY-9

LABORATORY CONSTANT HEAD PERMEABILITY TEST

Specimen ID:

TY-10

PVC Cell Height, h_m	149.61	mm	Height of PVC cell
PVC Cell Weight,w	219.79	g	Weight of PVC cell
PVC Internal Diameter, D	77.47	mm	Internal Diameter of PVC cell
Top Gap Height, d_T	12.48	mm	Depth of the top surface of the PLDCC specimen to the cell rim (average)
Botton Gap Height, d_B	16.53	mm	Depth of the bottom surface of the PLDCC specimen to the cell rim (average)
Equipment Weight, W_E	1555.50	g	Weight of Permeameter with monometer plugs
Equipment + Dry sample, W_{dry}	1983.50	g	Weight of Permeameter cantained in un-saturated PLDCC sample
Equipment + Sat sample, W_{sat}	2379.00	g	Weight of Permeameter cantained in saturated PLDCC sample
Assembly Excess Water, EW	48.14	g	Weight of excess water contained in the Permeameter assembly
PLDCC Sample Height, Hs	12.06	cm	
PLDCC Cross-sectional Area, A	47.14	cm^2	
Unsat. PLDCC Weight	206.51	g	
PLDCC Vol, V	568.46	cm3	
Unsat. PLDCC Unit Weight, W_{unsat}	0.36	g/cm^3	
	22.67	lb/ft^3	
Total Weight of Water, W_w	395.50	g	
Weight of Excess Cell Water, E_{wc}	136.73	g	
Weight of Saturated PLDCC, W_{sat}	417.14	g	
Saturated PLDCC Unit Weight, Uw_{sat}	**0.73**	**g/cm^3**	
	45.79	**lb/ft^3**	
Vol. Water in PLDCC	210632.94	mm^3	
Vol. PLDCC	568460.4	mm^3	
Vol. Water/Vol. PLDCC	**37.05%**		%Water contained in PLDCC when saturated (water storage capacity)

Constant Head Permeability Test

Tare Weight, W_A	0.00	g
Tare Weight, W_B	0.00	g
Tare Weight, W_C	0.00	g
Manometer H1	0.00	mm
Manometer H2	532.00	mm
Δh	53.20	cm
Vol. of Water + Tare A	346.70	cm^3
Vol. of Water + Tare B	340.30	cm^3
Vol. of Water + Tare C	333.00	cm^3
Average Flow, Q	340.00	cm^3
Length of Specimen Along Pa	7.62	cm
Interval of Time, t	60.00	sec
Hydraulic Conductivity, K	**1.72E-02**	**cm/sec**

Permeability Test Report of Specimen TY-10

LABORATORY CONSTANT HEAD PERMEABILITY TEST

Specimen ID:

TY-11

PVC Cell Height, h_m	149.32	mm	Height of PVC cell
PVC Cell Weight,w	219.39	g	Weight of PVC cell
PVC Internal Diameter, D	77.37	mm	Internal Diameter of PVC cell
Top Gap Height, d_T	9.79	mm	Depth of the top surface of the PLDCC specimen to the cell rim (average)
Botton Gap Height, d_B	19.41	mm	Depth of the bottom surface of the PLDCC specimen to the cell rim (average)
Equipment Weight, W_E	1557.30	g	Weight of Permeameter with monometer plugs
Equipment + Dry sample, W_{dry}	1981.30	g	Weight of Permeameter cantained in un-saturated PLDCC sample
Equipment + Sat sample, W_{sat}	2391.90	g	Weight of Permeameter cantained in saturated PLDCC sample
Assembly Excess Water, EW	48.14	g	Weight of excess water contained in the Permeameter assembly
PLDCC Sample Height, Hs	12.01	cm	
PLDCC Cross-sectional Area, A	47.02	cm^2	
Unsat. PLDCC Weight	204.51	g	
PLDCC Vol, V	564.81	cm3	
Unsat. PLDCC Unit Weight, W_{unsat}	0.36	g/cm^3	
	22.59	lb/ft^3	
Total Weight of Water, W_w	410.60	g	
Weight of Excess Cell Water, E_{wc}	137.30	g	
Weight of Saturated PLDCC, W_{sat}	429.67	g	
Saturated PLDCC Unit Weight, Uw_{sat}	**0.76**	**g/cm^3**	
	47.47	**lb/ft^3**	
Vol. Water in PLDCC	225162.13	mm^3	
Vol. PLDCC	564812.9	mm^3	
Vol. Water/Vol. PLDCC	**39.86%**		%Water contained in PLDCC when saturated (water storage capacity)

Constant Head Permeability Test

Tare Weight, W_A	0.00	g
Tare Weight, W_B	0.00	g
Tare Weight, W_C	0.00	g
Manometer H1	350.00	mm
Manometer H2	980.00	mm
Δh	63.00	cm
Vol. of Water + Tare A	180.41	cm^3
Vol. of Water + Tare B	153.61	cm^3
Vol. of Water + Tare C	159.80	cm^3
Average Flow, Q	164.23	cm^3
Length of Specimen Along Pa	7.62	cm
Interval of Time, t	30.00	sec
Hydraulic Conductivity, K	**1.41E-02**	**cm/sec**

Permeability Test Report of Specimen TY-11

LABORATORY CONSTANT HEAD PERMEABILITY TEST

Specimen ID:

TY-12

PVC Cell Height, h_m	149.49	mm	Height of PVC cell
PVC Cell Weight,w	219.93	g	Weight of PVC cell
PVC Internal Diameter, D	77.13	mm	Internal Diameter of PVC cell
Top Gap Height, d_T	11.98	mm	Depth of the top surface of the PLDCC specimen to the cell rim (average)
Botton Gap Height, d_B	19.01	mm	Depth of the bottom surface of the PLDCC specimen to the cell rim (average)
Equipment Weight, W_E	1547.80	g	Weight of Permeameter with monometer plugs
Equipment + Dry sample, W_{dry}	1953.30	g	Weight of Permeameter cantained in un-saturated PLDCC sample
Equipment + Sat sample, W_{sat}	2417.00	g	Weight of Permeameter cantained in saturated PLDCC sample
Assembly Excess Water, EW	48.14	g	Weight of excess water contained in the Permeameter assembly
PLDCC Sample Height, Hs	11.85	cm	
PLDCC Cross-sectional Area, A	46.73	cm^2	
Unsat. PLDCC Weight	186.67	g	
PLDCC Vol, V	553.70	cm3	
Unsat. PLDCC Unit Weight, W_{unsat}	0.34	g/cm^3	
	21.04	lb/ft^3	
Total Weight of Water, W_w	463.70	g	
Weight of Excess Cell Water, E_{wc}	144.85	g	
Weight of Saturated PLDCC, W_{sat}	457.39	g	
Saturated PLDCC Unit Weight, Uw_{sat}	**0.83**	**g/cm^3**	
	51.55	**lb/ft^3**	
Vol. Water in PLDCC	270716.5362	mm^3	
Vol. PLDCC	553696.1	mm^3	
Vol. Water/Vol. PLDCC	**48.89%**		%Water contained in PLDCC when saturated (water storage capacity)

Constant Head Permeability Test

Tare Weight, W_A	104.10	g
Tare Weight, W_B	95.70	g
Tare Weight, W_C	103.00	g
Manometer H1	460.00	mm
Manometer H2	1260.00	mm
Δh	80.00	cm
Vol. of Water + Tare A	292.70	cm^3
Vol. of Water + Tare B	280.40	cm^3
Vol. of Water + Tare C	282.80	cm^3
Average Flow, Q	184.37	cm^3
Length of Specimen Along Path (	7.62	cm
Interval of Time, t	30.00	sec
Hydraulic Conductivity, K	**1.25E-02**	**cm/sec**

Permeability Test Report of Specimen TY-12

LABORATORY CONSTANT HEAD PERMEABILITY TEST

Specimen ID:

TY-13

PVC Cell Height, h_m	150.16	mm	Height of PVC cell
PVC Cell Weight,w	220.32	g	Weight of PVC cell
PVC Internal Diameter, D	77.28	mm	Internal Diameter of PVC cell
Top Gap Height, d_T	10.12	mm	Depth of the top surface of the PLDCC specimen to the cell rim (average)
Botton Gap Height, d_B	18.93	mm	Depth of the bottom surface of the PLDCC specimen to the cell rim (average)
Equipment Weight, W_E	1558.30	g	Weight of Permeameter with monometer plugs
Equipment + Dry sample, W_{dry}	1979.50	g	Weight of Permeameter cantained in un-saturated PLDCC sample
Equipment + Sat sample, W_{sat}	2414.60	g	Weight of Permeameter cantained in saturated PLDCC sample
Assembly Excess Water, EW	48.14	g	Weight of excess water contained in the Permeameter assembly
PLDCC Sample Height, Hs	12.11	cm	
PLDCC Cross-sectional Area, A	46.90	cm^2	
Unsat. PLDCC Weight	201.38	g	
PLDCC Vol, V	568.09	cm3	
Unsat. PLDCC Unit Weight, W_{unsat}	0.35	g/cm^3	
	22.12	lb/ft^3	
Total Weight of Water, W_w	435.10	g	
Weight of Excess Cell Water, E_{wc}	136.25	g	
Weight of Saturated PLDCC, W_{sat}	452.09	g	
Saturated PLDCC Unit Weight, Uw_{sat}	**0.80**	**g/cm^3**	
	49.66	**lb/ft^3**	
Vol. Water in PLDCC	250708.744	mm^3	
Vol. PLDCC	568093.3	mm^3	
Vol. Water/Vol. PLDCC	**44.13%**		%Water contained in PLDCC when saturated (water storage capacity)

Constant Head Permeability Test

Tare Weight, W_A	104.10	g
Tare Weight, W_B	95.70	g
Tare Weight, W_C	103.00	g
Manometer H1	863.00	mm
Manometer H2	1265.00	mm
Δh	40.20	cm
Vol. of Water + Tare A	207.50	cm^3
Vol. of Water + Tare B	195.60	cm^3
Vol. of Water + Tare C	200.00	cm^3
Average Flow, Q	100.10	cm^3
Length of Specimen Along Path (	7.62	cm
Interval of Time, t	30.00	sec
Hydraulic Conductivity, K	**1.35E-02**	**cm/sec**

Permeability Test Report of Specimen TY-13

LABORATORY CONSTANT HEAD PERMEABILITY TEST

Specimen ID:

TY-14

PVC Cell Height, h_m	149.75	mm	Height of PVC cell
PVC Cell Weight,w	219.62	g	Weight of PVC cell
PVC Internal Diameter, D	77.46	mm	Internal Diameter of PVC cell
Top Gap Height, d_T	14.10	mm	Depth of the top surface of the PLDCC specimen to the cell rim (average)
Botton Gap Height, d_B	18.79	mm	Depth of the bottom surface of the PLDCC specimen to the cell rim (average)
Equipment Weight, W_E	1547.30	g	Weight of Permeameter with monometer plugs
Equipment + Dry sample, W_{dry}	1961.20	g	Weight of Permeameter cantained in un-saturated PLDCC sample
Equipment + Sat sample, W_{sat}	2396.70	g	Weight of Permeameter cantained in saturated PLDCC sample
Assembly Excess Water, EW	48.14	g	Weight of excess water contained in the Permeameter assembly
PLDCC Sample Height, Hs	11.69	cm	
PLDCC Cross-sectional Area, A	47.13	cm^2	
Unsat. PLDCC Weight	194.68	g	
PLDCC Vol, V	550.70	cm3	
Unsat. PLDCC Unit Weight, W_{unsat}	0.35	g/cm^3	
	22.06	lb/ft^3	
Total Weight of Water, W_w	435.50	g	
Weight of Excess Cell Water, E_{wc}	155.03	g	
Weight of Saturated PLDCC, W_{sat}	427.01	g	
Saturated PLDCC Unit Weight, Uw_{sat}	**0.78**	**g/cm^3**	
	48.38	**lb/ft^3**	
Vol. Water in PLDCC	232329.10	mm^3	
Vol. PLDCC	550699.3	mm^3	
Vol. Water/Vol. PLDCC	**42.19%**		%Water contained in PLDCC when saturated (water storage capacity)

Constant Head Permeability Test

Tare Weight, W_A	0.00	g
Tare Weight, W_B	0.00	g
Tare Weight, W_C	0.00	g
Manometer H1	390.00	mm
Manometer H2	1040.00	mm
Δh	65.00	cm
Vol. of Water + Tare A	250.81	cm^3
Vol. of Water + Tare B	238.30	cm^3
Vol. of Water + Tare C	232.81	cm^3
Average Flow, Q	230.16	cm^3
Length of Specimen Along Pa	7.62	cm
Interval of Time, t	30.00	sec
Hydraulic Conductivity, K	**1.91E-02**	**cm/sec**

Permeability Test Report of Specimen TY-14

LABORATORY CONSTANT HEAD PERMEABILITY TEST

Specimen ID:

TY-16

PVC Cell Height, h_m	150.65	mm	Height of PVC cell
PVC Cell Weight,w	220.91	g	Weight of PVC cell
PVC Internal Diameter, D	77.37	mm	Internal Diameter of PVC cell
Top Gap Height, d_T	15.97	mm	Depth of the top surface of the PLDCC specimen to the cell rim (average)
Botton Gap Height, d_B	18.22	mm	Depth of the bottom surface of the PLDCC specimen to the cell rim (average)
Equipment Weight, W_E	1558.30	g	Weight of Permeameter with monometer plugs
Equipment + Dry sample, W_{dry}	1960.10	g	Weight of Permeameter cantained in un-saturated PLDCC sample
Equipment + Sat sample, W_{sat}	2428.10	g	Weight of Permeameter cantained in saturated PLDCC sample
Assembly Excess Water, EW	48.14	g	Weight of excess water contained in the Permeameter assembly
PLDCC Sample Height, Hs	11.65	cm	
PLDCC Cross-sectional Area, A	47.02	cm^2	
Unsat. PLDCC Weight	182.09	g	
PLDCC Vol, V	547.62	cm3	
Unsat. PLDCC Unit Weight, W_{unsat}	0.33	g/cm^3	
	20.75	lb/ft^3	
Total Weight of Water, W_w	468.00	g	
Weight of Excess Cell Water, E_{wc}	160.74	g	
Weight of Saturated PLDCC, W_{sat}	441.21	g	
Saturated PLDCC Unit Weight, Uw_{sat}	**0.81**	**g/cm^3**	
	50.28	**lb/ft^3**	
Vol. Water in PLDCC	259124.9576	mm^3	
Vol. PLDCC	547616.1	mm^3	
Vol. Water/Vol. PLDCC	**47.32%**		%Water contained in PLDCC when saturated (water storage capacity)

Constant Head Permeability Test

Tare Weight, W_A	104.10	g
Tare Weight, W_B	95.70	g
Tare Weight, W_C	103.00	g
Manometer H1	285.00	mm
Manometer H2	1140.00	mm
Δh	85.50	cm
Vol. of Water + Tare A	231.70	cm^3
Vol. of Water + Tare B	220.30	cm^3
Vol. of Water + Tare C	225.30	cm^3
Average Flow, Q	124.83	cm^3
Length of Specimen Along Path (	7.62	cm
Interval of Time, t	30.00	sec
Hydraulic Conductivity, K	**7.89E-03**	**cm/sec**

Permeability Test Report of Specimen TY-16

LABORATORY CONSTANT HEAD PERMEABILITY TEST

Specimen ID:

TY-17

PVC Cell Height, h_m	150.77	mm	Height of PVC cell
PVC Cell Weight,w	220.65	g	Weight of PVC cell
PVC Internal Diameter, D	77.20	mm	Internal Diameter of PVC cell
Top Gap Height, d_T	9.03	mm	Depth of the top surface of the PLDCC specimen to the cell rim (average)
Botton Gap Height, d_B	18.91	mm	Depth of the bottom surface of the PLDCC specimen to the cell rim (average)
Equipment Weight, W_E	1547.80	g	Weight of Permeameter with monometer plugs
Equipment + Dry sample, W_{dry}	1957.50	g	Weight of Permeameter cantained in un-saturated PLDCC sample
Equipment + Sat sample, W_{sat}	2409.90	g	Weight of Permeameter cantained in saturated PLDCC sample
Assembly Excess Water, EW	48.14	g	Weight of excess water contained in the Permeameter assembly
PLDCC Sample Height, Hs	12.28	cm	
PLDCC Cross-sectional Area, A	46.80	cm^2	
Unsat. PLDCC Weight	190.15	g	
PLDCC Vol, V	574.90	cm3	
Unsat. PLDCC Unit Weight, W_{unsat}	0.33	g/cm^3	
	20.64	lb/ft^3	
Total Weight of Water, W_w	452.40	g	
Weight of Excess Cell Water, E_{wc}	130.79	g	
Weight of Saturated PLDCC, W_{sat}	463.62	g	
Saturated PLDCC Unit Weight, Uw_{sat}	**0.81**	**g/cm^3**	
	50.32	**lb/ft^3**	
Vol. Water in PLDCC	273469.0079	mm^3	
Vol. PLDCC	574902.8	mm^3	
Vol. Water/Vol. PLDCC	**47.57%**		%Water contained in PLDCC when saturated (water storage capacity)

Constant Head Permeability Test

Tare Weight, W_A	104.10	g
Tare Weight, W_B	95.70	g
Tare Weight, W_C	103.00	g
Manometer H1	370.00	mm
Manometer H2	1325.00	mm
Δh	95.50	cm
Vol. of Water + Tare A	241.30	cm^3
Vol. of Water + Tare B	229.30	cm^3
Vol. of Water + Tare C	233.20	cm^3
Average Flow, Q	133.67	cm^3
Length of Specimen Along Path (	7.62	cm
Interval of Time, t	30.00	sec
Hydraulic Conductivity, K	**7.60E-03**	**cm/sec**

Permeability Test Report of Specimen TY-17

LABORATORY CONSTANT HEAD PERMEABILITY TEST

Specimen ID:

TY-18

PVC Cell Height, h_m	150.76	mm	Height of PVC cell
PVC Cell Weight,w	220.64	g	Weight of PVC cell
PVC Internal Diameter, D	77.37	mm	Internal Diameter of PVC cell
Top Gap Height, d_T	15.38	mm	Depth of the top surface of the PLDCC specimen to the cell rim (average)
Botton Gap Height, d_B	19.08	mm	Depth of the bottom surface of the PLDCC specimen to the cell rim (average)
Equipment Weight, W_E	1558.90	g	Weight of Permeameter with monometer plugs
Equipment + Dry sample, W_{dry}	1973.50	g	Weight of Permeameter cantained in un-saturated PLDCC sample
Equipment + Sat sample, W_{sat}	2418.80	g	Weight of Permeameter cantained in saturated PLDCC sample
Assembly Excess Water, EW	48.14	g	Weight of excess water contained in the Permeameter assembly
PLDCC Sample Height, Hs	11.63	cm	
PLDCC Cross-sectional Area, A	47.01	cm^2	
Unsat. PLDCC Weight	194.56	g	
PLDCC Vol, V	546.76	cm3	
Unsat. PLDCC Unit Weight, W_{unsat}	0.36	g/cm^3	
	22.20	lb/ft^3	
Total Weight of Water, W_w	445.30	g	
Weight of Excess Cell Water, E_{wc}	161.99	g	
Weight of Saturated PLDCC, W_{sat}	429.73	g	
Saturated PLDCC Unit Weight, Uw_{sa}	**0.79**	**g/cm^3**	
	49.04	**lb/ft^3**	
Vol. Water in PLDCC	235174.53	mm^3	
Vol. PLDCC	546756.9	mm^3	
Vol. Water/Vol. PLDCC	**43.01%**		%Water contained in PLDCC when saturated (water storage capacity)

Constant Head Permeability Test

Tare Weight, W_A	0.00	g
Tare Weight, W_B	0.00	g
Tare Weight, W_C	0.00	g
Manometer H1	450.00	mm
Manometer H2	890.00	mm
Δh	44.00	cm
Vol. of Water + Tare A	302.11	cm^3
Vol. of Water + Tare B	289.30	cm^3
Vol. of Water + Tare C	286.81	cm^3
Average Flow, Q	232.65	cm^3
Length of Specimen Along Pa	7.62	cm
Interval of Time, t	30.00	sec
Hydraulic Conductivity, K	**2.86E-02**	**cm/sec**

Permeability Test Report of Specimen TY-18

LABORATORY CONSTANT HEAD PERMEABILITY TEST

Specimen ID:

TY-19

PVC Cell Height, h_m	150.04	mm	Height of PVC cell
PVC Cell Weight,w	220.88	g	Weight of PVC cell
PVC Internal Diameter, D	77.22	mm	Internal Diameter of PVC cell
Top Gap Height, d_T	16.97	mm	Depth of the top surface of the PLDCC specimen to the cell rim (average)
Botton Gap Height, d_B	18.69	mm	Depth of the bottom surface of the PLDCC specimen to the cell rim (average)
Equipment Weight, W_E	1543.50	g	Weight of Permeameter with monometer plugs
Equipment + Dry sample, W_{dry}	1959.69	g	Weight of Permeameter cantained in un-saturated PLDCC sample
Equipment + Sat sample, W_{sat}	2406.80	g	Weight of Permeameter cantained in saturated PLDCC sample
Assembly Excess Water, EW	48.14	g	Weight of excess water contained in the Permeameter assembly
PLDCC Sample Height, Hs	11.44	cm	
PLDCC Cross-sectional Area, A	46.83	cm^2	
Unsat. PLDCC Weight	193.72	g	
PLDCC Vol, V	535.62	cm3	
Unsat. PLDCC Unit Weight, W_{unsat}	0.36	g/cm^3	
	22.57	lb/ft^3	
Total Weight of Water, W_w	447.11	g	
Weight of Excess Cell Water, E_{wc}	166.98	g	
Weight of Saturated PLDCC, W_{sat}	425.71	g	
Saturated PLDCC Unit Weight, Uw_{sat}	**0.79**	**g/cm^3**	
	49.60	**lb/ft^3**	
Vol. Water in PLDCC	231992.50	mm^3	
Vol. PLDCC	535615.3	mm^3	
Vol. Water/Vol. PLDCC	**43.31%**		%Water contained in PLDCC when saturated (water storage capacity)

Constant Head Permeability Test

Tare Weight, W_A	0.00	g
Tare Weight, W_B	0.00	g
Tare Weight, W_C	0.00	g
Manometer H1	50.00	mm
Manometer H2	845.00	mm
Δh	79.50	cm
Vol. of Water + Tare A	320.20	cm^3
Vol. of Water + Tare B	320.10	cm^3
Vol. of Water + Tare C	312.90	cm^3
Average Flow, Q	317.73	cm^3
Length of Specimen Along Pa	7.62	cm
Interval of Time, t	60.00	sec
Hydraulic Conductivity, K	**1.08E-02**	**cm/sec**

Permeability Test Report of Specimen TY-19

LABORATORY CONSTANT HEAD PERMEABILITY TEST

Specimen ID:

TY-20

PVC Cell Height, h_m	149.96	mm	Height of PVC cell
PVC Cell Weight,w	220.19	g	Weight of PVC cell
PVC Internal Diameter, D	77.57	mm	Internal Diameter of PVC cell
Top Gap Height, d_T	7.55	mm	Depth of the top surface of the PLDCC specimen to the cell rim (average)
Botton Gap Height, d_B	14.33	mm	Depth of the bottom surface of the PLDCC specimen to the cell rim (average)
Equipment Weight, W_E	1557.00	g	Weight of Permeameter with monometer plugs
Equipment + Dry sample, W_{dry}	2057.40	g	Weight of Permeameter cantained in un-saturated PLDCC sample
Equipment + Sat sample, W_{sat}	2417.40	g	Weight of Permeameter cantained in saturated PLDCC sample
Assembly Excess Water, EW	48.14	g	Weight of excess water contained in the Permeameter assembly
PLDCC Sample Height, Hs	12.81	cm	
PLDCC Cross-sectional Area, A	47.25	cm^2	
Unsat. PLDCC Weight	281.01	g	
PLDCC Vol, V	605.20	cm3	
Unsat. PLDCC Unit Weight, W_{unsat}	0.46	g/cm^3	
	28.97	lb/ft^3	
Total Weight of Water, W_w	360.00	g	
Weight of Excess Cell Water, E_{wc}	103.41	g	
Weight of Saturated PLDCC, W_{sat}	489.46	g	
Saturated PLDCC Unit Weight, Uw_{sat}	**0.81**	**g/cm^3**	
	50.47	**lb/ft^3**	
Vol. Water in PLDCC	208453.0	mm^3	
Vol. PLDCC	605195.9	mm^3	
Vol. Water/Vol. PLDCC	**34.44%**		%Water contained in PLDCC when saturated (water storage capacity)

Constant Head Permeability Test

Tare Weight, W_A	104.10	g
Tare Weight, W_B	95.60	g
Tare Weight, W_C	102.90	g
Manometer H1	445.00	mm
Manometer H2	1400.00	mm
Δh	95.50	cm
Vol. of Water + Tare A	131.70	cm^3
Vol. of Water + Tare B	120.40	cm^3
Vol. of Water + Tare C	124.50	cm^3
Average Flow, Q	24.67	cm^3
Length of Specimen Along Path (	7.62	cm
Interval of Time, t	30.00	sec
Hydraulic Conductivity, K	**1.39E-03**	**cm/sec**

Permeability Test Report of Specimen TY-20

LABORATORY CONSTANT HEAD PERMEABILITY TEST

Specimen ID:

TY-21

PVC Cell Height, h_m	151.27	mm	Height of PVC cell
PVC Cell Weight,w	221.47	g	Weight of PVC cell
PVC Internal Diameter, D	77.24	mm	Internal Diameter of PVC cell
Top Gap Height, d_T	7.02	mm	Depth of the top surface of the PLDCC specimen to the cell rim (average)
Botton Gap Height, d_B	11.27	mm	Depth of the bottom surface of the PLDCC specimen to the cell rim (average)
Equipment Weight, W_E	1547.40	g	Weight of Permeameter with monometer plugs
Equipment + Dry sample, W_{dry}	2052.00	g	Weight of Permeameter cantained in un-saturated PLDCC sample
Equipment + Sat sample, W_{sat}	2407.60	g	Weight of Permeameter cantained in saturated PLDCC sample
Assembly Excess Water, EW	48.14	g	Weight of excess water contained in the Permeameter assembly
PLDCC Sample Height, Hs	13.30	cm	
PLDCC Cross-sectional Area, A	46.85	cm^2	
Unsat. PLDCC Weight	284.03	g	
PLDCC Vol, V	623.02	cm3	
Unsat. PLDCC Unit Weight, W_{unsat}	0.46	g/cm^3	
	28.45	lb/ft^3	
Total Weight of Water, W_w	355.60	g	
Weight of Excess Cell Water, E_{wc}	85.70	g	
Weight of Saturated PLDCC, W_{sat}	505.80	g	
Saturated PLDCC Unit Weight, Uw_{sat}	**0.81**	**g/cm^3**	
	50.66	**lb/ft^3**	
Vol. Water in PLDCC	221766.7	mm^3	
Vol. PLDCC	623017.8	mm^3	
Vol. Water/Vol. PLDCC	**35.60%**		%Water contained in PLDCC when saturated (water storage capacity)

Constant Head Permeability Test

Tare Weight, W_A	104.10	g
Tare Weight, W_B	95.60	g
Tare Weight, W_C	102.90	g
Manometer H1	490.00	mm
Manometer H2	1410.00	mm
Δh	92.00	cm
Vol. of Water + Tare A	119.20	cm^3
Vol. of Water + Tare B	109.70	cm^3
Vol. of Water + Tare C	115.80	cm^3
Average Flow, Q	14.03	cm^3
Length of Specimen Along Path (	7.62	cm
Interval of Time, t	30.00	sec
Hydraulic Conductivity, K	**8.27E-04**	**cm/sec**

Permeability Test Report of Specimen TY-21

LABORATORY CONSTANT HEAD PERMEABILITY TEST

Specimen ID:

TY-22

PVC Cell Height, h_m	150.87	mm	Height of PVC cell
PVC Cell Weight,w	221.68	g	Weight of PVC cell
PVC Internal Diameter, D	77.92	mm	Internal Diameter of PVC cell
Top Gap Height, d_T	8.29	mm	Depth of the top surface of the PLDCC specimen to the cell rim (average)
Botton Gap Height, d_B	13.66	mm	Depth of the bottom surface of the PLDCC specimen to the cell rim (average)
Equipment Weight, W_E	1557.00	g	Weight of Permeameter with monometer plugs
Equipment + Dry sample, W_{dry}	2063.50	g	Weight of Permeameter cantained in un-saturated PLDCC sample
Equipment + Sat sample, W_{sat}	2425.20	g	Weight of Permeameter cantained in saturated PLDCC sample
Assembly Excess Water, EW	48.14	g	Weight of excess water contained in the Permeameter assembly
PLDCC Sample Height, Hs	12.89	cm	
PLDCC Cross-sectional Area, A	47.69	cm^2	
Unsat. PLDCC Weight	283.62	g	
PLDCC Vol, V	614.75	cm3	
Unsat. PLDCC Unit Weight, W_{unsat}	0.46	g/cm^3	
	28.79	lb/ft^3	
Total Weight of Water, W_w	361.70	g	
Weight of Excess Cell Water, E_{wc}	104.69	g	
Weight of Saturated PLDCC, W_{sat}	492.49	g	
Saturated PLDCC Unit Weight, Uw_{sat}	**0.80**	**g/cm^3**	
	49.99	**lb/ft^3**	
Vol. Water in PLDCC	208868.9	mm^3	
Vol. PLDCC	614754.0	mm^3	
Vol. Water/Vol. PLDCC	**33.98%**		%Water contained in PLDCC when saturated (water storage capacity)

Constant Head Permeability Test

Tare Weight, W_A	104.10	g
Tare Weight, W_B	95.60	g
Tare Weight, W_C	102.90	g
Manometer H1	500.00	mm
Manometer H2	1420.00	mm
Δh	92.00	cm
Vol. of Water + Tare A	136.60	cm^3
Vol. of Water + Tare B	124.90	cm^3
Vol. of Water + Tare C	129.50	cm^3
Average Flow, Q	29.47	cm^3
Length of Specimen Along Path (	7.62	cm
Interval of Time, t	30.00	sec
Hydraulic Conductivity, K	**1.71E-03**	**cm/sec**

Permeability Test Report of Specimen TY-22

LABORATORY CONSTANT HEAD PERMEABILITY TEST

Specimen ID:

TY-23

PVC Cell Height, h_m	150.98	mm	Height of PVC cell
PVC Cell Weight,w	221.90	g	Weight of PVC cell
PVC Internal Diameter, D	77.51	mm	Internal Diameter of PVC cell
Top Gap Height, d_T	12.11	mm	Depth of the top surface of the PLDCC specimen to the cell rim (average)
Botton Gap Height, d_B	13.52	mm	Depth of the bottom surface of the PLDCC specimen to the cell rim (average)
Equipment Weight, W_E	1547.40	g	Weight of Permeameter with monometer plugs
Equipment + Dry sample, W_{dry}	2040.50	g	Weight of Permeameter cantained in un-saturated PLDCC sample
Equipment + Sat sample, W_{sat}	2420.90	g	Weight of Permeameter cantained in saturated PLDCC sample
Assembly Excess Water, EW	48.14	g	Weight of excess water contained in the Permeameter assembly
PLDCC Sample Height, Hs	12.54	cm	
PLDCC Cross-sectional Area, A	47.19	cm^2	
Unsat. PLDCC Weight	270.40	g	
PLDCC Vol, V	591.55	cm3	
Unsat. PLDCC Unit Weight, W_{unsat}	0.46	g/cm^3	
	28.52	lb/ft^3	
Total Weight of Water, W_w	380.40	g	
Weight of Excess Cell Water, E_{wc}	120.95	g	
Weight of Saturated PLDCC, W_{sat}	481.71	g	
Saturated PLDCC Unit Weight, Uw_{sat}	**0.81**	**g/cm^3**	
	50.81	**lb/ft^3**	
Vol. Water in PLDCC	211308	mm^3	
Vol. PLDCC	591547.2	mm^3	
Vol. Water/Vol. PLDCC	**35.72%**		%Water contained in PLDCC when saturated (water storage capacity)

Constant Head Permeability Test

Tare Weight, W_A	104.10	g
Tare Weight, W_B	95.60	g
Tare Weight, W_C	102.90	g
Manometer H1	490.00	mm
Manometer H2	1350.00	mm
Δh	86.00	cm
Vol. of Water + Tare A	131.90	cm^3
Vol. of Water + Tare B	121.00	cm^3
Vol. of Water + Tare C	126.20	cm^3
Average Flow, Q	25.50	cm^3
Length of Specimen Along Path (	7.62	cm
Interval of Time, t	30.00	sec
Hydraulic Conductivity, K	**1.60E-03**	**cm/sec**

Permeability Test Report of Specimen TY-23

LABORATORY CONSTANT HEAD PERMEABILITY TEST

Specimen ID:

TY-24

PVC Cell Height, h_m	148.69	mm	Height of PVC cell
PVC Cell Weight,w	217.47	g	Weight of PVC cell
PVC Internal Diameter, D	77.39	mm	Internal Diameter of PVC cell
Top Gap Height, d_T	11.26	mm	Depth of the top surface of the PLDCC specimen to the cell rim (average)
Botton Gap Height, d_B	12.34	mm	Depth of the bottom surface of the PLDCC specimen to the cell rim (average)
Equipment Weight, W_E	1547.80	g	Weight of Permeameter with monometer plugs
Equipment + Dry sample, W_{dry}	2032.00	g	Weight of Permeameter cantained in un-saturated PLDCC sample
Equipment + Sat sample, W_{sat}	2404.90	g	Weight of Permeameter cantained in saturated PLDCC sample
Assembly Excess Water, EW	48.14	g	Weight of excess water contained in the Permeameter assembly
PLDCC Sample Height, Hs	12.51	cm	
PLDCC Cross-sectional Area, A	47.04	cm^2	
Unsat. PLDCC Weight	267.63	g	
PLDCC Vol, V	588.45	cm3	
Unsat. PLDCC Unit Weight, W_{unsat}	0.45	g/cm^3	
	28.38	lb/ft^3	
Total Weight of Water, W_w	372.90	g	
Weight of Excess Cell Water, E_{wc}	111.02	g	
Weight of Saturated PLDCC, W_{sat}	481.37	g	
Saturated PLDCC Unit Weight, Uw_{sat}	**0.82**	**g/cm^3**	
	51.05	**lb/ft^3**	
Vol. Water in PLDCC	213739	mm^3	
Vol. PLDCC	588448.3	mm^3	
Vol. Water/Vol. PLDCC	**36.32%**		%Water contained in PLDCC when saturated (water storage capacity)

Constant Head Permeability Test

Tare Weight, W_A	104.10	g
Tare Weight, W_B	95.70	g
Tare Weight, W_C	102.90	g
Manometer H1	545.00	mm
Manometer H2	1390.00	mm
Δh	84.50	cm
Vol. of Water + Tare A	126.90	cm^3
Vol. of Water + Tare B	116.60	cm^3
Vol. of Water + Tare C	122.50	cm^3
Average Flow, Q	21.10	cm^3
Length of Specimen Along Path (	7.62	cm
Interval of Time, t	30.00	sec
Hydraulic Conductivity, K	**1.35E-03**	**cm/sec**

Permeability Test Report of Specimen TY-24

LABORATORY CONSTANT HEAD PERMEABILITY TEST

Specimen ID:

TY-25

PVC Cell Height, h_m	150.66	mm	Height of PVC cell
PVC Cell Weight,w	220.55	g	Weight of PVC cell
PVC Internal Diameter, D	77.55	mm	Internal Diameter of PVC cell
Top Gap Height, d_T	13.41	mm	Depth of the top surface of the PLDCC specimen to the cell rim (average)
Botton Gap Height, d_B	10.29	mm	Depth of the bottom surface of the PLDCC specimen to the cell rim (average)
Equipment Weight, W_E	1557.30	g	Weight of Permeameter with monometer plugs
Equipment + Dry sample, W_{dry}	2046.10	g	Weight of Permeameter cantained in un-saturated PLDCC sample
Equipment + Sat sample, W_{sat}	2424.70	g	Weight of Permeameter cantained in saturated PLDCC sample
Assembly Excess Water, EW	48.14	g	Weight of excess water contained in the Permeameter assembly
PLDCC Sample Height, Hs	12.70	cm	
PLDCC Cross-sectional Area, A	47.24	cm^2	
Unsat. PLDCC Weight	269.15	g	
PLDCC Vol, V	599.69	cm3	
Unsat. PLDCC Unit Weight, W_{unsat}	0.45	g/cm^3	
	28.01	lb/ft^3	
Total Weight of Water, W_w	378.60	g	
Weight of Excess Cell Water, E_{wc}	111.98	g	
Weight of Saturated PLDCC, W_{sat}	487.63	g	
Saturated PLDCC Unit Weight, Uw_{sat}	**0.81**	**g/cm^3**	
	50.74	**lb/ft^3**	
Vol. Water in PLDCC	218484.5	mm^3	
Vol. PLDCC	599694.8	mm^3	
Vol. Water/Vol. PLDCC	**36.43%**		%Water contained in PLDCC when saturated (water storage capacity)

Constant Head Permeability Test

Tare Weight, W_A	104.10	g
Tare Weight, W_B	95.70	g
Tare Weight, W_C	102.90	g
Manometer H1	590.00	mm
Manometer H2	1250.00	mm
Δh	66.00	cm
Vol. of Water + Tare A	132.80	cm^3
Vol. of Water + Tare B	121.80	cm^3
Vol. of Water + Tare C	127.00	cm^3
Average Flow, Q	26.30	cm^3
Length of Specimen Along Path (	7.62	cm
Interval of Time, t	30.00	sec
Hydraulic Conductivity, K	**2.14E-03**	**cm/sec**

Permeability Test Report of Specimen TY-25

LABORATORY CONSTANT HEAD PERMEABILITY TEST

Specimen ID:

TY-26

PVC Cell Height, h_m	151.10	mm	Height of PVC cell
PVC Cell Weight,w	221.18	g	Weight of PVC cell
PVC Internal Diameter, D	77.32	mm	Internal Diameter of PVC cell
Top Gap Height, d_T	13.95	mm	Depth of the top surface of the PLDCC specimen to the cell rim (average)
Botton Gap Height, d_B	11.25	mm	Depth of the bottom surface of the PLDCC specimen to the cell rim (average)
Equipment Weight, W_E	1548.50	g	Weight of Permeameter with monometer plugs
Equipment + Dry sample, W_{dry}	2038.10	g	Weight of Permeameter cantained in un-saturated PLDCC sample
Equipment + Sat sample, W_{sat}	2423.30	g	Weight of Permeameter cantained in saturated PLDCC sample
Assembly Excess Water, EW	48.14	g	Weight of excess water contained in the Permeameter assembly
PLDCC Sample Height, Hs	12.59	cm	
PLDCC Cross-sectional Area, A	46.96	cm^2	
Unsat. PLDCC Weight	270.42	g	
PLDCC Vol, V	591.19	cm3	
Unsat. PLDCC Unit Weight, W_{unsat}	0.46	g/cm^3	
	28.54	lb/ft^3	
Total Weight of Water, W_w	385.20	g	
Weight of Excess Cell Water, E_{wc}	118.35	g	
Weight of Saturated PLDCC, W_{sat}	489.13	g	
Saturated PLDCC Unit Weight, Uw_{sat}	**0.83**	**g/cm^3**	
	51.63	**lb/ft^3**	
Vol. Water in PLDCC	218710.3	mm^3	
Vol. PLDCC	591188.7	mm^3	
Vol. Water/Vol. PLDCC	**36.99%**		%Water contained in PLDCC when saturated (water storage capacity)

Constant Head Permeability Test

Tare Weight, W_A	104.10	g
Tare Weight, W_B	95.70	g
Tare Weight, W_C	102.90	g
Manometer H1	448.00	mm
Manometer H2	1310.00	mm
Δh	86.20	cm
Vol. of Water + Tare A	130.50	cm^3
Vol. of Water + Tare B	119.90	cm^3
Vol. of Water + Tare C	125.70	cm^3
Average Flow, Q	24.47	cm^3
Length of Specimen Along Path (	7.62	cm
Interval of Time, t	30.00	sec
Hydraulic Conductivity, K	**1.54E-03**	**cm/sec**

Permeability Test Report of Specimen TY-26

LABORATORY CONSTANT HEAD PERMEABILITY TEST

Specimen ID:

TY-27

PVC Cell Height, h_m	151.23	mm	Height of PVC cell
PVC Cell Weight,w	221.80	g	Weight of PVC cell
PVC Internal Diameter, D	77.36	mm	Internal Diameter of PVC cell
Top Gap Height, d_T	6.65	mm	Depth of the top surface of the PLDCC specimen to the cell rim (average)
Botton Gap Height, d_B	12.80	mm	Depth of the bottom surface of the PLDCC specimen to the cell rim (average)
Equipment Weight, W_E	1558.80	g	Weight of Permeameter with monometer plugs
Equipment + Dry sample, W_{dry}	2063.80	g	Weight of Permeameter cantained in un-saturated PLDCC sample
Equipment + Sat sample, W_{sat}	2423.30	g	Weight of Permeameter cantained in saturated PLDCC sample
Assembly Excess Water, EW	48.14	g	Weight of excess water contained in the Permeameter assembly
PLDCC Sample Height, Hs	13.18	cm	
PLDCC Cross-sectional Area, A	47.00	cm^2	
Unsat. PLDCC Weight	284.80	g	
PLDCC Vol, V	619.33	cm3	
Unsat. PLDCC Unit Weight, W_{unsat}	0.46	g/cm^3	
	28.69	lb/ft^3	
Total Weight of Water, W_w	359.50	g	
Weight of Excess Cell Water, E_{wc}	91.39	g	
Weight of Saturated PLDCC, W_{sat}	504.77	g	
Saturated PLDCC Unit Weight, Uw_{sat}	**0.82**	**g/cm^3**	
	50.86	**lb/ft^3**	
Vol. Water in PLDCC	219973.2	mm^3	
Vol. PLDCC	619331.3	mm^3	
Vol. Water/Vol. PLDCC	**35.52%**		%Water contained in PLDCC when saturated (water storage capacity)

Constant Head Permeability Test

Tare Weight, W_A	104.10	g
Tare Weight, W_B	95.70	g
Tare Weight, W_C	102.90	g
Manometer H1	495.00	mm
Manometer H2	1272.00	mm
Δh	77.70	cm
Vol. of Water + Tare A	144.80	cm^3
Vol. of Water + Tare B	132.50	cm^3
Vol. of Water + Tare C	136.20	cm^3
Average Flow, Q	36.93	cm^3
Length of Specimen Along Path (	7.62	cm
Interval of Time, t	30.00	sec
Hydraulic Conductivity, K	**2.57E-03**	**cm/sec**

Permeability Test Report of Specimen TY-27

LABORATORY CONSTANT HEAD PERMEABILITY TEST

Specimen ID:

TY-28

PVC Cell Height, h_m	150.40	mm	Height of PVC cell
PVC Cell Weight,w	219.84	g	Weight of PVC cell
PVC Internal Diameter, D	77.48	mm	Internal Diameter of PVC cell
Top Gap Height, d_T	11.87	mm	Depth of the top surface of the PLDCC specimen to the cell rim (average)
Botton Gap Height, d_B	12.92	mm	Depth of the bottom surface of the PLDCC specimen to the cell rim (average)
Equipment Weight, W_E	1546.30	g	Weight of Permeameter with monometer plugs
Equipment + Dry sample, W_{dry}	2039.20	g	Weight of Permeameter cantained in un-saturated PLDCC sample
Equipment + Sat sample, W_{sat}	2417.80	g	Weight of Permeameter cantained in saturated PLDCC sample
Assembly Excess Water, EW	48.14	g	Weight of excess water contained in the Permeameter assembly
PLDCC Sample Height, Hs	12.56	cm	
PLDCC Cross-sectional Area, A	47.15	cm^2	
Unsat. PLDCC Weight	276.56	g	
PLDCC Vol, V	592.26	cm3	
Unsat. PLDCC Unit Weight, W_{unsat}	0.47	g/cm^3	
	29.14	lb/ft^3	
Total Weight of Water, W_w	378.60	g	
Weight of Excess Cell Water, E_{wc}	116.90	g	
Weight of Saturated PLDCC, W_{sat}	490.12	g	
Saturated PLDCC Unit Weight, Uw_{sat}	**0.83**	**g/cm^3**	
	51.64	**lb/ft^3**	
Vol. Water in PLDCC	213562.3	mm^3	
Vol. PLDCC	592263.6	mm^3	
Vol. Water/Vol. PLDCC	**36.06%**		%Water contained in PLDCC when saturated (water storage capacity)

Constant Head Permeability Test

Tare Weight, W_A	104.10	g
Tare Weight, W_B	95.60	g
Tare Weight, W_C	102.90	g
Manometer H1	450.00	mm
Manometer H2	1055.00	mm
Δh	60.50	cm
Vol. of Water + Tare A	129.90	cm^3
Vol. of Water + Tare B	119.40	cm^3
Vol. of Water + Tare C	125.50	cm^3
Average Flow, Q	24.07	cm^3
Length of Specimen Along Path (	7.62	cm
Interval of Time, t	30.00	sec
Hydraulic Conductivity, K	**2.14E-03**	**cm/sec**

Permeability Test Report of Specimen TY-28

LABORATORY CONSTANT HEAD PERMEABILITY TEST

Specimen ID:

TY-29

PVC Cell Height, h_m	150.50	mm	Height of PVC cell
PVC Cell Weight,w	220.46	g	Weight of PVC cell
PVC Internal Diameter, D	77.55	mm	Internal Diameter of PVC cell
Top Gap Height, d_T	11.89	mm	Depth of the top surface of the PLDCC specimen to the cell rim (average)
Botton Gap Height, d_B	9.31	mm	Depth of the bottom surface of the PLDCC specimen to the cell rim (average)
Equipment Weight, W_E	1558.40	g	Weight of Permeameter with monometer plugs
Equipment + Dry sample, W_{dry}	2055.00	g	Weight of Permeameter cantained in un-saturated PLDCC sample
Equipment + Sat sample, W_{sat}	2418.10	g	Weight of Permeameter cantained in saturated PLDCC sample
Assembly Excess Water, EW	48.14	g	Weight of excess water contained in the Permeameter assembly
PLDCC Sample Height, Hs	12.93	cm	
PLDCC Cross-sectional Area, A	47.24	cm^2	
Unsat. PLDCC Weight	277.34	g	
PLDCC Vol, V	610.75	cm3	
Unsat. PLDCC Unit Weight, W_{unsat}	0.45	g/cm^3	
	28.34	lb/ft^3	
Total Weight of Water, W_w	363.10	g	
Weight of Excess Cell Water, E_{wc}	100.14	g	
Weight of Saturated PLDCC, W_{sat}	492.16	g	
Saturated PLDCC Unit Weight, Uw_{sat}	**0.81**	**g/cm^3**	
	50.28	**lb/ft^3**	
Vol. Water in PLDCC	214820	mm^3	
Vol. PLDCC	610750.4	mm^3	
Vol. Water/Vol. PLDCC	**35.17%**		%Water contained in PLDCC when saturated (water storage capacity)

Constant Head Permeability Test

Tare Weight, W_A	104.10	g
Tare Weight, W_B	95.60	g
Tare Weight, W_C	102.90	g
Manometer H1	525.00	mm
Manometer H2	1297.00	mm
Δh	77.20	cm
Vol. of Water + Tare A	128.40	cm^3
Vol. of Water + Tare B	118.30	cm^3
Vol. of Water + Tare C	123.90	cm^3
Average Flow, Q	22.67	cm^3
Length of Specimen Along Path (	7.62	cm
Interval of Time, t	30.00	sec
Hydraulic Conductivity, K	**1.58E-03**	**cm/sec**

Permeability Test Report of Specimen TY-29

LABORATORY CONSTANT HEAD PERMEABILITY TEST

Specimen ID:

TY-30

PVC Cell Height, h_m	150.76	mm	Height of PVC cell
PVC Cell Weight,w	220.45	g	Weight of PVC cell
PVC Internal Diameter, D	77.72	mm	Internal Diameter of PVC cell
Top Gap Height, d_T	7.10	mm	Depth of the top surface of the PLDCC specimen to the cell rim (average)
Botton Gap Height, d_B	11.50	mm	Depth of the bottom surface of the PLDCC specimen to the cell rim (average)
Equipment Weight, W_E	1547.70	g	Weight of Permeameter with monometer plugs
Equipment + Dry sample, W_{dry}	2045.20	g	Weight of Permeameter cantained in un-saturated PLDCC sample
Equipment + Sat sample, W_{sat}	2399.30	g	Weight of Permeameter cantained in saturated PLDCC sample
Assembly Excess Water, EW	48.14	g	Weight of excess water contained in the Permeameter assembly
PLDCC Sample Height, Hs	13.22	cm	
PLDCC Cross-sectional Area, A	47.44	cm^2	
Unsat. PLDCC Weight	278.45	g	
PLDCC Vol, V	626.95	cm3	
Unsat. PLDCC Unit Weight, W_{unsat}	0.44	g/cm^3	
	27.71	lb/ft^3	
Total Weight of Water, W_w	354.10	g	
Weight of Excess Cell Water, E_{wc}	88.24	g	
Weight of Saturated PLDCC, W_{sat}	496.18	g	
Saturated PLDCC Unit Weight, Uw_{sat}	**0.79**	**g/cm^3**	
	49.38	**lb/ft^3**	
Vol. Water in PLDCC	217727.1	mm^3	
Vol. PLDCC	626952.8	mm^3	
Vol. Water/Vol. PLDCC	**34.73%**		%Water contained in PLDCC when saturated (water storage capacity)

Constant Head Permeability Test

Tare Weight, W_A	104.10	g
Tare Weight, W_B	95.60	g
Tare Weight, W_C	102.90	g
Manometer H1	460.00	mm
Manometer H2	1335.00	mm
Δh	87.50	cm
Vol. of Water + Tare A	119.40	cm^3
Vol. of Water + Tare B	110.40	cm^3
Vol. of Water + Tare C	117.40	cm^3
Average Flow, Q	14.87	cm^3
Length of Specimen Along Path (	7.62	cm
Interval of Time, t	30.00	sec
Hydraulic Conductivity, K	**9.10E-04**	**cm/sec**

Permeability Test Report of Specimen TY-30

LABORATORY CONSTANT HEAD PERMEABILITY TEST

Specimen ID:

TY-31

PVC Cell Height, h_m	149.78	mm	Height of PVC cell
PVC Cell Weight,w	218.76	g	Weight of PVC cell
PVC Internal Diameter, D	77.52	mm	Internal Diameter of PVC cell
Top Gap Height, d_T	10.26	mm	Depth of the top surface of the PLDCC specimen to the cell rim (average)
Botton Gap Height, d_B	14.17	mm	Depth of the bottom surface of the PLDCC specimen to the cell rim (average)
Equipment Weight, W_E	1555.80	g	Weight of Permeameter with monometer plugs
Equipment + Dry sample, W_{dry}	2052.10	g	Weight of Permeameter cantained in un-saturated PLDCC sample
Equipment + Sat sample, W_{sat}	2357.40	g	Weight of Permeameter cantained in saturated PLDCC sample
Assembly Excess Water, EW	48.14	g	Weight of excess water contained in the Permeameter assembly
PLDCC Sample Height, Hs	12.53	cm	
PLDCC Cross-sectional Area, A	47.20	cm^2	
Unsat. PLDCC Weight	276.74	g	
PLDCC Vol, V	591.63	cm3	
Unsat. PLDCC Unit Weight, W_{unsat}	0.47	g/cm^3	
	29.19	lb/ft^3	
Total Weight of Water, W_w	305.30	g	
Weight of Excess Cell Water, E_{wc}	115.32	g	
Weight of Saturated PLDCC, W_{sat}	418.58	g	
Saturated PLDCC Unit Weight, Uw_{sat}	**0.71**	**g/cm^3**	
	44.15	**lb/ft^3**	
Vol. Water in PLDCC	141838.55	mm^3	
Vol. PLDCC	591630.3	mm^3	
Vol. Water/Vol. PLDCC	**23.97%**		%Water contained in PLDCC when saturated (water storage capacity)

Constant Head Permeability Test

Tare Weight, W_A	0.00	g
Tare Weight, W_B	0.00	g
Tare Weight, W_C	0.00	g
Manometer H1	0.00	mm
Manometer H2	100.00	mm
Δh	10.00	cm
Vol. of Water + Tare A	40.50	cm^3
Vol. of Water + Tare B	48.30	cm^3
Vol. of Water + Tare C	48.70	cm^3
Average Flow, Q	46.33	cm^3
Length of Specimen Along Pa	7.62	cm
Interval of Time, t	60.00	sec
Hydraulic Conductivity, K	**1.25E-02**	**cm/sec**

Permeability Test Report of Specimen TY-31

LABORATORY CONSTANT HEAD PERMEABILITY TEST

Specimen ID:

TY-32

PVC Cell Height, h_m	149.75	mm	Height of PVC cell
PVC Cell Weight,w	219.69	g	Weight of PVC cell
PVC Internal Diameter, D	77.38	mm	Internal Diameter of PVC cell
Top Gap Height, d_T	13.70	mm	Depth of the top surface of the PLDCC specimen to the cell rim (average)
Botton Gap Height, d_B	13.11	mm	Depth of the bottom surface of the PLDCC specimen to the cell rim (average)
Equipment Weight, W_E	1559.80	g	Weight of Permeameter with monometer plugs
Equipment + Dry sample, W_{dry}	2038.00	g	Weight of Permeameter cantained in un-saturated PLDCC sample
Equipment + Sat sample, W_{sat}	2424.00	g	Weight of Permeameter cantained in saturated PLDCC sample
Assembly Excess Water, EW	48.14	g	Weight of excess water contained in the Permeameter assembly
PLDCC Sample Height, Hs	12.29	cm	
PLDCC Cross-sectional Area, A	47.03	cm^2	
Unsat. PLDCC Weight	259.81	g	
PLDCC Vol, V	578.15	cm3	
Unsat. PLDCC Unit Weight, W_{unsat}	0.45	g/cm^3	
	28.04	lb/ft^3	
Total Weight of Water, W_w	386.00	g	
Weight of Excess Cell Water, E_{wc}	126.11	g	
Weight of Saturated PLDCC, W_{sat}	471.56	g	
Saturated PLDCC Unit Weight, Uw_{sat}	**0.82**	**g/cm^3**	
	50.90	**lb/ft^3**	
Vol. Water in PLDCC	211753.2	mm^3	
Vol. PLDCC	578150.0	mm^3	
Vol. Water/Vol. PLDCC	**36.63%**		%Water contained in PLDCC when saturated (water storage capacity)

Constant Head Permeability Test

Tare Weight, W_A	104.10	g
Tare Weight, W_B	95.60	g
Tare Weight, W_C	102.90	g
Manometer H1	430.00	mm
Manometer H2	1282.00	mm
Δh	85.20	cm
Vol. of Water + Tare A	139.90	cm^3
Vol. of Water + Tare B	128.30	cm^3
Vol. of Water + Tare C	132.20	cm^3
Average Flow, Q	32.60	cm^3
Length of Specimen Along Path (	7.62	cm
Interval of Time, t	30.00	sec
Hydraulic Conductivity, K	**2.07E-03**	**cm/sec**

Permeability Test Report of Specimen TY-32

LABORATORY CONSTANT HEAD PERMEABILITY TEST
Specimen ID:
TY-33

PVC Cell Height, h_m	150.56	mm	Height of PVC cell
PVC Cell Weight,w	220.55	g	Weight of PVC cell
PVC Internal Diameter, D	77.43	mm	Internal Diameter of PVC cell
Top Gap Height, d_T	12.63	mm	Depth of the top surface of the PLDCC specimen to the cell rim (average)
Botton Gap Height, d_B	10.26	mm	Depth of the bottom surface of the PLDCC specimen to the cell rim (average)
Equipment Weight, W_E	1548.00	g	Weight of Permeameter with monometer plugs
Equipment + Dry sample, W_{dry}	2044.90	g	Weight of Permeameter cantained in un-saturated PLDCC sample
Equipment + Sat sample, W_{sat}	2413.20	g	Weight of Permeameter cantained in saturated PLDCC sample
Assembly Excess Water, EW	48.14	g	Weight of excess water contained in the Permeameter assembly
PLDCC Sample Height, Hs	12.77	cm	
PLDCC Cross-sectional Area, A	47.08	cm^2	
Unsat. PLDCC Weight	277.35	g	
PLDCC Vol, V	601.07	cm3	
Unsat. PLDCC Unit Weight, W_{unsat}	0.46	g/cm^3	
	28.79	lb/ft^3	
Total Weight of Water, W_w	368.30	g	
Weight of Excess Cell Water, E_{wc}	107.79	g	
Weight of Saturated PLDCC, W_{sat}	489.72	g	
Saturated PLDCC Unit Weight, Uw_{sat}	**0.81**	**g/cm^3**	
	50.84	**lb/ft^3**	
Vol. Water in PLDCC	212370	mm^3	
Vol. PLDCC	601072.9	mm^3	
Vol. Water/Vol. PLDCC	**35.33%**		%Water contained in PLDCC when saturated (water storage capacity)

Constant Head Permeability Test

Tare Weight, W_A	104.10	g
Tare Weight, W_B	95.60	g
Tare Weight, W_C	102.90	g
Manometer H1	331.00	mm
Manometer H2	1243.00	mm
Δh	91.20	cm
Vol. of Water + Tare A	129.20	cm^3
Vol. of Water + Tare B	118.80	cm^3
Vol. of Water + Tare C	125.10	cm^3
Average Flow, Q	23.50	cm^3
Length of Specimen Along Path (	7.62	cm
Interval of Time, t	30.00	sec
Hydraulic Conductivity, K	**1.39E-03**	**cm/sec**

Permeability Test Report of Specimen TY-33

LABORATORY CONSTANT HEAD PERMEABILITY TEST

Specimen ID:

TY-34

PVC Cell Height, h_m	149.29	mm	Height of PVC cell
PVC Cell Weight,w	218.75	g	Weight of PVC cell
PVC Internal Diameter, D	77.30	mm	Internal Diameter of PVC cell
Top Gap Height, d_T	13.02	mm	Depth of the top surface of the PLDCC specimen to the cell rim (average)
Botton Gap Height, d_B	12.47	mm	Depth of the bottom surface of the PLDCC specimen to the cell rim (average)
Equipment Weight, W_E	1560.20	g	Weight of Permeameter with monometer plugs
Equipment + Dry sample, W_{dry}	2046.60	g	Weight of Permeameter cantained in un-saturated PLDCC sample
Equipment + Sat sample, W_{sat}	2423.80	g	Weight of Permeameter cantained in saturated PLDCC sample
Assembly Excess Water, EW	48.14	g	Weight of excess water contained in the Permeameter assembly
PLDCC Sample Height, Hs	12.38	cm	
PLDCC Cross-sectional Area, A	46.93	cm^2	
Unsat. PLDCC Weight	269.45	g	
PLDCC Vol, V	581.00	cm3	
Unsat. PLDCC Unit Weight, W_{unsat}	0.46	g/cm^3	
	28.94	lb/ft^3	
Total Weight of Water, W_w	377.20	g	
Weight of Excess Cell Water, E_{wc}	119.61	g	
Weight of Saturated PLDCC, W_{sat}	478.90	g	
Saturated PLDCC Unit Weight, Uw_{sat}	**0.82**	**g/cm^3**	
	51.43	**lb/ft^3**	
Vol. Water in PLDCC	209447.9	mm^3	
Vol. PLDCC	580997.3	mm^3	
Vol. Water/Vol. PLDCC	**36.05%**		%Water contained in PLDCC when saturated (water storage capacity)

Constant Head Permeability Test

Tare Weight, W_A	104.10	g
Tare Weight, W_B	95.60	g
Tare Weight, W_C	102.90	g
Manometer H1	514.00	mm
Manometer H2	1252.00	mm
Δh	73.80	cm
Vol. of Water + Tare A	135.40	cm^3
Vol. of Water + Tare B	123.20	cm^3
Vol. of Water + Tare C	127.80	cm^3
Average Flow, Q	27.93	cm^3
Length of Specimen Along Path (	7.62	cm
Interval of Time, t	30.00	sec
Hydraulic Conductivity, K	**2.05E-03**	**cm/sec**

Permeability Test Report of Specimen TY-34

LABORATORY CONSTANT HEAD PERMEABILITY TEST

Specimen ID:

TY-35

PVC Cell Height, h_m	149.88	mm	Height of PVC cell
PVC Cell Weight,w	220.07	g	Weight of PVC cell
PVC Internal Diameter, D	77.46	mm	Internal Diameter of PVC cell
Top Gap Height, d_T	10.32	mm	Depth of the top surface of the PLDCC specimen to the cell rim (average)
Botton Gap Height, d_B	10.90	mm	Depth of the bottom surface of the PLDCC specimen to the cell rim (average)
Equipment Weight, W_E	1558.30	g	Weight of Permeameter with monometer plugs
Equipment + Dry sample, W_{dry}	2048.90	g	Weight of Permeameter cantained in un-saturated PLDCC sample
Equipment + Sat sample, W_{sat}	2420.00	g	Weight of Permeameter cantained in saturated PLDCC sample
Assembly Excess Water, EW	48.14	g	Weight of excess water contained in the Permeameter assembly
PLDCC Sample Height, Hs	12.87	cm	
PLDCC Cross-sectional Area, A	47.13	cm^2	
Unsat. PLDCC Weight	273.13	g	
PLDCC Vol, V	606.34	cm3	
Unsat. PLDCC Unit Weight, W_{unsat}	0.45	g/cm^3	
	28.11	lb/ft^3	
Total Weight of Water, W_w	371.10	g	
Weight of Excess Cell Water, E_{wc}	100.02	g	
Weight of Saturated PLDCC, W_{sat}	496.07	g	
Saturated PLDCC Unit Weight, Uw_{sat}	**0.82**	**g/cm^3**	
	51.05	**lb/ft^3**	
Vol. Water in PLDCC	222939	mm^3	
Vol. PLDCC	606338.1	mm^3	
Vol. Water/Vol. PLDCC	**36.77%**		%Water contained in PLDCC when saturated (water storage capacity)

Constant Head Permeability Test

Tare Weight, W_A	104.10	g
Tare Weight, W_B	95.60	g
Tare Weight, W_C	103.00	g
Manometer H1	430.00	mm
Manometer H2	1160.00	mm
Δh	73.00	cm
Vol. of Water + Tare A	120.90	cm^3
Vol. of Water + Tare B	111.60	cm^3
Vol. of Water + Tare C	118.20	cm^3
Average Flow, Q	16.00	cm^3
Length of Specimen Along Path (	7.62	cm
Interval of Time, t	30.00	sec
Hydraulic Conductivity, K	**1.18E-03**	**cm/sec**

Permeability Test Report of Specimen TY-35

LABORATORY CONSTANT HEAD PERMEABILITY TEST

Specimen ID:

TY-36

PVC Cell Height, h_m	150.37	mm	Height of PVC cell
PVC Cell Weight,w	220.03	g	Weight of PVC cell
PVC Internal Diameter, D	77.67	mm	Internal Diameter of PVC cell
Top Gap Height, d_T	18.62	mm	Depth of the top surface of the PLDCC specimen to the cell rim (average)
Botton Gap Height, d_B	12.72	mm	Depth of the bottom surface of the PLDCC specimen to the cell rim (average)
Equipment Weight, W_E	1546.10	g	Weight of Permeameter with monometer plugs
Equipment + Dry sample, W_{dry}	2020.20	g	Weight of Permeameter cantained in un-saturated PLDCC sample
Equipment + Sat sample, W_{sat}	2414.30	g	Weight of Permeameter cantained in saturated PLDCC sample
Assembly Excess Water, EW	48.14	g	Weight of excess water contained in the Permeameter assembly
PLDCC Sample Height, Hs	11.90	cm	
PLDCC Cross-sectional Area, A	47.38	cm^2	
Unsat. PLDCC Weight	254.87	g	
PLDCC Vol, V	564.02	cm3	
Unsat. PLDCC Unit Weight, W_{unsat}	0.45	g/cm^3	
	28.20	lb/ft^3	
Total Weight of Water, W_w	394.10	g	
Weight of Excess Cell Water, E_{wc}	148.51	g	
Weight of Saturated PLDCC, W_{sat}	452.32	g	
Saturated PLDCC Unit Weight, Uw_{sat}	**0.80**	**g/cm^3**	
	50.04	**lb/ft^3**	
Vol. Water in PLDCC	197450.2	mm^3	
Vol. PLDCC	564022.6	mm^3	
Vol. Water/Vol. PLDCC	**35.01%**		%Water contained in PLDCC when saturated (water storage capacity)

Constant Head Permeability Test

Tare Weight, W_A	104.10	g
Tare Weight, W_B	95.60	g
Tare Weight, W_C	103.00	g
Manometer H1	664.00	mm
Manometer H2	1365.00	mm
Δh	70.10	cm
Vol. of Water + Tare A	134.30	cm^3
Vol. of Water + Tare B	122.70	cm^3
Vol. of Water + Tare C	126.90	cm^3
Average Flow, Q	27.07	cm^3
Length of Specimen Along Path (	7.62	cm
Interval of Time, t	30.00	sec
Hydraulic Conductivity, K	**2.07E-03**	**cm/sec**

Permeability Test Report of Specimen TY-36

LABORATORY CONSTANT HEAD PERMEABILITY TEST

Specimen ID:

TY-37

PVC Cell Height, h_m	149.07	mm	Height of PVC cell
PVC Cell Weight,w	218.44	g	Weight of PVC cell
PVC Internal Diameter, D	77.81	mm	Internal Diameter of PVC cell
Top Gap Height, d_T	13.89	mm	Depth of the top surface of the PLDCC specimen to the cell rim (average)
Botton Gap Height, d_B	11.58	mm	Depth of the bottom surface of the PLDCC specimen to the cell rim (average)
Equipment Weight, W_E	1547.30	g	Weight of Permeameter with monometer plugs
Equipment + Dry sample, W_{dry}	2026.00	g	Weight of Permeameter cantained in un-saturated PLDCC sample
Equipment + Sat sample, W_{sat}	2402.30	g	Weight of Permeameter cantained in saturated PLDCC sample
Assembly Excess Water, EW	48.14	g	Weight of excess water contained in the Permeameter assembly
PLDCC Sample Height, Hs	12.36	cm	
PLDCC Cross-sectional Area, A	47.55	cm^2	
Unsat. PLDCC Weight	260.76	g	
PLDCC Vol, V	587.70	cm3	
Unsat. PLDCC Unit Weight, W_{unsat}	0.44	g/cm^3	
	27.69	lb/ft^3	
Total Weight of Water, W_w	376.30	g	
Weight of Excess Cell Water, E_{wc}	121.06	g	
Weight of Saturated PLDCC, W_{sat}	467.86	g	
Saturated PLDCC Unit Weight, Uw_{sat}	**0.80**	**g/cm^3**	
	49.68	**lb/ft^3**	
Vol. Water in PLDCC	207102.7	mm^3	
Vol. PLDCC	587704.1	mm^3	
Vol. Water/Vol. PLDCC	**35.24%**		%Water contained in PLDCC when saturated (water storage capacity)

Constant Head Permeability Test

Tare Weight, W_A	104.10	g
Tare Weight, W_B	95.60	g
Tare Weight, W_C	103.00	g
Manometer H1	480.00	mm
Manometer H2	1350.00	mm
Δh	87.00	cm
Vol. of Water + Tare A	121.40	cm^3
Vol. of Water + Tare B	111.80	cm^3
Vol. of Water + Tare C	118.20	cm^3
Average Flow, Q	16.23	cm^3
Length of Specimen Along Path (	7.62	cm
Interval of Time, t	30.00	sec
Hydraulic Conductivity, K	**9.97E-04**	**cm/sec**

Permeability Test Report of Specimen TY-37

LABORATORY CONSTANT HEAD PERMEABILITY TEST

Specimen ID:

TY-38

PVC Cell Height, h_m	150.80	mm	Height of PVC cell
PVC Cell Weight,w	221.61	g	Weight of PVC cell
PVC Internal Diameter, D	77.34	mm	Internal Diameter of PVC cell
Top Gap Height, d_T	16.59	mm	Depth of the top surface of the PLDCC specimen to the cell rim (average)
Botton Gap Height, d_B	9.58	mm	Depth of the bottom surface of the PLDCC specimen to the cell rim (average)
Equipment Weight, W_E	1560.10	g	Weight of Permeameter with monometer plugs
Equipment + Dry sample, W_{dry}	2058.50	g	Weight of Permeameter cantained in un-saturated PLDCC sample
Equipment + Sat sample, W_{sat}	2432.70	g	Weight of Permeameter cantained in saturated PLDCC sample
Assembly Excess Water, EW	48.14	g	Weight of excess water contained in the Permeameter assembly
PLDCC Sample Height, Hs	12.46	cm	
PLDCC Cross-sectional Area, A	46.97	cm^2	
Unsat. PLDCC Weight	278.09	g	
PLDCC Vol, V	585.45	cm3	
Unsat. PLDCC Unit Weight, W_{unsat}	0.48	g/cm^3	
	29.64	lb/ft^3	
Total Weight of Water, W_w	374.20	g	
Weight of Excess Cell Water, E_{wc}	122.93	g	
Weight of Saturated PLDCC, W_{sat}	481.23	g	
Saturated PLDCC Unit Weight, Uw_{sat}	**0.82**	**g/cm^3**	
	51.29	**lb/ft^3**	
Vol. Water in PLDCC	203135.8	mm^3	
Vol. PLDCC	585445.4	mm^3	
Vol. Water/Vol. PLDCC	**34.70%**		%Water contained in PLDCC when saturated (water storage capacity)

Constant Head Permeability Test

Tare Weight, W_A	104.10	g
Tare Weight, W_B	95.60	g
Tare Weight, W_C	103.00	g
Manometer H1	354.00	mm
Manometer H2	1400.00	mm
Δh	104.60	cm
Vol. of Water + Tare A	126.00	cm^3
Vol. of Water + Tare B	116.40	cm^3
Vol. of Water + Tare C	122.60	cm^3
Average Flow, Q	20.77	cm^3
Length of Specimen Along Path (	7.62	cm
Interval of Time, t	30.00	sec
Hydraulic Conductivity, K	**1.07E-03**	**cm/sec**

Permeability Test Report of Specimen TY-38

LABORATORY CONSTANT HEAD PERMEABILITY TEST

Specimen ID:

A1

PVC Cell Height, h_m	152.92	mm	Height of PVC cell
PVC Cell Weight,w	331.20	g	Weight of PVC cell
PVC Internal Diameter, D	77.30	mm	Internal Diameter of PVC cell
Top Gap Height, d_T	7.90	mm	Depth of the top surface of the PLDCC specimen to the cell rim (average)
Botton Gap Height, d_B	18.96	mm	Depth of the bottom surface of the PLDCC specimen to the cell rim (average)
Equipment Weight, W_E	1547.20	g	Weight of Permeameter with monometer plugs
Equipment + Dry sample, W_{dry}	2126.40	g	Weight of Permeameter cantained in un-saturated PLDCC sample
Equipment + Sat sample, W_{sat}	2663.40	g	Weight of Permeameter cantained in saturated PLDCC sample
Assembly Excess Water, EW	48.14	g	Weight of excess water contained in the Permeameter assembly
PLDCC Sample Height, Hs	12.61	cm	
PLDCC Cross-sectional Area, A	46.93	cm^2	
Unsat. PLDCC Weight	248.10	g	
PLDCC Vol, V	591.60	cm3	
Unsat. PLDCC Unit Weight, W_{unsat}	0.42	g/cm^3	
	26.17	lb/ft^3	
Total Weight of Water, W_w	537.00	g	
Weight of Excess Cell Water, E_{wc}	126.09	g	
Weight of Saturated PLDCC, W_{sat}	610.87	g	
Saturated PLDCC Unit Weight, Uw_{sat}	**1.03**	**g/cm^3**	
	64.43	**lb/ft^3**	
Vol. Water in PLDCC	362774.6	mm^3	
Vol. PLDCC	591597.7	mm^3	
Vol. Water/Vol. PLDCC	**61.32%**		%Water contained in PLDCC when saturated (water storage capacity)

Constant Head Permeability Test

Tare Weight, W_A	104.20	g
Tare Weight, W_B	95.80	g
Tare Weight, W_C	102.80	g
Manometer H1	330.00	mm
Manometer H2	435.00	mm
Δh	10.50	cm
Vol. of Water + Tare A	562.30	cm^3
Vol. of Water + Tare B	545.70	cm^3
Vol. of Water + Tare C	554.60	cm^3
Average Flow, Q	453.27	cm^3
Length of Specimen Along Path (	7.62	cm
Interval of Time, t	30.00	sec
Hydraulic Conductivity, K	**2.34E-01**	**cm/sec**

Permeability Test Report of Specimen A1

LABORATORY CONSTANT HEAD PERMEABILITY TEST
Specimen ID:
A2

PVC Cell Height, h_m	152.72	mm	Height of PVC cell
PVC Cell Weight,w	334.50	g	Weight of PVC cell
PVC Internal Diameter, D	77.10	mm	Internal Diameter of PVC cell
Top Gap Height, d_T	6.78	mm	Depth of the top surface of the PLDCC specimen to the cell rim (average)
Botton Gap Height, d_B	16.32	mm	Depth of the bottom surface of the PLDCC specimen to the cell rim (average)
Equipment Weight, W_E	1557.80	g	Weight of Permeameter with monometer plugs
Equipment + Dry sample, W_{dry}	2142.30	g	Weight of Permeameter cantained in un-saturated PLDCC sample
Equipment + Sat sample, W_{sat}	2664.60	g	Weight of Permeameter cantained in saturated PLDCC sample
Assembly Excess Water, EW	48.14	g	Weight of excess water contained in the Permeameter assembly
PLDCC Sample Height, Hs	12.96	cm	
PLDCC Cross-sectional Area, A	46.69	cm^2	
Unsat. PLDCC Weight	250.20	g	
PLDCC Vol, V	605.18	cm3	
Unsat. PLDCC Unit Weight, W_{unsat}	0.41	g/cm^3	
	25.80	lb/ft^3	
Total Weight of Water, W_w	522.30	g	
Weight of Excess Cell Water, E_{wc}	107.83	g	
Weight of Saturated PLDCC, W_{sat}	616.54	g	
Saturated PLDCC Unit Weight, Uw_{sat}	**1.02**	**g/cm^3**	
	63.57	**lb/ft^3**	
Vol. Water in PLDCC	366335.5	mm^3	
Vol. PLDCC	605181.4	mm^3	
Vol. Water/Vol. PLDCC	**60.53%**		%Water contained in PLDCC when saturated (water storage capacity)

Constant Head Permeability Test

Tare Weight, W_A	104.20	g
Tare Weight, W_B	95.70	g
Tare Weight, W_C	102.90	g
Manometer H1	210.00	mm
Manometer H2	305.00	mm
Δh	9.50	cm
Vol. of Water + Tare A	377.40	cm^3
Vol. of Water + Tare B	368.10	cm^3
Vol. of Water + Tare C	368.50	cm^3
Average Flow, Q	270.40	cm^3
Length of Specimen Along Path (	7.62	cm
Interval of Time, t	30.00	sec
Hydraulic Conductivity, K	**1.55E-01**	**cm/sec**

Permeability Test Report of Specimen A2

LABORATORY CONSTANT HEAD PERMEABILITY TEST

Specimen ID:

A3

PVC Cell Height, h_m	152.81	mm	Height of PVC cell
PVC Cell Weight,w	330.60	g	Weight of PVC cell
PVC Internal Diameter, D	77.13	mm	Internal Diameter of PVC cell
Top Gap Height, d_T	10.95	mm	Depth of the top surface of the PLDCC specimen to the cell rim (average)
Botton Gap Height, d_B	15.85	mm	Depth of the bottom surface of the PLDCC specimen to the cell rim (average)
Equipment Weight, W_E	1547.80	g	Weight of Permeameter with monometer plugs
Equipment + Dry sample, W_{dry}	2117.90	g	Weight of Permeameter cantained in un-saturated PLDCC sample
Equipment + Sat sample, W_{sat}	2633.60	g	Weight of Permeameter cantained in saturated PLDCC sample
Assembly Excess Water, EW	48.14	g	Weight of excess water contained in the Permeameter assembly
PLDCC Sample Height, Hs	12.60	cm	
PLDCC Cross-sectional Area, A	46.72	cm^2	
Unsat. PLDCC Weight	241.00	g	
PLDCC Vol, V	588.76	cm3	
Unsat. PLDCC Unit Weight, W_{unsat}	0.41	g/cm^3	
	25.54	lb/ft^3	
Total Weight of Water, W_w	515.70	g	
Weight of Excess Cell Water, E_{wc}	125.18	g	
Weight of Saturated PLDCC, W_{sat}	583.38	g	
Saturated PLDCC Unit Weight, Uw_{sat}	**0.99**	**g/cm^3**	
	61.83	**lb/ft^3**	
Vol. Water in PLDCC	342382.3	mm^3	
Vol. PLDCC	588757.4	mm^3	
Vol. Water/Vol. PLDCC	**58.15%**		%Water contained in PLDCC when saturated (water storage capacity)

Constant Head Permeability Test

Tare Weight, W_A	104.20	g
Tare Weight, W_B	95.70	g
Tare Weight, W_C	102.90	g
Manometer H1	345.00	mm
Manometer H2	423.00	mm
Δh	7.80	cm
Vol. of Water + Tare A	622.30	cm^3
Vol. of Water + Tare B	-	cm^3
Vol. of Water + Tare C	-	cm^3
Average Flow, Q	518.10	cm^3
Length of Specimen Along Path (	7.62	cm
Interval of Time, t	30.00	sec
Hydraulic Conductivity, K	**3.61E-01**	**cm/sec**

Permeability Test Report of Specimen A3

LABORATORY CONSTANT HEAD PERMEABILITY TEST

Specimen ID:

A4

PVC Cell Height, h_m	152.81	mm	Height of PVC cell
PVC Cell Weight,w	334.70	g	Weight of PVC cell
PVC Internal Diameter, D	77.09	mm	Internal Diameter of PVC cell
Top Gap Height, d_T	11.91	mm	Depth of the top surface of the PLDCC specimen to the cell rim (average)
Botton Gap Height, d_B	19.49	mm	Depth of the bottom surface of the PLDCC specimen to the cell rim (average)
Equipment Weight, W_E	1557.80	g	Weight of Permeameter with monometer plugs
Equipment + Dry sample, W_{dry}	2130.60	g	Weight of Permeameter cantained in un-saturated PLDCC sample
Equipment + Sat sample, W_{sat}	2654.00	g	Weight of Permeameter cantained in saturated PLDCC sample
Assembly Excess Water, EW	48.14	g	Weight of excess water contained in the Permeameter assembly
PLDCC Sample Height, Hs	12.14	cm	
PLDCC Cross-sectional Area, A	46.67	cm^2	
Unsat. PLDCC Weight	237.20	g	
PLDCC Vol, V	566.65	cm3	
Unsat. PLDCC Unit Weight, W_{unsat}	0.42	g/cm^3	
	26.12	lb/ft^3	
Total Weight of Water, W_w	523.40	g	
Weight of Excess Cell Water, E_{wc}	146.53	g	
Weight of Saturated PLDCC, W_{sat}	565.93	g	
Saturated PLDCC Unit Weight, Uw_{sat}	**1.00**	**g/cm^3**	
	62.32	**lb/ft^3**	
Vol. Water in PLDCC	328727.4	mm^3	
Vol. PLDCC	566650.5	mm^3	
Vol. Water/Vol. PLDCC	**58.01%**		%Water contained in PLDCC when saturated (water storage capacity)

Constant Head Permeability Test

Tare Weight, W_A	104.20	g
Tare Weight, W_B	95.60	g
Tare Weight, W_C	103.10	g
Manometer H1	230.00	mm
Manometer H2	291.00	mm
Δh	6.10	cm
Vol. of Water + Tare A	321.90	cm^3
Vol. of Water + Tare B	312.10	cm^3
Vol. of Water + Tare C	319.90	cm^3
Average Flow, Q	217.00	cm^3
Length of Specimen Along Path (	7.62	cm
Interval of Time, t	20.00	sec
Hydraulic Conductivity, K	**2.90E-01**	**cm/sec**

Permeability Test Report of Specimen A4

LABORATORY CONSTANT HEAD PERMEABILITY TEST

Specimen ID:

A5

PVC Cell Height, h_m	152.34	mm	Height of PVC cell
PVC Cell Weight,w	333.50	g	Weight of PVC cell
PVC Internal Diameter, D	76.72	mm	Internal Diameter of PVC cell
Top Gap Height, d_T	10.32	mm	Depth of the top surface of the PLDCC specimen to the cell rim (average)
Botton Gap Height, d_B	17.69	mm	Depth of the bottom surface of the PLDCC specimen to the cell rim (average)
Equipment Weight, W_E	1547.80	g	Weight of Permeameter with monometer plugs
Equipment + Dry sample, W_{dry}	2128.40	g	Weight of Permeameter cantained in un-saturated PLDCC sample
Equipment + Sat sample, W_{sat}	2629.30	g	Weight of Permeameter cantained in saturated PLDCC sample
Assembly Excess Water, EW	48.14	g	Weight of excess water contained in the Permeameter assembly
PLDCC Sample Height, Hs	12.43	cm	
PLDCC Cross-sectional Area, A	46.23	cm^2	
Unsat. PLDCC Weight	246.60	g	
PLDCC Vol, V	574.71	cm3	
Unsat. PLDCC Unit Weight, W_{unsat}	0.43	g/cm^3	
	26.77	lb/ft^3	
Total Weight of Water, W_w	500.90	g	
Weight of Excess Cell Water, E_{wc}	129.51	g	
Weight of Saturated PLDCC, W_{sat}	569.86	g	
Saturated PLDCC Unit Weight, Uw_{sat}	**0.99**	**g/cm^3**	
	61.87	**lb/ft^3**	
Vol. Water in PLDCC	323256.6	mm^3	
Vol. PLDCC	574711.7	mm^3	
Vol. Water/Vol. PLDCC	**56.25%**		%Water contained in PLDCC when saturated (water storage capacity)

Constant Head Permeability Test

Tare Weight, W_A	104.20	g
Tare Weight, W_B	95.70	g
Tare Weight, W_C	102.90	g
Manometer H1	345.00	mm
Manometer H2	425.00	mm
Δh	8.00	cm
Vol. of Water + Tare A	448.80	cm^3
Vol. of Water + Tare B	439.40	cm^3
Vol. of Water + Tare C	446.10	cm^3
Average Flow, Q	343.83	cm^3
Length of Specimen Along Path (	7.62	cm
Interval of Time, t	20.00	sec
Hydraulic Conductivity, K	**3.54E-01**	**cm/sec**

Permeability Test Report of Specimen A5

LABORATORY CONSTANT HEAD PERMEABILITY TEST

Specimen ID:

A6

PVC Cell Height, h_m	152.63	mm	Height of PVC cell
PVC Cell Weight,w	335.50	g	Weight of PVC cell
PVC Internal Diameter, D	76.89	mm	Internal Diameter of PVC cell
Top Gap Height, d_T	6.27	mm	Depth of the top surface of the PLDCC specimen to the cell rim (average)
Botton Gap Height, d_B	21.54	mm	Depth of the bottom surface of the PLDCC specimen to the cell rim (average)
Equipment Weight, W_E	1547.30	g	Weight of Permeameter with monometer plugs
Equipment + Dry sample, W_{dry}	2121.30	g	Weight of Permeameter cantained in un-saturated PLDCC sample
Equipment + Sat sample, W_{sat}	2642.30	g	Weight of Permeameter cantained in saturated PLDCC sample
Assembly Excess Water, EW	48.14	g	Weight of excess water contained in the Permeameter assembly
PLDCC Sample Height, Hs	12.48	cm	
PLDCC Cross-sectional Area, A	46.43	cm^2	
Unsat. PLDCC Weight	238.50	g	
PLDCC Vol, V	579.53	cm3	
Unsat. PLDCC Unit Weight, W_{unsat}	0.41	g/cm^3	
	25.68	lb/ft^3	
Total Weight of Water, W_w	521.00	g	
Weight of Excess Cell Water, E_{wc}	129.09	g	
Weight of Saturated PLDCC, W_{sat}	582.27	g	
Saturated PLDCC Unit Weight, Uw_{sat}	**1.00**	**g/cm^3**	
	62.70	**lb/ft^3**	
Vol. Water in PLDCC	343773.9	mm^3	
Vol. PLDCC	579530.9	mm^3	
Vol. Water/Vol. PLDCC	**59.32%**		%Water contained in PLDCC when saturated (water storage capacity)

Constant Head Permeability Test

Tare Weight, W_A	104.20	g
Tare Weight, W_B	95.60	g
Tare Weight, W_C	103.10	g
Manometer H1	340.00	mm
Manometer H2	430.00	mm
Δh	9.00	cm
Vol. of Water + Tare A	449.40	cm^3
Vol. of Water + Tare B	440.40	cm^3
Vol. of Water + Tare C	444.90	cm^3
Average Flow, Q	343.93	cm^3
Length of Specimen Along Path (	7.62	cm
Interval of Time, t	20.00	sec
Hydraulic Conductivity, K	**3.14E-01**	**cm/sec**

Permeability Test Report of Specimen A6

LABORATORY CONSTANT HEAD PERMEABILITY TEST

Specimen ID:

A7

PVC Cell Height, h_m	152.27	mm	Height of PVC cell
PVC Cell Weight,w	327.60	g	Weight of PVC cell
PVC Internal Diameter, D	77.23	mm	Internal Diameter of PVC cell
Top Gap Height, d_T	11.89	mm	Depth of the top surface of the PLDCC specimen to the cell rim (average)
Botton Gap Height, d_B	19.07	mm	Depth of the bottom surface of the PLDCC specimen to the cell rim (average)
Equipment Weight, W_E	1557.80	g	Weight of Permeameter with monometer plugs
Equipment + Dry sample, W_{dry}	2129.60	g	Weight of Permeameter cantained in un-saturated PLDCC sample
Equipment + Sat sample, W_{sat}	2641.70	g	Weight of Permeameter cantained in saturated PLDCC sample
Assembly Excess Water, EW	48.14	g	Weight of excess water contained in the Permeameter assembly
PLDCC Sample Height, Hs	12.13	cm	
PLDCC Cross-sectional Area, A	46.84	cm^2	
Unsat. PLDCC Weight	242.60	g	
PLDCC Vol, V	568.21	cm3	
Unsat. PLDCC Unit Weight, W_{unsat}	0.43	g/cm^3	
	26.64	lb/ft^3	
Total Weight of Water, W_w	512.10	g	
Weight of Excess Cell Water, E_{wc}	145.05	g	
Weight of Saturated PLDCC, W_{sat}	561.51	g	
Saturated PLDCC Unit Weight, Uw_{sat}	**0.99**	**g/cm^3**	
	61.66	**lb/ft^3**	
Vol. Water in PLDCC	318908.8	mm^3	
Vol. PLDCC	568207.0	mm^3	
Vol. Water/Vol. PLDCC	**56.13%**		%Water contained in PLDCC when saturated (water storage capacity)

Constant Head Permeability Test

Tare Weight, W_A	104.10	g
Tare Weight, W_B	95.70	g
Tare Weight, W_C	102.90	g
Manometer H1	333.00	mm
Manometer H2	508.00	mm
Δh	17.50	cm
Vol. of Water + Tare A	397.40	cm^3
Vol. of Water + Tare B	391.90	cm^3
Vol. of Water + Tare C	397.30	cm^3
Average Flow, Q	294.63	cm^3
Length of Specimen Along Path (	7.62	cm
Interval of Time, t	20.00	sec
Hydraulic Conductivity, K	**1.37E-01**	**cm/sec**

Permeability Test Report of Specimen A7

LABORATORY CONSTANT HEAD PERMEABILITY TEST

Specimen ID:

A8

PVC Cell Height, h_m	153.64	mm	Height of PVC cell
PVC Cell Weight,w	331.40	g	Weight of PVC cell
PVC Internal Diameter, D	77.07	mm	Internal Diameter of PVC cell
Top Gap Height, d_T	8.63	mm	Depth of the top surface of the PLDCC specimen to the cell rim (average)
Botton Gap Height, d_B	18.53	mm	Depth of the bottom surface of the PLDCC specimen to the cell rim (average)
Equipment Weight, W_E	1547.30	g	Weight of Permeameter with monometer plugs
Equipment + Dry sample, W_{dry}	2126.00	g	Weight of Permeameter cantained in un-saturated PLDCC sample
Equipment + Sat sample, W_{sat}	2634.80	g	Weight of Permeameter cantained in saturated PLDCC sample
Assembly Excess Water, EW	48.14	g	Weight of excess water contained in the Permeameter assembly
PLDCC Sample Height, Hs	12.65	cm	
PLDCC Cross-sectional Area, A	46.64	cm^2	
Unsat. PLDCC Weight	245.90	g	
PLDCC Vol, V	589.93	cm3	
Unsat. PLDCC Unit Weight, W_{unsat}	0.42	g/cm^3	
	26.01	lb/ft^3	
Total Weight of Water, W_w	508.80	g	
Weight of Excess Cell Water, E_{wc}	126.70	g	
Weight of Saturated PLDCC, W_{sat}	579.86	g	
Saturated PLDCC Unit Weight, Uw_{sat}	**0.98**	**g/cm^3**	
	61.34	**lb/ft^3**	
Vol. Water in PLDCC	333959.2	mm^3	
Vol. PLDCC	589925.9	mm^3	
Vol. Water/Vol. PLDCC	**56.61%**		%Water contained in PLDCC when saturated (water storage capacity)

Constant Head Permeability Test

Tare Weight, W_A	104.20	g
Tare Weight, W_B	95.60	g
Tare Weight, W_C	103.10	g
Manometer H1	337.00	mm
Manometer H2	430.00	mm
Δh	9.30	cm
Vol. of Water + Tare A	452.80	cm^3
Vol. of Water + Tare B	443.00	cm^3
Vol. of Water + Tare C	449.70	cm^3
Average Flow, Q	347.53	cm^3
Length of Specimen Along Path (	7.62	cm
Interval of Time, t	20.00	sec
Hydraulic Conductivity, K	**3.05E-01**	**cm/sec**

Permeability Test Report of Specimen A8

APPENDIX B - PRODUCTION PROCEDURE FOR PLDCC

Foam preparation:

a. Determine the amount of water and foaming agent needed. The recommended ratio of foam to water is 1:50, which means 20 grams of chemicals per liter of water.

b. Fill the mixing bucket with water.

c. Measure the amount of foaming agent in a graduate cylinder.

d. Pour the foaming agent into the mixing bucket and thoroughly mix it with water.

e. Insert the recirculating tube into the mixing bucket.

Adjusting the foam density:

a. Prepare several disposable cups.

b. Develop a spreadsheet with the following measuring parameters: measure the weight and volume of the disposable cups.

Cup weight (g)	Cup volume (cm^3)	Weight of foam + cup (g)	Weight of foam (g)	Foam density (g/cm^3)	Foam density (PCF)

c. Turn on the foam generator, and allow the foam to run from the foaming tube for at least 30

seconds.

d. Collect the foam in the disposable cups and measure the weight of the foam + cup. Calculate the weight of the foam and determine the foam density. The recommended foam density is 2.5 PCF (AERIX INDUSTRIES™), but it could change based on the mix design.

e. If the foam density is not as expected, adjust the foam density by turning the recirculate knob on the foam generator clockwise or counterclockwise. Repeat the process from (c) to (e) to calculate the foam density.

Mixing Slurry and Foam:

a. Determine the water-to-cement ratio. The recommended W/C is 0.55 (AERIX INDUSTRY™), but it could change based on the mix design. Weigh the cement and water accordingly.

b. Sprinkle water inside a slurry mixing bucket (Note: the slurry mixing bucket is different from the foam mixing bucket).

c. Pour the water into the slurry mixing bucket, followed by the cement.

d. Mix the cement and water for 2 minutes thoroughly using a handheld cement mixer.

e. Set aside two to three cups of cement slurry separately in case of foam overshooting.

f. Add a good amount of foam to the slurry mixing bucket and mix for at least 20 seconds.

g. Collect a full cup of foam-slurry mixture and calculate the density. If the density of the mix is

not as expected, add more slurry (from (e)) or foam to increase or lower the density of the mixture until the desired value is achieved. After adding extra slurry or foam, the slurry-foam mixture needs to be thoroughly mixed.

Pouring and curing of the PLDCC Samples:

a. After the desired density of the PLDCC sample is achieved, pour the slurry mixture into the concrete mold and gently tap the mold to ensure uniform density across the sample.

b. Wet a towel, cover the concrete mold, and allow the concrete to cure for at least 10 days for permeability testing and 28 days for compressive strength testing.

APPENDIX C.1 - MODIFIED ASTM D2434 CONSTANT HEAD PERMEABILITY

CASTLE ROCK CONSULTING
ENHANCING TRADITIONAL SOLUTIONS WITH INNOVATION

CRC Modifications of ASTM D2434 Constant Head Permeability Testing for Pervious Low Density Cellular Concrete (PLDCC)

Overview:

The modifications made to the D2434 test as relates to testing Pervious Low Density Cellular Concrete (PLDCC), concern sample fabrication and preparation for testing.

These modifications are based on the nature of PLDCC, and how it differs from permeable soils, for which the D2434 test is intended.

Once the PLDCC sample has been fabricated and prepared for testing, the testing procedure for determining the hydraulic conductivity of the PLDCC, including measurements taken, calculations, and application of Darcy's Law are the same as specified in the D2434 protocol for soils.

These modifications and protocols are outlined in the following text, with drawings for illustration attached in the appendix.

PLDCC Sampling:

PLDCC, being a cohesive cementitious material does not require the same sample preparation as a non-cohesive granular soil. As such, the details specified in the D2434 procedure concerning sample gradation, filling, and compaction in the permeameter cell are not applicable. The use of porous stones or manometer port screens are not necessary, so they are omitted. Instead, the PLDCC samples are cast in place in a PVC cell that replaces the acrylic cell that is supplied with the permeameter (figures 1 and 2).

The PVC cells are fabricated from schedule 40 PVC pipe, to the same dimensions and tolerances as the acrylic cells that they replace, with the exception that the PVC cells do not have the circumferential grooves around the inside wall at the manometer ports (figures 3 and 4).

The manometer ports are located at the requisite distance for the cell diameter and are drilled and tapped to accommodate threaded hose barbs for connecting to manometers. These manometer ports are plugged with screws prior to casting the PLDCC in the cell.

Additionally standard PVC "knock-out" pressure test caps are used to stop the open ends of the cell to contain the PLDCC when cast in the cell. The bottom cap is taped in place around its circumference to prevent material from seeping out. The top cap has its center

knocked out and is taped around its circumference to provide a protective ring to prevent damage to the cell rim. A vented slip cap is placed over the top of the cell after filling (figure 5).

The interior wall of the PVC cell is roughened with sandpaper prior to filling, to ensure a good bond of the PLDCC to the walls, in an effort to eliminate sidewall leakage, as well as ensure that the PLDCC remains in place during vacuum saturation.

These PVC cells are an economical alternative to using the acrylic cells and can be fabricated in large numbers, to be shipped off to various projects where they can be filled, and returned to a lab for testing. The cells are also more durable than their acrylic counterparts, and can be cleaned out and reused.

Sample Preparation:

After the PLDCC samples have been cast, and have had sufficient time to cure and develop the permeable structure (usually 7 to 10 days), they may be prepared for testing.

The slip cap is removed, as well as the top ring and bottom cap. Depending on how the cell was filled, excess material may need to be removed, or scraped down below the cell rim. A metal putty knife or chisel works well as a scraping tool and helps keep the surfaces flat and relatively square to the cell ends. Both top and bottom surfaces should be scarified and blown off with compressed air to expose the cellular structure.

The cell can now be placed into the permeameter for testing. The manometer port plugs remain in place during saturation and vacuum saturation of the sample.

After saturation, the permeameter is placed on its side, with the monometer ports face up while connected to the water source with the inlet vale open, and the outlet valve closed. The plug screws are removed and a 1/8” drill with a pilot is used to drill through the sample at the manometer port, stopping at the opposite wall with water flowing through the sample to purge debris from the hole. This provides a pathway for the cross-sectional flow velocity to the manometers and permits the manometers to respond more quickly to flow changes.

Threaded hose barbs may now be installed in the manometer ports and connected to the manometers and the permeameter can be turned upright for testing.

The testing procedure from this point on is the same as that specified in the D2434 protocol when testing soils.

Appendix

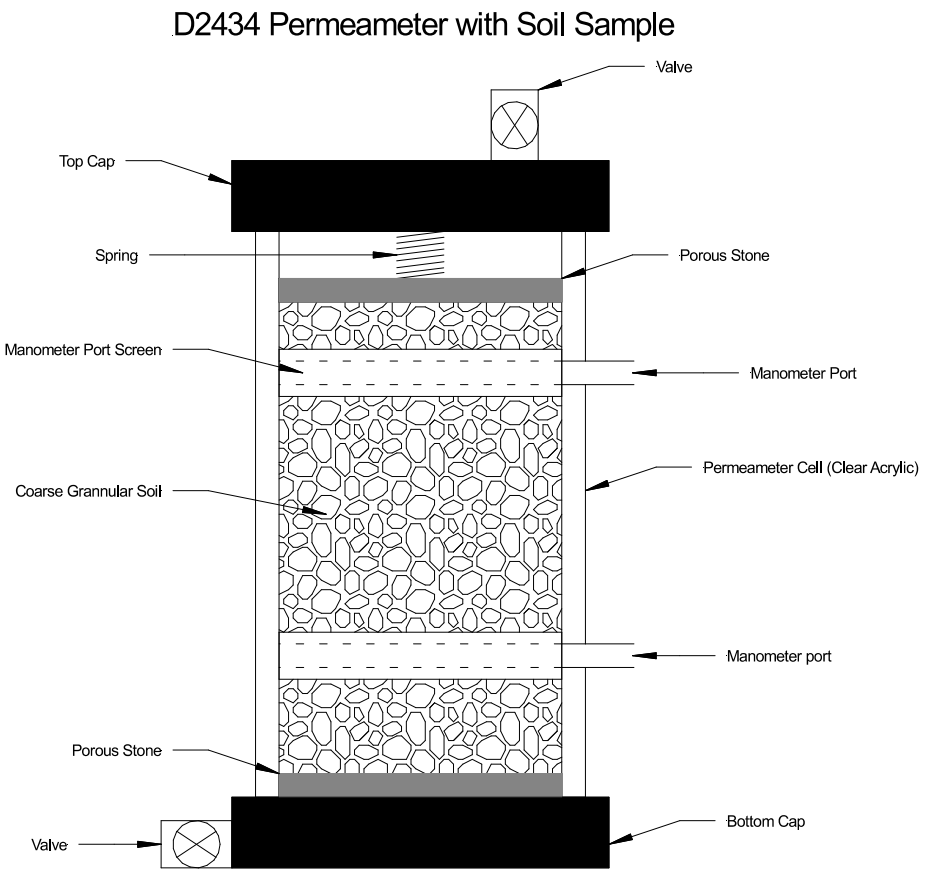

Figure 1

Appendix

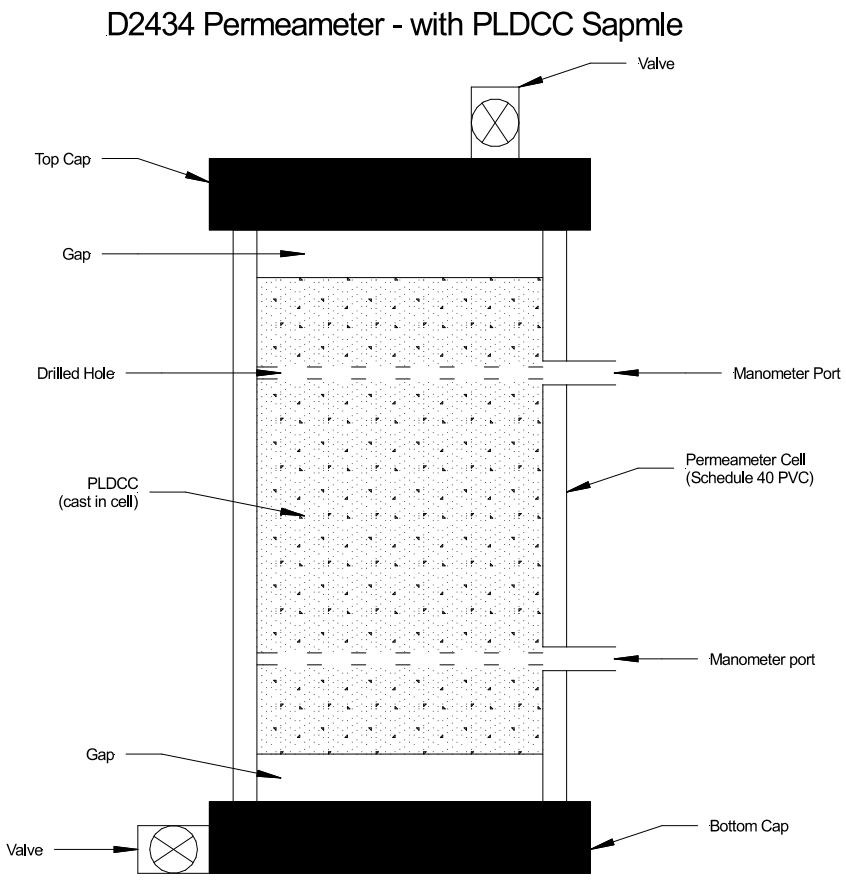

Figure 2

Appendix

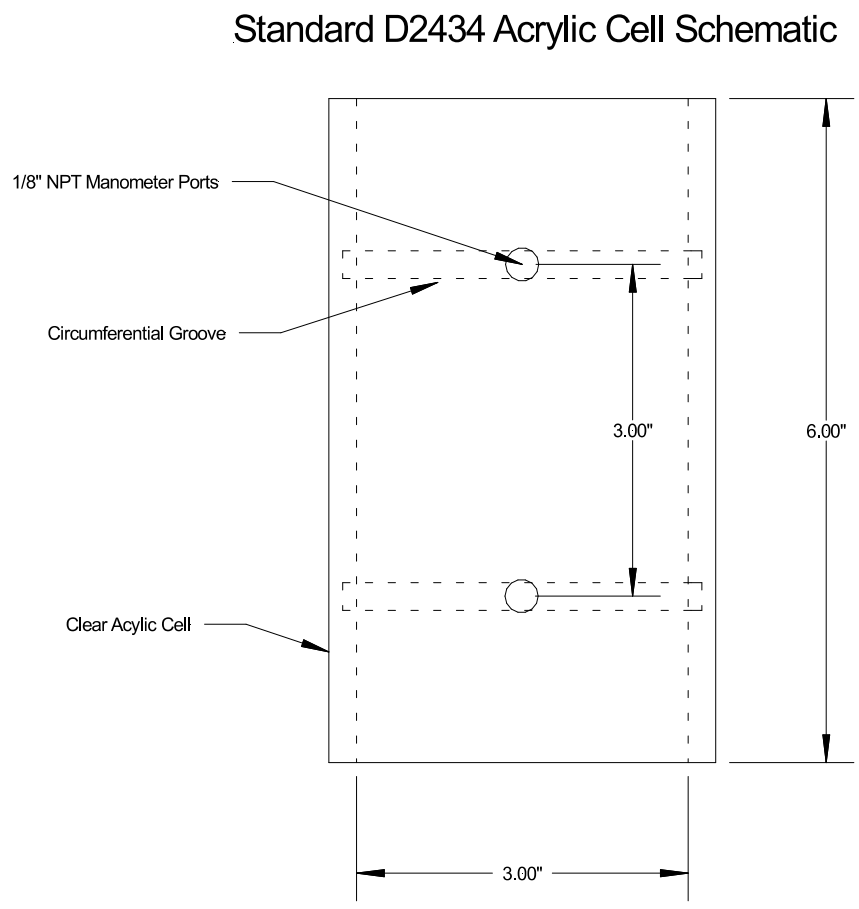

Figure 3

Appendix

PVC Cell Schematic

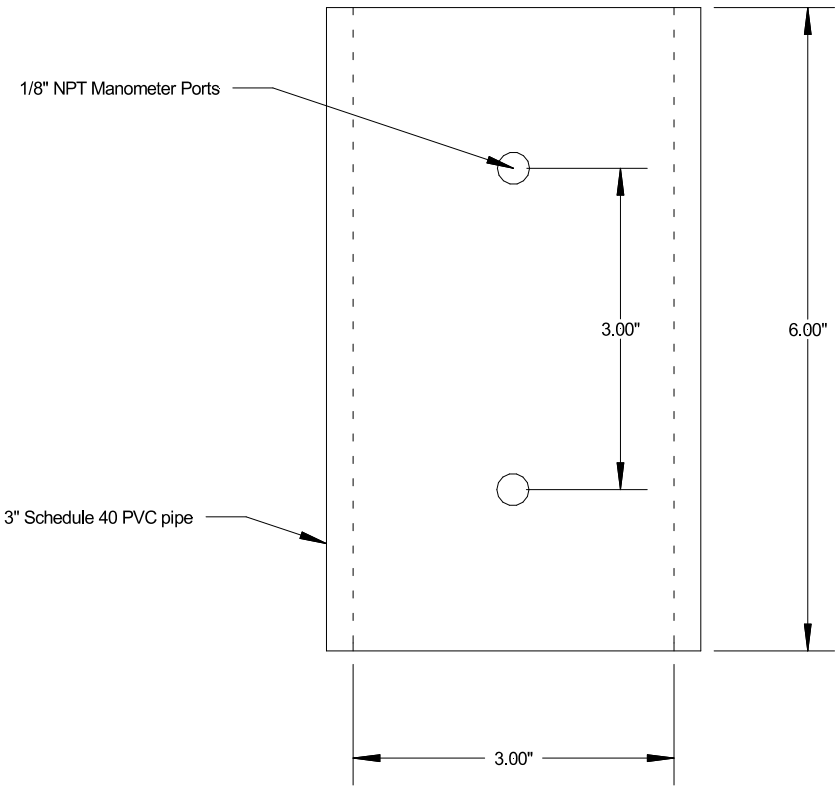

Figure 4

Appendix

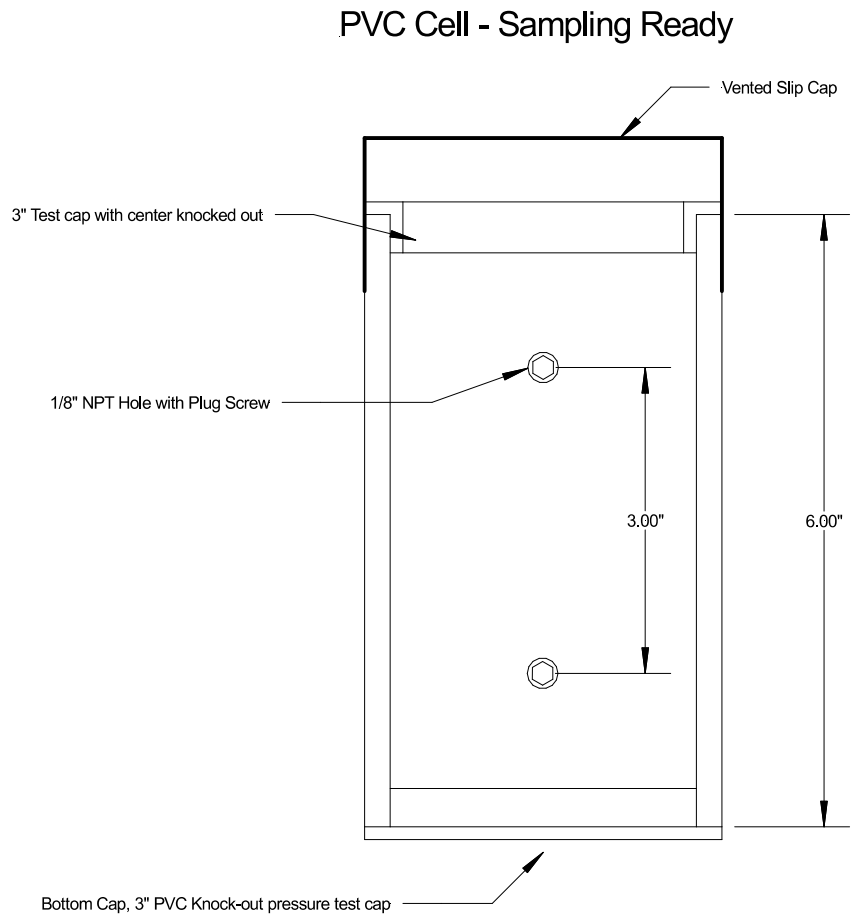

Figure 5

APPENDIX C.2 - NATURALLY SATURATED UNIT WEIGHT MEASUREMENT OF PLDCC

CASTLE ROCK CONSULTING
ENHANCING TRADITIONAL SOLUTIONS WITH INNOVATION

CRC Method for Measuring Naturally Saturated Unit Weight of PLDCC using the ASTM D2434 Testing Apparatus

Overview:

In some instances, it is desirable to know the saturated unit weight achieved by the PLDCC under service conditions. This saturated unit weight is achieved under "natural" conditions as groundwater infiltrates the PLDCC after placement.

The estimation of this saturated unit weight can be measured using the D2434 apparatus and the same PLDCC samples intended for measurement of the hydraulic conductivity. The saturated unit weight is measured prior to testing for hydraulic conductivity. The following procedure is based on a series of trials conducted by CRC in which samples were saturated under varying amounts of elevation head over various time intervals and determined to be sufficient for establishing a "natural" saturation condition.

The protocol is outlined in the following text, with drawings and sample calculations for demonstration in the attached appendix.

Method for Estimating Saturated Unit Weight of PLDCC:

If the saturated unit weight is to be measured, the PVC cell should have a tare weight recorded prior to being filled. The tare weight should not include the caps, only the cell, with manometer plug screws in place and any label for sample identification. The tare weight can be written on the cell ID label. It is best for the testing lab to ensure that this is done before sending the cells out for sampling.

After the cell has been filled and returned for testing, any excess material or spillage on the outside of the cell is cleaned off. The caps and ring are removed. Excess material on the top surface is removed to below the top rim, and both the top and bottom surfaces are scarified and blown off with compressed air to expose the cellular structure, taking care to keep the top and bottom surfaces as square as possible to the cell ends. The weight of the filled and prepped cell is recorded.

The overall height of the cell is recorded, along with the depth from the cell rim to the surface of the PLDCC at both the top and bottom ends. An average of three depth measurements around the circumference can be taken. These measurements will be used to calculate the volume of water in the gaps between the cell ends and the PLDCC surface that is excess water not contained within the PLDCC after saturation.

The cell with the unsaturated PLDCC is placed in the permeameter assembly. The tare weight of the permeameter assembly, with the PLDCC sample cell is recorded.

The permeameter is connected to the constant head water source with the inflow through the bottom valve and the purge plug removed from the top cap. Saturation is conducted under 2' of constant head. Water is allowed to flow freely though the sample until flowing out of the top vent in the permeameter, at which point the flow rate is adjusted to a slow trickle and left for a period of 30 minutes. The upward flow through the sample aids in dislodging trapped air and mimics upward infiltration of ground water through the sample at low flow.

After a period of 30 minutes, the inflow valve is closed and the purge plug replace in the top cap. The permeameter is disconnected from the reservoir, thoroughly dried off and weighed. The assembly weight with the saturated PLDCC sample and the excess assembly water is recorded.

Volume and weight measurements are used to calculate the estimated saturated unit weight of the PLDCC as follows:

The depth measurements from the top and bottom surfaces to the cell rim can be subtracted from the cell height to determine the height of the PLDCC sample within the cell. The sample height in conjunction with the cross-sectional area can be used to determine the volume of the PLDCC in the cell.

The cell tare weight can be subtracted from the unsaturated cell weight to determine the weight of the PLDCC sample, which can be used in conjunction with the calculated volume, to verify the un-saturated unit weight of the PLDCC.

The weight of the permeameter assembly containing the saturated PLDCC cell can be subtracted from the tare weight of the permeameter assembly containing the un-saturated PLDCC cell. The difference is the weight of water in the PLDCC and the assembly after saturation, from which excess water not contained within the PLDCC must be subtracted.

This excess water is a combination of the water occupying the spaces between the PLDCC surfaces and the ends of the cell, as well as water occupying the space between the top end of the cell and the bottom of the top cap of the permeameter, and water in the valves and boreholes in the permeameter base and cap.

The weight of water contained in the valves, boreholes, and gap between the cell and top cap can be measured for a particular permeameter as follows:

1. Place an empty permeameter cell with plugs in the manometer ports in the permeameter.
2. Connect the permeameter to a water source, inflow from the bottom valve.
3. Fill the cell completely with water and purge all of the air.
4. Close the valves and disconnect from the water source.
5. Tare a pan.
6. Carefully remove the top cap, open the valve to prevent suction from holding it in place.
7. Holding the top cap over the pan, shake the excess water off into the pan.
8. Carefully decant the water from the top of the cell with a pipette, past the top of the retaining ring until even with the interface between the top rim of the cell and the retaining ring.
9. Add the water to the pan.
10. Open the bottom valve and allow the water to drain from the cell.
11. Carefully remove the retaining ring and the empty cell.
12. Shake the bottom base over the pan to recover the excess water.
13. Repeating the process a few times gives a good average of the water weight that will be occupying the valves, boreholes and gap.

This excess water from the assembly can be added to the calculated weight of water occupying the gaps between the PLDCC surfaces and cell rims (based on volume from depth measurements.)

This excess water is subtracted from the difference between the tared assembly and saturated assembly weights, giving the weight of water contained within the PLDCC.

Adding the weight of water contained within the PLDCC to the initial un-saturated sample weight and dividing by the calculated volume of the PLDCC will yield the estimated natural saturated unit weight.

Figure 1 conceptualizes the excess water that must be accounted for, as well as relevant dimensions.

An example of measurements and calculations is contained in the appendix.

Appendix

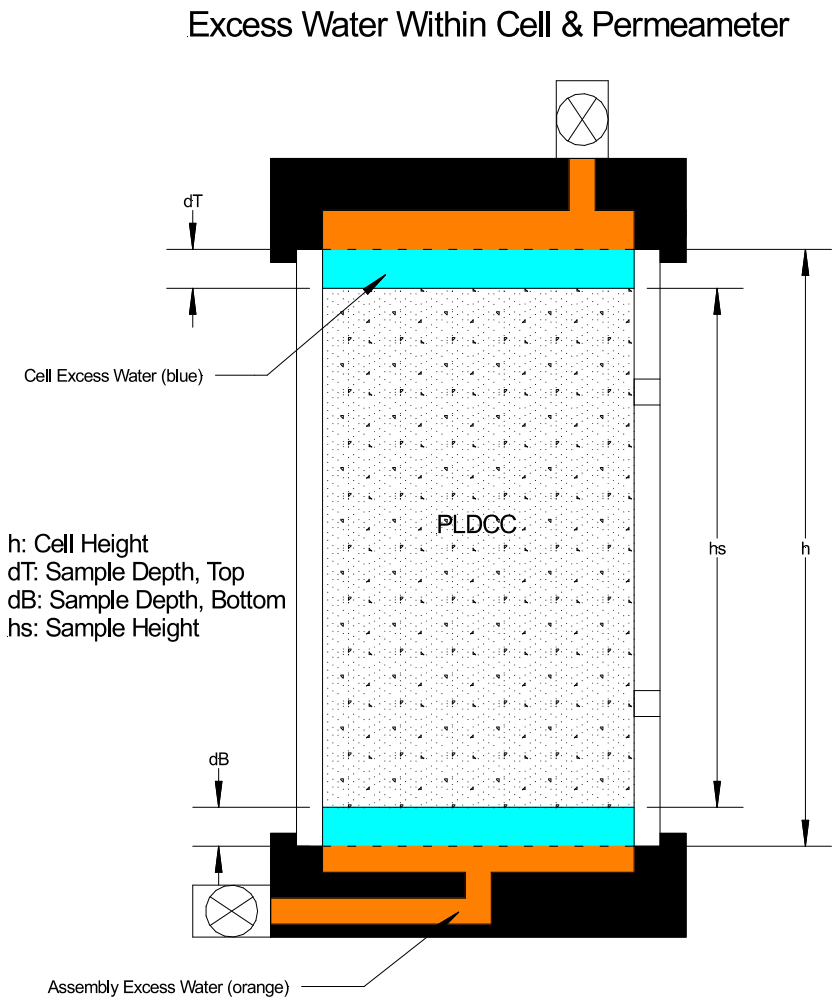

Figure 1

CASTLE ROCK CONSULTING
ENHANCING TRADITIONAL SOLUTIONS WITH INNOVATION

Appendix

Sample Determination of Natural Saturation Unit Weight

Measured Values

Cell Tare Weight, C_T :	330.0	g	Weight of empty cell with manometer plugs and Id label.
Prepared Cell Weight, C :	584.4	g	Weight of cell containing PLDCC sample after trimming & scarifying.
Assembly Tare Weight, P_T :	2201.6	g	Weight of Permeameter containin g un-saturated PLDCC cell.
Saturated Assembly Weight, P_s :	2665.8	g	Weight of dried permeameter containing saturated PLDCC sample.
Cell Diameter, D:	7.6	cm	Internal diameter of the cell.
Cell Height, h :	15.2	cm	Height of the cell.
Top Surface depth, d_T :	1.3	cm	Depth of the top surface of the PLDCC to the cell rim (average).
Bottom Surface Depth, d_B :	1.3	cm	Depth of the bottom surface of the PLDCC to the cell rim (average).
Assembly Excess Water, EW_A:	58.0	g	Weight of excess water contained in the Permeameter assembly as described.

Calculations

PLDCC Sample Height, h_s :	12.6	cm	$h_s = h - d_T - d_B$
PLDCC Sample Cross-sectional Area, A :	45.4	cm^2	$A = \frac{\pi D^2}{4}$
Unsaturated PLDCC Sample Weight, W_U :	254.4	g	$W_U = C - C_T$
PLDCC Sample Volume, V :	571.6	cm^3	$V = h_s \times A$
Unsaturated PLDCC Unit Weight, UW:	0.445	g/cm	$UW = \frac{W_U}{V}$
Unsaturated PLDCC Unit Weight, UW:	**27.8**	**lb/ft^3**	$UW = \left(\frac{W_U}{V}\right) \times 62.4 \frac{lb}{ft^3}$
Total Weight of Water, W_W :	464.2	g	$W_W = P_S - P_T$
Weight of Excess Cell Water, EW_C :	117.9	g	$EW_C = A \times (d_T + d_B) \times 1.0 \frac{g}{cm^3}$
Weight of Saturated PLDCC, W_S :	542.7	g	$W_S = W_U + W_W - EW_C - EW_A$
Natural Saturated PLDCC Unit Weight, $UW_{sat.}$:	0.949	g/cm^3	$UW_{sat.} = \frac{W_S}{V}$
Natural Saturated PLDCC Unit Weight, $UW_{sat.}$:	**59.2**	**lb/ft^3**	$UW_{sat.} = \left(\frac{W_S}{V}\right) \times 62.4 \frac{lb}{ft^3}$

APPENDIX D – RESILIENT MODULUS TESTS

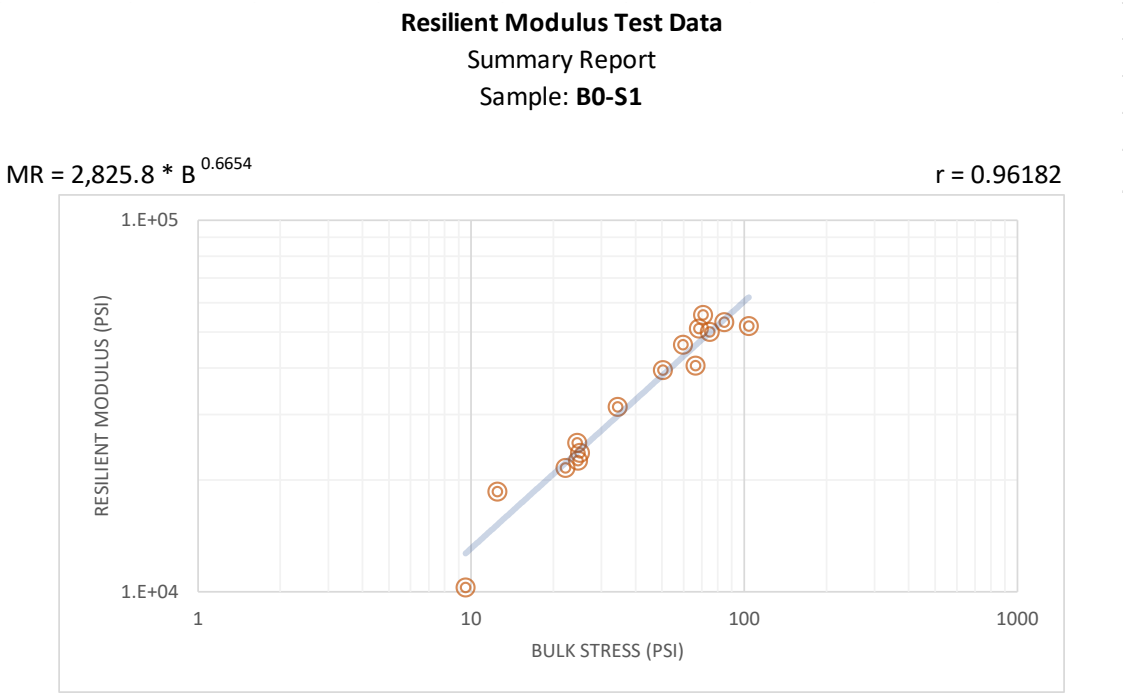

Figure D1. Resilient modulus test data of sample 1 of batch 0 (B0-S1)

Test Date: 01/13/2023

Confining Stress, S3 (psi)	Nom. Max. Deviator Stress (psi)	Mean Deviator Stress (psi)	Std. Dev. Deviator Stress (psi)	Mean Bulk Stress (psi)	Mean Resilient Strain (%)	Std. Dev. Resilient Strain (%)	Mean Resilient Modulus (psi)	Std. Dev. Resilient Modulus (psi)
3.198	3	-0.04671	0.1720	9.549	0.00	0.00	10252	670.0
3.033	6	3.379	3.9375	12.48	0.02	0.02	18582	1,222.5
3.041	9	15.32	7.2000	24.44	0.06	0.03	25112	1,300.5
5.197	5	9.428	4.5853	25.02	0.04	0.02	23617	440.9
4.875	10	9.984	1.4420	24.61	0.04	0.01	22515	275.8
4.989	15	7.219	0.6999	22.18	0.03	0.00	21495	642.0
10.14	10	3.984	0.8502	34.39	0.01	0.00	31427	1,420.4
10.21	20	19.75	2.8994	50.37	0.05	0.01	39420	897.0
9.95	30	29.87	2.6294	59.72	0.06	0.00	46185	1,679.9
14.89	10	10.62	4.5896	66.28	0.03	0.01	40543	2,100.4
15.17	15	22.666	3.0929	68.17	0.04	0.00	51017	2,396.3
14.96	30	29.92	3.9326	74.81	0.06	0.01	49986	1,418.4
20.01	15	10.7	4.8921	70.73	0.02	0.01	55571	4,293.0
20.07	20	24.26	4.6967	84.48	0.04	0.01	53086	3,642.2
20.01	40	43.82	5.1144	103.9	0.08	0.01	51843	437.6

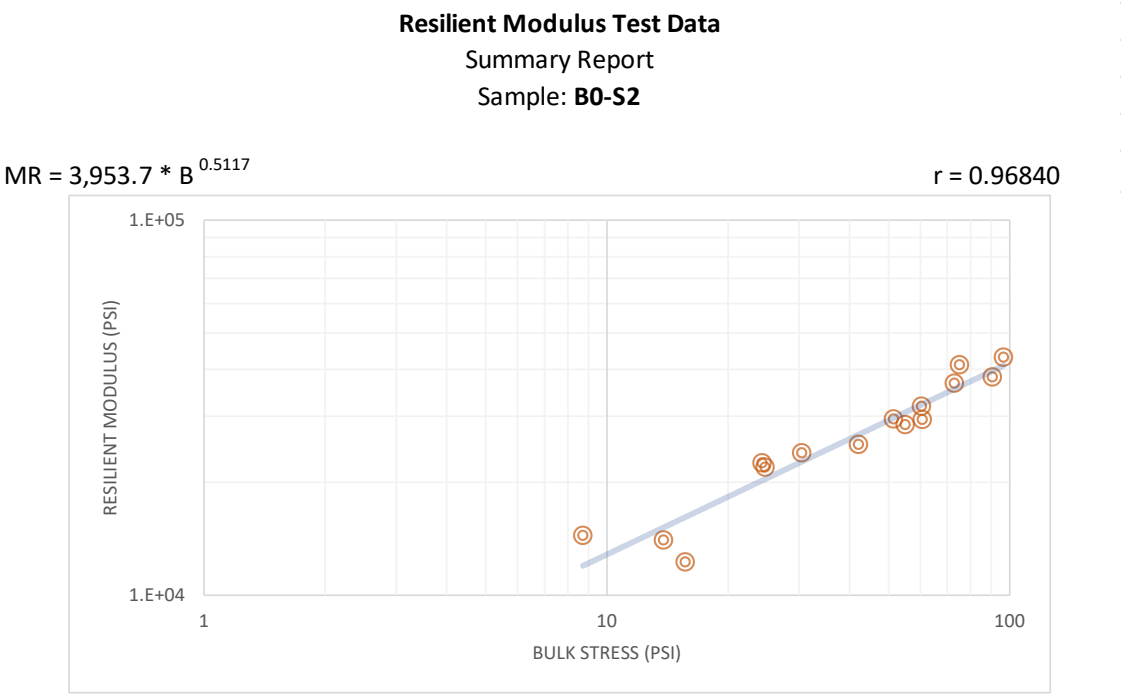

Figure D2. Resilient modulus test data of sample 2 of batch 0 (B0-S2)

Test Date: 01/13/2023

Confining Stress, S3 (psi)	Nom. Max. Deviator Stress (psi)	Mean Deviator Stress (psi)	Std. Dev. Deviator Stress (psi)	Mean Bulk Stress (psi)	Mean Resilient Strain (%)	Std. Dev. Resilient Strain (%)	Mean Resilient Modulus (psi)	Std. Dev. Resilient Modulus (psi)
2.985	3	-0.2292	0.0855	8.726	0.00	0.00	14429	243.7
3.357	6	3.759	3.2626	13.83	0.02	0.02	14036	760.5
3.029	9	15.21	6.7613	24.29	0.07	0.03	22536	122.8
5.156	5	0.195	0.2745	15.66	0.00	0.00	12260	699.2
4.967	10	9.83	1.7175	24.73	0.05	0.01	21946	245.6
5.143	15	15.04	0.1652	30.47	0.06	0.00	23971	162.6
10.3	10	11.29	2.7683	42.18	0.04	0.01	25212	1,491.1
10.18	20	20.98	3.2353	51.51	0.07	0.01	29486	488.3
10.14	30	30.02	0.0390	60.45	0.09	0.00	31916	60.8
15.06	10	9.881	0.2620	55.05	0.04	0.00	28475	360.8
15.27	15	14.94	0.7441	60.74	0.05	0.00	29414	241.9
15.16	30	27.36	3.0460	72.85	0.07	0.01	36775	948.2
20.05	15	14.91	0.6292	75.07	0.04	0.00	41175	680.0
19.92	20	30.87	2.1604	90.63	0.08	0.00	38192	1,151.7
20.02	40	36.53	6.3928	96.59	0.08	0.01	43132	892.1

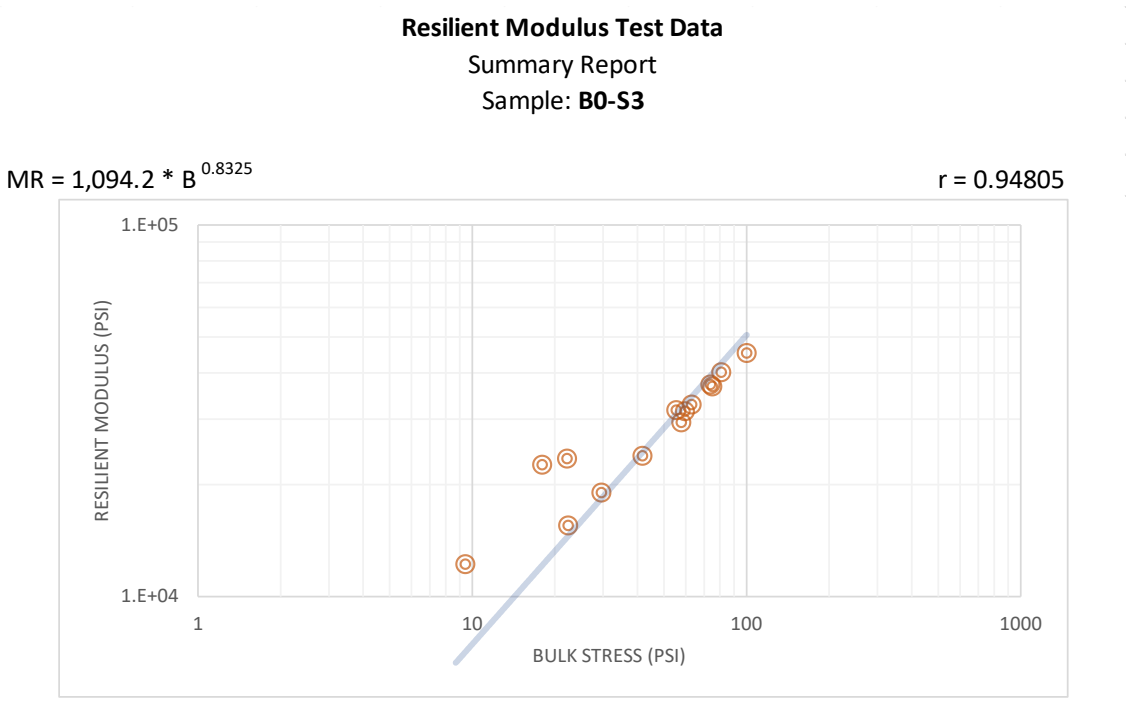

Figure D3. Resilient modulus test data of sample 3 of batch 0 (B0-S3)

Test Date: 01/14/2023

Confining Stress, S3 (psi)	Nom. Max. Deviator Stress (psi)	Mean Deviator Stress (psi)	Std. Dev. Deviator Stress (psi)	Mean Bulk Stress (psi)	Mean Resilient Strain (%)	Std. Dev. Resilient Strain (%)	Mean Resilient Modulus (psi)	Std. Dev. Resilient Modulus (psi)
2.992	3	0.4609	1.4804	9.437	0.01	0.01	12205	982.2
2.946	6	-0.1337	0.0897	8.704	0.00	0.00	1887	-
3.131	9	13	4.0501	22.39	0.08	0.02	15519	892.3
5.167	5	2.501	4.2175	18	0.01	0.02	22607	2,809.8
5.115	10	6.815	4.0319	22.16	0.03	0.02	23485	1,177.0
5.553	15	12.91	0.5610	29.57	0.07	0.00	19014	499.0
10.05	10	11.66	0.3716	41.8	0.05	0.00	23889	347.5
10.25	20	27.06	1.4074	57.83	0.09	0.00	29374	892.3
10.03	30	29.63	0.1224	59.72	0.09	0.00	31482	159.0
15.12	10	10.19	0.6566	55.55	0.03	0.00	31719	550.5
15.19	15	17.62	0.7173	63.2	0.05	0.00	32836	405.6
15.14	30	29.75	3.5061	75.16	0.08	0.01	36729	1,463.4
19.92	15	14.14	4.8916	73.9	0.04	0.01	37163	2,239.1
20.01	20	20.93	1.7583	80.96	0.05	0.00	40099	314.3
19.85	40	40.51	5.6885	100.1	0.09	0.01	45153	759.4

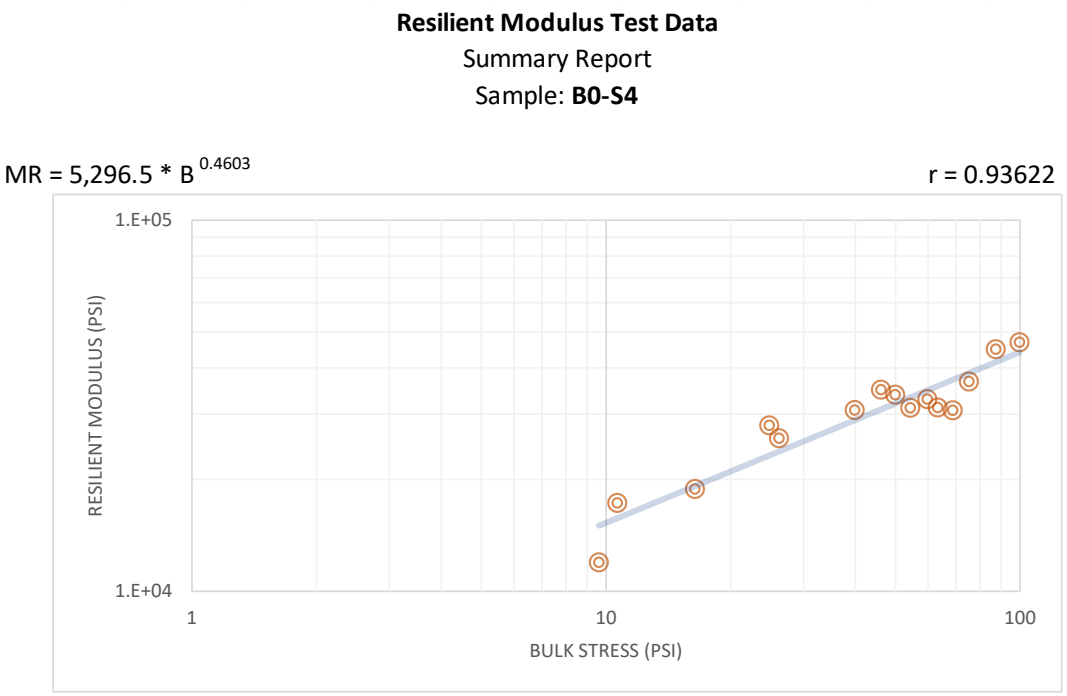

Figure D4. Resilient modulus test data of sample 4 of batch 0 (B0-S4)

Test Date: 01/14/2023

Confining Stress, S3 (psi)	Nom. Max. Deviator Stress (psi)	Mean Deviator Stress (psi)	Std. Dev. Deviator Stress (psi)	Mean Bulk Stress (psi)	Mean Resilient Strain (%)	Std. Dev. Resilient Strain (%)	Mean Resilient Modulus (psi)	Std. Dev. Resilient Modulus (psi)
3.297	3	-0.2675	0.0716	9.623	0.00	0.00	11962	1,223.8
3.18	6	1.105	1.4216	10.65	0.01	0.01	17307	1,826.3
2.995	9	17.22	6.8833	26.2	0.07	0.02	25860	130.2
4.968	5	1.51	1.8806	16.42	0.01	0.01	18849	2,469.0
5.068	10	9.605	6.2899	24.81	0.04	0.02	27958	965.1
5.014	15	24.83	0.7080	39.88	0.08	0.00	30759	199.0
9.999	10	16.13	1.0104	46.13	0.05	0.00	34894	301.1
10.03	20	19.85	2.8147	49.93	0.06	0.01	33855	349.5
10.09	30	29.48	2.4726	59.77	0.09	0.01	32911	1,145.2
15.06	10	9.178	0.5206	54.37	0.03	0.00	31223	243.9
15.05	15	18.07	4.0016	63.23	0.06	0.01	31245	858.2
15.04	30	30.21	3.7148	75.32	0.08	0.01	36749	2,377.1
19.85	15	9.281	4.1064	68.82	0.03	0.01	30749	4,048.7
19.96	20	27.5	2.2732	87.39	0.06	0.00	44907	1,759.1
20.01	40	39.67	4.7052	99.71	0.08	0.01	46866	560.0

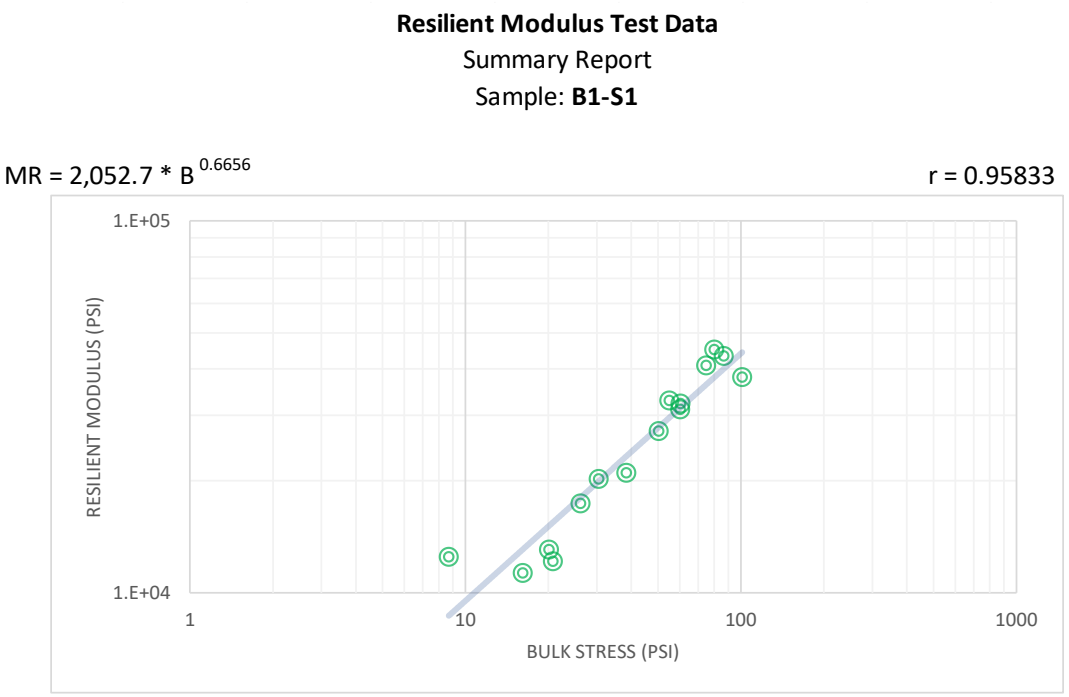

Figure D5. Resilient modulus test data of sample 1 of batch 1 (B1-S

Test Date: 01/07/2023

Confining Stress, S3 (psi)	Nom. Max. Deviator Stress (psi)	Mean Deviator Stress (psi)	Std. Dev. Deviator Stress (psi)	Mean Bulk Stress (psi)	Mean Resilient Strain (%)	Std. Dev. Resilient Strain (%)	Mean Resilient Modulus (psi)	Std. Dev. Resilient Modulus (psi)
2.99	3	-0.269	0.0171	8.702	0.00	0.00	12460	1,294.8
2.981	6	11.83	3.6822	20.77	0.10	0.02	12122	347.1
2.978	9	11.18	5.4249	20.12	0.09	0.04	13037	267.5
5.069	5	0.9385	0.8725	16.15	0.01	0.01	11285	1,051.7
5.196	10	10.6	0.4628	26.19	0.06	0.00	17344	183.1
5.041	15	15.31	0.1564	30.43	0.07	0.00	20192	132.3
10.14	10	7.934	0.9206	38.34	0.04	0.00	20992	300.6
10.06	20	20.09	0.9153	50.28	0.07	0.00	27157	94.3
10.16	30	29.86	0.2685	60.33	0.09	0.00	32243	236.0
14.98	10	9.987	0.5458	54.94	0.03	0.00	32852	980.7
15.05	15	15.1	3.3636	60.26	0.05	0.01	31060	658.0
15	30	29.87	2.3871	74.86	0.07	0.01	40808	549.0
20.23	15	25.93	1.1372	86.6	0.06	0.00	43242	760.0
20.05	20	19.84	0.0706	80.09	0.04	0.00	44997	239.7
20.28	40	40.27	4.3636	101.1	0.10	0.01	37924	651.5

1)

Resilient Modulus Test Data

Summary Report

Sample: **B1-S2**

$MR = 2{,}774.3 * B^{0.5434}$ r = 0.98742

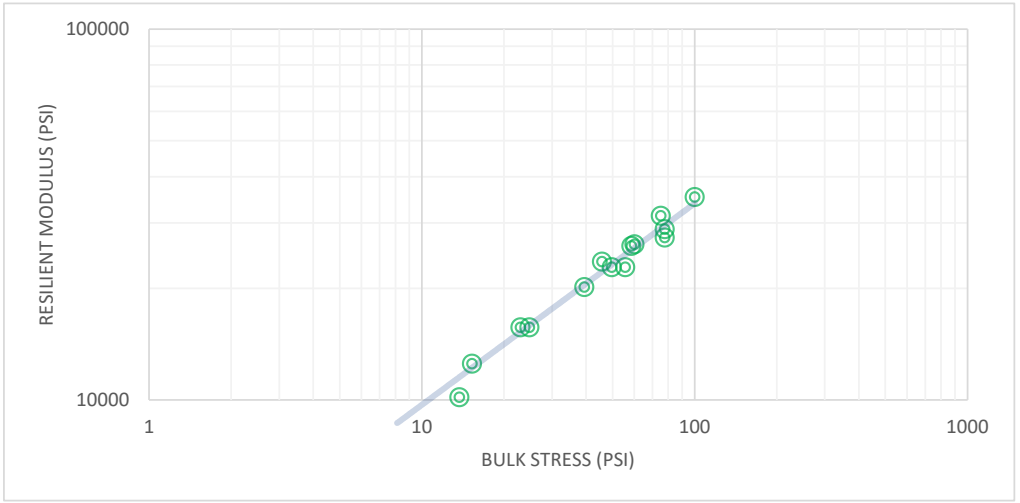

Figure D6. Resilient modulus test data of sample 2 of batch 1 (B2-S1)

Test Date: 01/13/2023

Confining Stress, S3 (psi)	Nom. Max. Deviator Stress (psi)	Mean Deviator Stress (psi)	Std. Dev. Deviator Stress (psi)	Mean Bulk Stress (psi)	Mean Resilient Strain (%)	Std. Dev. Resilient Strain (%)	Mean Resilient Modulus (psi)	Std. Dev. Resilient Modulus (psi)
2.729	3	-0.06757	0.2305	8.118	0.00	0.00	9305	461.1
3.527	6	4.721	3.6558	15.3	0.04	0.02	12529	1,030.7
2.881	9	5.119	7.4964	13.76	0.04	0.05	10167	716.6
5.17	5	7.506	3.6580	23.02	0.05	0.02	15693	883.8
5.035	10	9.745	5.9917	24.85	0.06	0.03	15698	1,516.7
4.932	15	24.7	1.0667	39.5	0.12	0.00	20153	257.7
9.988	10	15.87	1.7333	45.84	0.07	0.01	23587	521.9
10.04	20	19.68	0.9395	49.8	0.08	0.00	22808	142.2
10.12	30	29.84	0.1093	60.21	0.11	0.00	26274	136.0
15.07	10	10.52	0.1109	55.71	0.05	0.00	22774	117.7
15.09	15	13.43	1.1137	58.69	0.05	0.00	26007	941.9
15.14	30	29.82	0.1084	75.24	0.09	0.00	31350	308.6
19.89	15	18.08	3.3575	77.75	0.06	0.01	28882	1,506.9
19.97	20	17.92	2.6495	77.84	0.06	0.00	27397	1,920.7
20.07	40	39.87	3.2738	100.1	0.11	0.01	35232	604.0

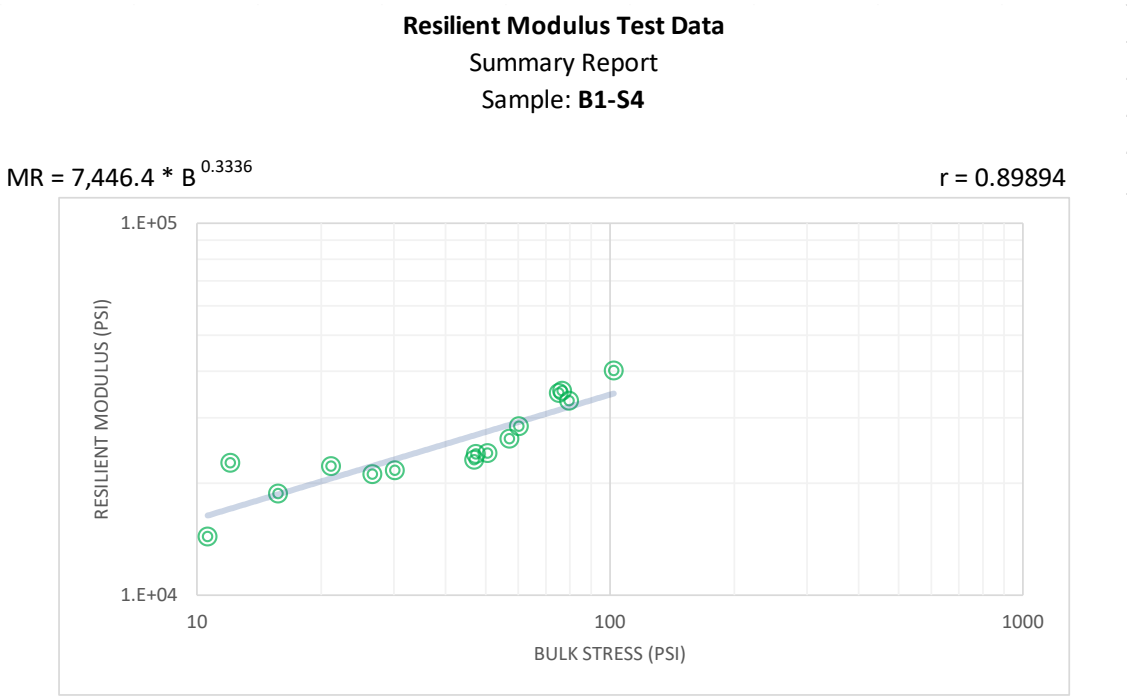

Figure D7. Resilient modulus test data of sample 4 of batch 1 (B4-S1)

Test Date: 01/07/2023

Confining Stress, S3 (psi)	Nom. Max. Deviator Stress (psi)	Mean Deviator Stress (psi)	Std. Dev. Deviator Stress (psi)	Mean Bulk Stress (psi)	Mean Resilient Strain (%)	Std. Dev. Resilient Strain (%)	Mean Resilient Modulus (psi)	Std. Dev. Resilient Modulus (psi)
2.689	3	2.532	3.2525	10.6	0.01	0.02	14386	1,092.7
2.9	6	3.356	5.6856	12.05	0.02	0.03	22686	1,289.4
3.08	9	11.89	4.7233	21.13	0.06	0.02	22237	1,172.8
5.222	5	0.04677	0.6499	15.71	0.00	0.00	18754	1,001.1
4.967	10	15.25	0.2412	30.15	0.07	0.00	21679	158.5
5.113	15	11.25	1.7633	26.59	0.05	0.01	21166	394.5
10.27	10	16.51	2.1461	47.33	0.07	0.01	23964	819.9
10.19	20	20	3.8043	50.56	0.08	0.01	24112	1,120.7
10.2	30	29.58	3.7819	60.18	0.10	0.01	28451	699.9
14.77	10	2.635	1.1687	46.94	0.01	0.00	23140	2,678.7
15.19	15	11.5	3.1438	57.08	0.04	0.00	26324	339.0
15.25	30	29.49	1.6110	75.23	0.08	0.00	34963	277.4
20	15	16.62	4.7603	76.61	0.05	0.02	35431	2,437.7
20.11	20	19.28	1.1573	79.62	0.06	0.00	33342	879.8
20.04	40	42.01	4.9015	102.1	0.10	0.01	40180	1,393.3

Resilient Modulus Test Data

Summary Report

Sample: **B1-S7**

$MR = 8{,}178.5 * B^{0.336}$ r = 0.90719

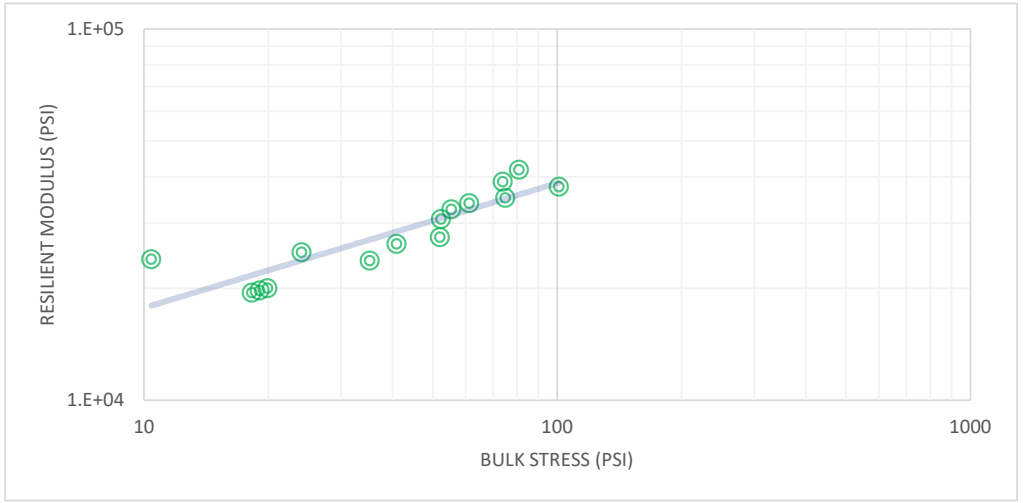

Figure D8. Resilient modulus test data of sample 7 of batch 1 (B7-S1)

Test Date: 01/07/2023

Confining Stress, S3 (psi)	Nom. Max. Deviator Stress (psi)	Mean Deviator Stress (psi)	Std. Dev. Deviator Stress (psi)	Mean Bulk Stress (psi)	Mean Resilient Strain (%)	Std. Dev. Resilient Strain (%)	Mean Resilient Modulus (psi)	Std. Dev. Resilient Modulus (psi)
3.588	3	-0.34	0.0148	10.43	0.00	0.00	23952	1,710.0
3.347	6	9.888	6.3393	19.93	0.05	0.03	20014	863.9
3.259	9	8.477	6.3249	18.26	0.05	0.03	19478	1,098.6
5.558	5	7.414	3.9930	24.09	0.03	0.02	25024	1,577.2
2.487	10	2.601	1.7680	19.06	0.01	0.01	19749	1,875.5
5.336	15	19.22	2.5182	35.23	0.08	0.01	23783	104.9
10.5	10	9.386	2.9548	40.87	0.04	0.01	26345	434.1
10.72	20	19.84	4.8695	52.02	0.07	0.01	27499	1,912.0
10.47	30	29.87	3.6712	61.28	0.09	0.01	33923	766.7
15.2	10	9.86	0.5614	55.46	0.03	0.00	32669	462.3
15.1	15	7.1	3.4054	52.39	0.02	0.01	30759	897.2
15.03	30	29.85	4.2399	74.94	0.08	0.01	35082	2,045.0
20.27	15	13.09	0.3237	73.9	0.03	0.00	38793	523.1
20.31	20	19.94	1.5430	80.88	0.05	0.00	41759	461.8
20.28	40	40.14	4.1859	101	0.10	0.01	37575	1,583.7

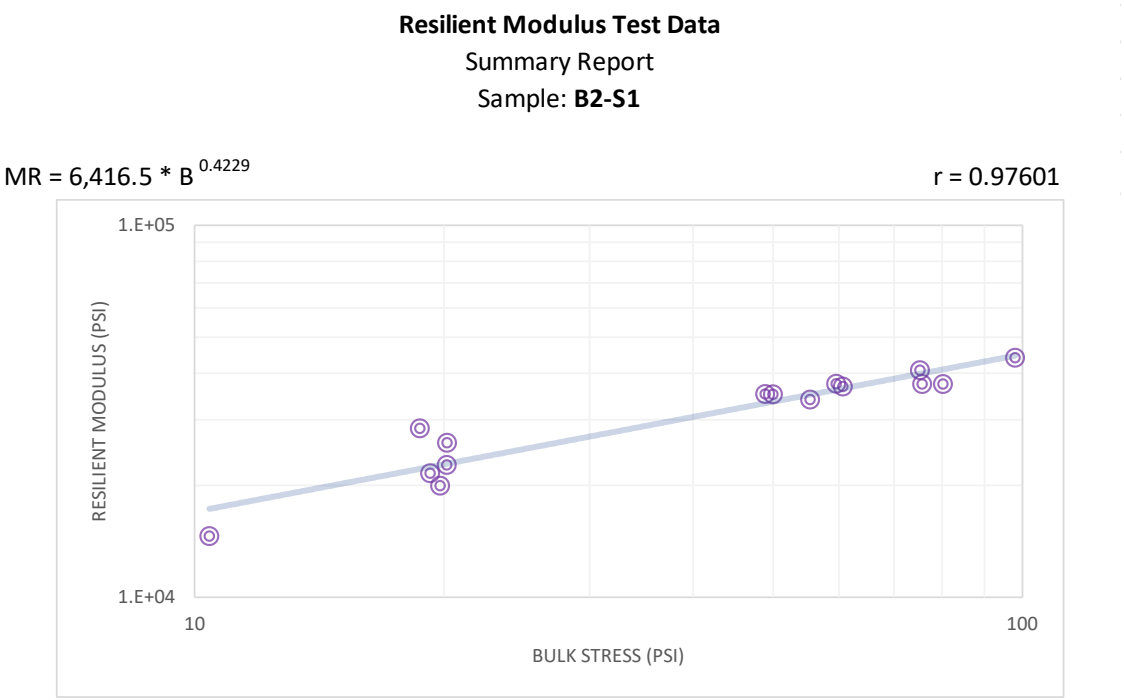

Figure D9. Resilient modulus test data of sample 1 of batch 2 (B1-S2)

Test Date: 01/14/2023

Confining Stress, S3 (psi)	Nom. Max. Deviator Stress (psi)	Mean Deviator Stress (psi)	Std. Dev. Deviator Stress (psi)	Mean Bulk Stress (psi)	Mean Resilient Strain (%)	Std. Dev. Resilient Strain (%)	Mean Resilient Modulus (psi)	Std. Dev. Resilient Modulus (psi)
2.603	3	2.611	3.9463	10.42	0.02	0.02	14602	1132.4
3.03	6	10.17	5.3077	19.26	0.05	0.02	21533	1889.1
2.887	9	11.5	4.5421	20.16	0.05	0.02	22683	2029.7
5.12	5	3.355	3.9304	18.71	0.02	0.02	28419	3910.2
5.056	10	5.014	5.7239	20.18	0.02	0.02	26009	976.2
5.035	15	4.686	0.2413	19.79	0.02	0.00	19925	552.0
10.23	10	18.23	1.0384	48.92	0.05	0.00	35163	286.1
10.11	20	19.65	4.7625	49.99	0.06	0.01	35128	231.8
10.14	30	30.29	5.1099	60.71	0.08	0.01	36836	1148.9
15.19	10	9.84	4.0349	55.4	0.03	0.01	33956	1477.7
15.1	15	14.27	3.6790	59.57	0.04	0.01	37482	1208.5
15.17	30	29.69	7.2233	75.21	0.07	0.02	40717	482.7
20.22	15	15.03	5.2061	75.69	0.04	0.01	37376	2783.1
20.01	20	20.17	5.2821	80.21	0.06	0.02	37429	1148.9
20.01	40	37.97	8.5568	98.02	0.08	0.02	43999	1477.7

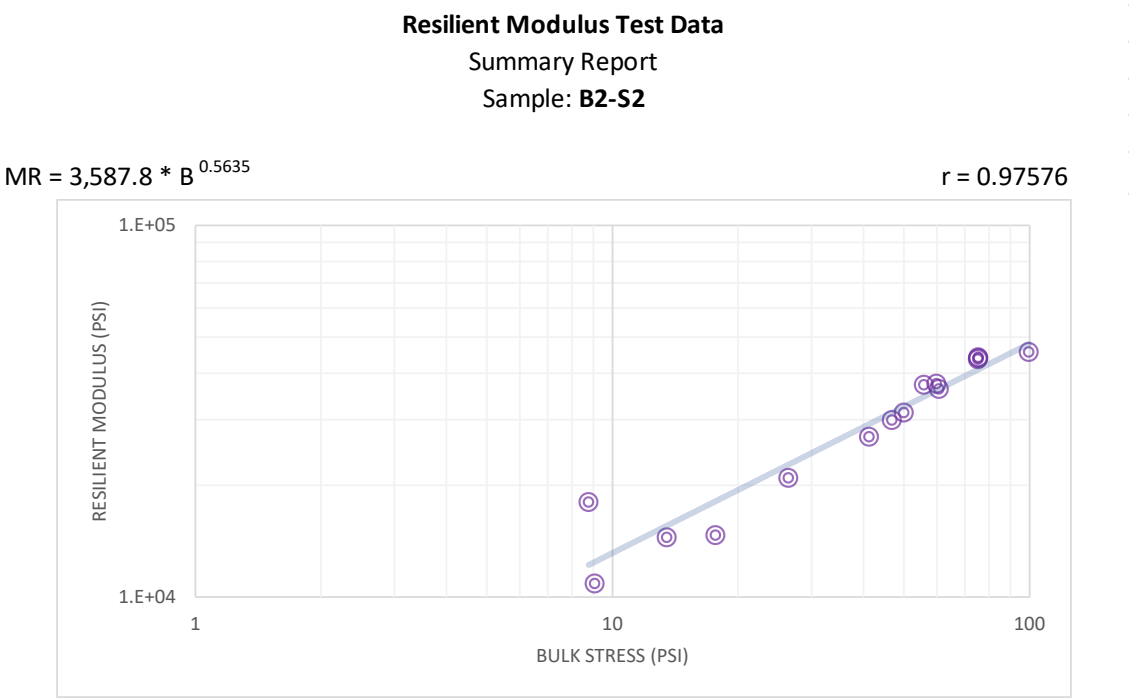

Figure D10. Resilient modulus test data of sample 2 of batch 2 (B2-S2)

Test Date: 01/16/2023

Confining Stress, S3 (psi)	Nom. Max. Deviator Stress (psi)	Mean Deviator Stress (psi)	Std. Dev. Deviator Stress (psi)	Mean Bulk Stress (psi)	Mean Resilient Strain (%)	Std. Dev. Resilient Strain (%)	Mean Resilient Modulus (psi)	Std. Dev. Resilient Modulus (psi)
3.063	3	-0.1166	0.2767	9.071	0.00	0.00	10877	2096
2.917	6	0.02217	0.3700	8.775	0.00	0.00	18017	6241
3.006	9	4.492	3.4850	13.51	0.03	0.02	14461	1989
5.187	5	2.105	2.9577	17.67	0.02	0.02	14667	2190
5.05	10	11.28	5.6504	26.43	0.05	0.03	20927	930
5.15	15	25.84	1.0944	41.29	0.10	0.00	26976	571
10.13	10	16.46	2.1289	46.83	0.05	0.01	29912	724
10.18	20	19.49	0.9680	50.04	0.06	0.00	31358	475
10.25	30	29.93	1.3699	60.68	0.08	0.00	36277	492
15.03	10	10.75	5.4843	55.86	0.03	0.02	37239	787
15.08	15	14.61	5.4993	59.86	0.04	0.01	37493	2028
15.08	30	30.01	0.1902	75.26	0.07	0.00	43602	292
20.17	15	14.81	1.6545	75.33	0.03	0.00	44194	869
20.11	20	15.12	2.6810	75.46	0.03	0.01	43971	1764
19.96	40	39.85	6.3854	99.73	0.08	0.01	45637	1546

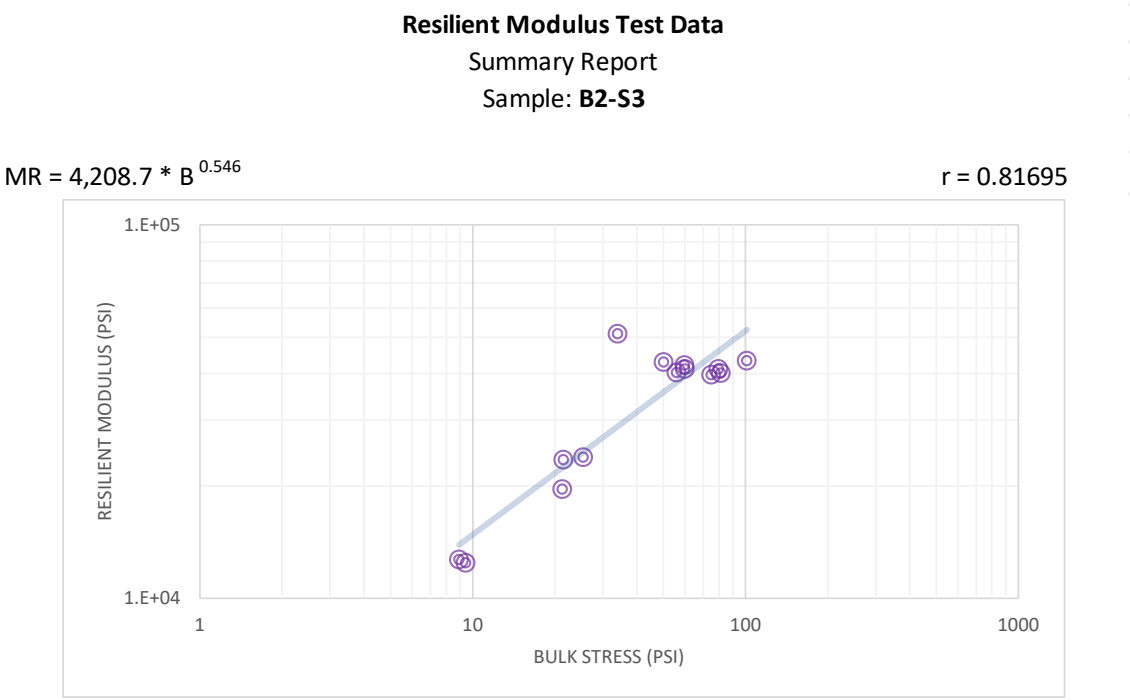

Figure D11. Resilient modulus test data of sample 3 of batch 2 (B2-S3)

Test Date: 01/16/2023

Confining Stress, S3 (psi)	Nom. Max. Deviator Stress (psi)	Mean Deviator Stress (psi)	Std. Dev. Deviator Stress (psi)	Mean Bulk Stress (psi)	Mean Resilient Strain (%)	Std. Dev. Resilient Strain (%)	Mean Resilient Modulus (psi)	Std. Dev. Resilient Modulus (psi)
2.906	3	0.7249	1.9279	9.444	0.01	0.01	12431	1861
2.843	6	0.3934	0.6396	8.924	0.01	0.01	12681	1634
3.001	9	12.51	5.4518	21.51	0.05	0.02	23469	1482
5.154	5	-0.1459	0.0736	15.32	0.00	0.00		
5.103	10	10.15	5.8908	25.45	0.04	0.02	23855	3143
5.038	15	6.229	1.1230	21.34	0.03	0.00	19584	1556
10.04	10	3.94	5.7120	34.05	0.01	0.01	51058	3837
10.07	20	19.93	2.2177	50.14	0.05	0.01	42886	1158
10	30	29.78	5.0107	59.78	0.07	0.01	42054	494
15.12	10	14.66	3.5748	60.02	0.04	0.01	41081	2839
15.04	15	10.86	1.1663	55.97	0.03	0.00	40217	984
15.07	30	29.69	6.9572	74.89	0.07	0.02	39651	332
20.08	15	21.03	1.6224	81.28	0.05	0.00	40050	224
19.96	20	19.75	6.5312	79.63	0.05	0.02	41113	707
20.04	40	41.07	5.7469	101.2	0.09	0.01	43220	567

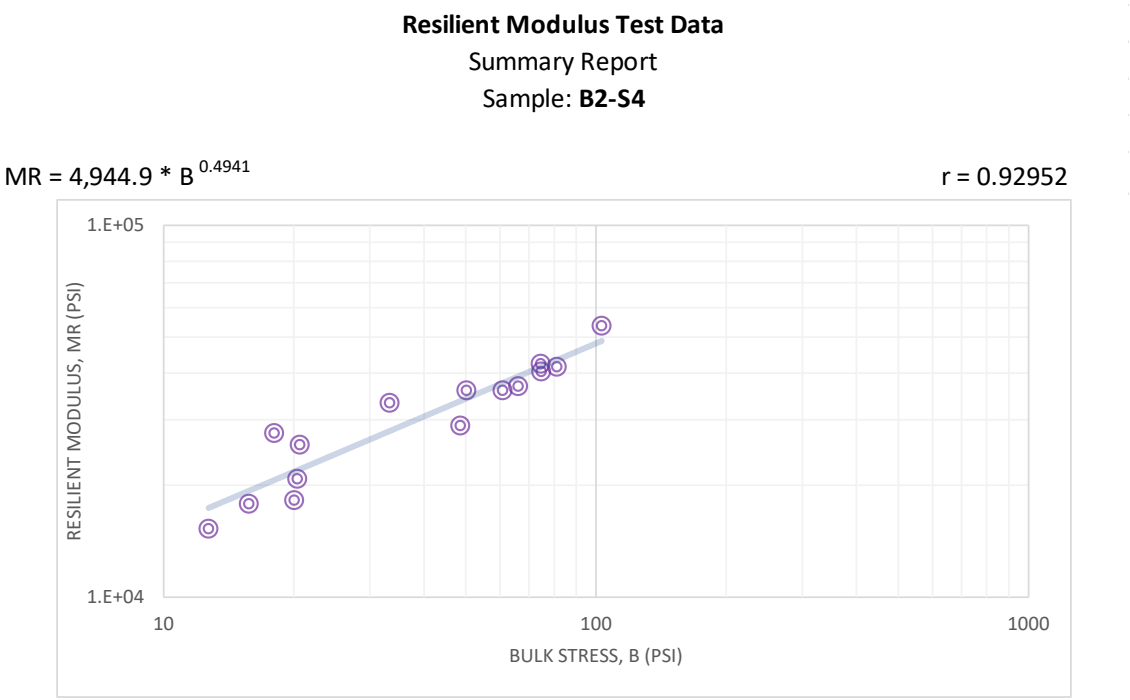

Figure D12. Resilient modulus test data of sample 4 of batch 2 (B2-S4)

Test Date: 01/16/2023

Confining Stress, S3 (psi)	Nom. Max. Deviator Stress (psi)	Mean Deviator Stress (psi)	Std. Dev. Deviator Stress (psi)	Mean Bulk Stress (psi)	Mean Resilient Strain (%)	Std. Dev. Resilient Strain (%)	Mean Resilient Modulus (psi)	Std. Dev. Resilient Modulus (psi)
2.898	3	4.022	3.6183	12.71	0.03	0.02	15268	1042
2.956	6	6.891	6.7773	15.76	0.04	0.03	17819	2941
3.087	9	10.8	5.1251	20.06	0.06	0.02	18198	4716
5.117	5	5.043	5.0763	20.39	0.03	0.02	20772	4774
5.119	10	2.666	2.2629	18.02	0.01	0.01	27604	1520
4.898	15	5.953	0.9507	20.65	0.02	0.00	25663	794
10.16	10	2.853	0.3657	33.32	0.01	0.00	33287	1765
10.03	20	20.11	4.7252	50.19	0.06	0.01	35957	940
10.03	30	30.74	4.6641	60.82	0.08	0.01	35944	381
15.16	10	3.044	1.4971	48.54	0.01	0.00	28923	1551
14.99	15	21.17	2.1991	66.12	0.06	0.01	36883	686
15.01	30	29.45	6.9283	74.47	0.07	0.01	42355	1547
19.88	15	15.03	4.7751	74.67	0.04	0.01	40366	1174
20.15	20	20.74	7.1300	81.18	0.05	0.02	41615	2675
20.11	40	42.74	6.6283	103.1	0.08	0.01	53593	2803

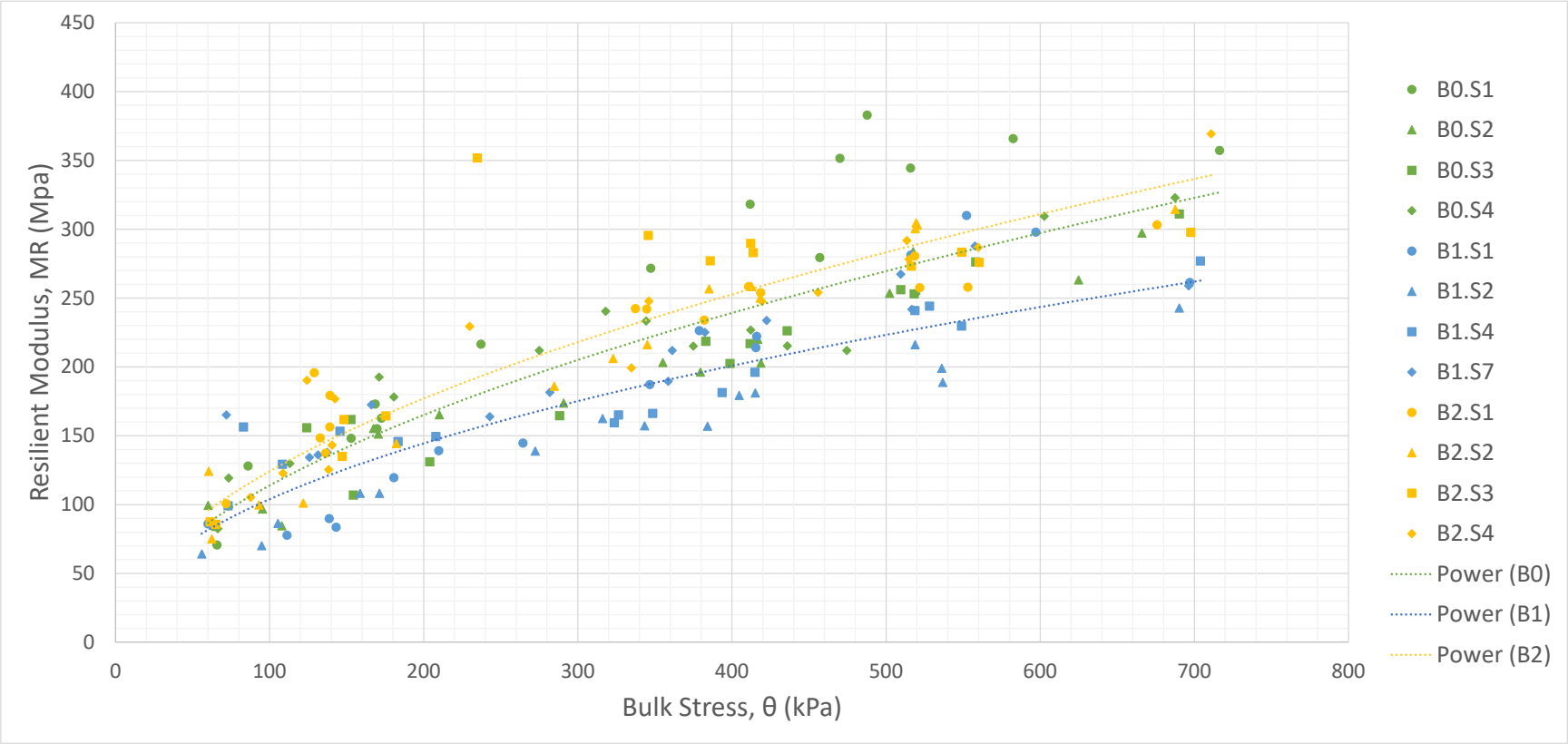

Figure D13. Graphical Results of the resilient modulus tests at a regular scale.

Table D1. Batch's 0 data.

Batch	Sample	Mean Bulk Stress, θ (kPa)	Mean Resilient Modulus, MR (mPa)	log(θ)	log(MR)
B 0	S 1	65.838	70.635	1.818	1.849
		86.047	128.028	1.935	2.107
		168.508	173.023	2.227	2.238
		172.507	162.723	2.237	2.211
		169.680	155.127	2.230	2.191
		152.926	148.101	2.184	2.171
		237.111	216.533	2.375	2.336
		347.289	271.605	2.541	2.434
		411.755	318.212	2.615	2.503
		456.985	279.341	2.660	2.446
		470.016	351.506	2.672	2.546
		515.797	344.402	2.712	2.537
		487.666	382.884	2.688	2.583
		582.469	365.765	2.765	2.563
		716.365	357.201	2.855	2.553
	S 2	60.164	99.416	1.779	1.997
		95.354	96.708	1.979	1.985
		167.474	155.275	2.224	2.191
		107.972	84.468	2.033	1.927
		170.507	151.208	2.232	2.180
		210.083	165.162	2.322	2.218
		290.821	173.713	2.464	2.240
		355.149	203.159	2.550	2.308
		416.788	219.898	2.620	2.342
		379.556	196.193	2.579	2.293
		418.788	202.664	2.622	2.307
		502.283	253.378	2.701	2.404
		517.589	283.699	2.714	2.453
		624.872	263.144	2.796	2.420
		665.965	297.178	2.823	2.473
	S 3	65.066	84.093	1.813	1.925
		154.374	106.926	2.189	2.029
		124.106	155.761	2.094	2.192
		152.788	161.813	2.184	2.209
		203.878	131.005	2.309	2.117
		288.201	164.597	2.460	2.216
		398.724	202.384	2.601	2.306
		411.755	216.912	2.615	2.336
		383.004	218.547	2.583	2.340
		435.749	226.241	2.639	2.355
		518.210	253.066	2.715	2.403
		509.523	256.052	2.707	2.408
		558.200	276.279	2.747	2.441
		690.165	311.101	2.839	2.493
		66.348	82.417	1.822	1.916
	S 4	73.429	119.244	1.866	2.076
		180.643	178.172	2.257	2.251
		113.212	129.869	2.054	2.114
		171.059	192.629	2.233	2.285
		274.963	211.928	2.439	2.326
		318.055	240.417	2.503	2.381
		344.255	233.261	2.537	2.368
		412.100	226.760	2.615	2.356
		374.868	215.129	2.574	2.333
		435.956	215.275	2.639	2.333
		519.313	253.202	2.715	2.403
		474.497	211.863	2.676	2.326
		602.533	309.408	2.780	2.491
		687.476	322.905	2.837	2.509
Equation in	power format	$MR = 9.6674\theta^{0.5355}$			
	linear format	$\log(MR) = 0.5355*\log(\theta) + 0.9853$			

Table D2. Batch's 0 data regression summary output.

Regular Scale

Regression Statistics	
Multiple R	0.88924386
R Square	0.790754643
Adjusted R Square	0.787083671
Standard Error	36.2052559
Observations	59

ANOVA

	df	*SS*	*MS*	*F*	*Significance F*
Regression	1	282360.5492	282360.5492	215.4074776	5.12674E-21
Residual	57	74716.77161	1310.820555		
Total	58	357077.3208			

	Coefficients	*Standard Error*	*t Stat*	*P-value*	*Lower 95%*	*Upper 95%*	*Lower 95.0%*	*Upper 95.0%*
Intercept	86.3231	9.7438	8.8593	0.0000	66.8114	105.8348	66.8114	105.8348
X Variable 1	0.3698	0.0252	14.6768	0.0000	0.3194	0.4203	0.3194	0.4203

Logarithmic Scale

Regression Statistics	
Multiple R	0.921837215
R Square	0.84978385
Adjusted R Square	0.847148479
Standard Error	0.069622125
Observations	59

ANOVA

	df	*SS*	*MS*	*F*	*Significance F*
Regression	1	1.5630	1.5630	322.4532	0.0000
Residual	57	0.2763	0.0048		
Total	58	1.8393			

	Coefficients	*Standard Error*	*t Stat*	*P-value*	*Lower 95%*	*Upper 95%*	*Lower 95.0%*	*Upper 95.0%*
Intercept	0.9853	0.0733	13.4340	0.0000	0.8384	1.1322	0.8384	1.1322
X Variable 1	0.5355	0.0298	17.9570	0.0000	0.4758	0.5952	0.4758	0.5952

Table D3. Batch's 1 data.

Batch	Sample	Mean Bulk Stress, θ (kPa)	Mean Resilient Modulus, MR (mPa)	log(θ)	log(MR)
B 1	S 1	59.998	85.850	1.778	1.934
		143.204	83.523	2.156	1.922
		138.723	89.825	2.142	1.953
		111.350	77.755	2.047	1.891
		180.574	119.502	2.257	2.077
		209.807	139.126	2.322	2.143
		264.345	144.635	2.422	2.160
		346.668	187.112	2.540	2.272
		415.961	222.153	2.619	2.347
		378.798	226.352	2.578	2.355
		415.478	214.003	2.619	2.330
		516.142	281.166	2.713	2.449
		597.086	297.940	2.776	2.474
		552.201	310.031	2.742	2.491
		697.060	261.295	2.843	2.417
	S 2	55.972	64.113	1.748	1.807
		105.490	86.323	2.023	1.936
		94.872	70.051	1.977	1.845
		158.717	108.125	2.201	2.034
		171.335	108.160	2.234	2.034
		272.343	138.853	2.435	2.143
		316.056	162.512	2.500	2.211
		343.359	157.146	2.536	2.196
		415.133	181.026	2.618	2.258
		384.107	156.913	2.584	2.196
		404.653	179.188	2.607	2.253
		518.762	216.002	2.715	2.334
		536.067	198.997	2.729	2.299
		536.688	188.764	2.730	2.276
		690.165	242.750	2.839	2.385
	S 4	73.084	99.122	1.864	1.996
		83.082	156.307	1.920	2.194
		145.686	153.213	2.163	2.185
		108.317	129.213	2.035	2.111
		207.877	149.367	2.318	2.174
		183.332	145.831	2.263	2.164
		326.329	165.115	2.514	2.218
		348.599	166.132	2.542	2.220
		414.926	196.027	2.618	2.292
		323.640	159.433	2.510	2.203
		393.553	181.371	2.595	2.259
		518.693	240.892	2.715	2.382
		528.207	244.121	2.723	2.388
		548.961	229.726	2.740	2.361
		703.955	276.842	2.848	2.442
	S 7	71.912	165.031	1.857	2.218
		137.413	137.895	2.138	2.140
		125.898	134.201	2.100	2.128
		166.095	172.415	2.220	2.237
		131.414	136.072	2.119	2.134
		242.902	163.868	2.385	2.214
		281.789	181.516	2.450	2.259
		358.665	189.468	2.555	2.278
		422.511	233.727	2.626	2.369
		382.383	225.091	2.582	2.352
		361.216	211.930	2.558	2.326
		516.693	241.715	2.713	2.383
		509.523	267.285	2.707	2.427
		557.648	287.717	2.746	2.459
Equation in	power format	$MR = 11.636\theta^{0.4754}$			
	linear format	$\log(MR) = 0.4757*\log(\theta) + 1.0651$			

Table D4. Batch's 1 data regression summary output.

Regular Scale

Regression Statistics	
Multiple R	0.778505509
R Square	0.606070828
Adjusted R Square	0.59915979
Standard Error	38.77990478
Observations	59

ANOVA

	df	*SS*	*MS*	*F*	*Significance F*
Regression	1	131884.4429	131884.4429	87.69606214	3.94085E-13
Residual	57	85721.21783	1503.881015		
Total	58	217605.6607			

	Coefficients	*Standard Error*	*t Stat*	*P-value*	*Lower 95%*	*Upper 95%*	*Lower 95.0%*	*Upper 95.0%*
Intercept	91.4068	10.4367	8.7582	0.0000	70.5076	112.3060	70.5076	112.3060
X Variable 1	0.2528	0.0270	9.3646	0.0000	0.1987	0.3068	0.1987	0.3068

Logarithmic Scale

Regression Statistics	
Multiple R	0.747823367
R Square	0.559239789
Adjusted R Square	0.551507153
Standard Error	0.11066214
Observations	59

ANOVA

	df	*SS*	*MS*	*F*	*Significance F*
Regression	1	0.885663334	0.885663334	72.32201803	1.00564E-11
Residual	57	0.698028227	0.012246109		
Total	58	1.583691562			

	Coefficients	*Standard Error*	*t Stat*	*P-value*	*Lower 95%*	*Upper 95%*	*Lower 95.0%*	*Upper 95.0%*
Intercept	1.2354	0.1166	10.5974	0.0000	1.0020	1.4689	1.0020	1.4689
X Variable 1	0.4031	0.0474	8.5042	0.0000	0.3082	0.4980	0.3082	0.4980

Table D5. Batch's 2 data.

Batch	Sample	Mean Bulk Stress, θ (kPa)	Mean Resilient Modulus, MR (mPa)	log(θ)	log(MR)
B 2	S 1	71.843	100.605	1.856	2.003
		132.793	148.364	2.123	2.171
		138.998	156.284	2.143	2.194
		129.001	195.809	2.111	2.292
		139.136	179.204	2.143	2.253
		136.447	137.286	2.135	2.138
		337.292	242.276	2.528	2.384
		344.669	242.033	2.537	2.384
		418.581	253.803	2.622	2.404
		381.970	233.957	2.582	2.369
		410.721	258.250	2.614	2.412
		518.555	280.540	2.715	2.448
		521.864	257.521	2.718	2.411
		553.028	257.883	2.743	2.411
		675.824	303.150	2.830	2.482
	S 2	62.542	74.939	1.796	1.875
		60.501	124.141	1.782	2.094
		93.148	99.633	1.969	1.998
		121.830	101.054	2.086	2.005
		182.228	144.190	2.261	2.159
		284.685	185.862	2.454	2.269
		322.881	206.091	2.509	2.314
		345.014	216.055	2.538	2.335
		418.374	249.946	2.622	2.398
		385.141	256.575	2.586	2.409
		412.720	258.330	2.616	2.412
		518.899	300.421	2.715	2.478
		519.382	304.495	2.715	2.484
		520.278	302.957	2.716	2.481
		687.614	314.438	2.837	2.498
	S 3	65.114	85.646	1.814	1.933
		61.529	87.373	1.789	1.941
		148.306	161.704	2.171	2.209
		175.472	164.361	2.244	2.216
		147.134	134.931	2.168	2.130
		234.766	351.791	2.371	2.546
		345.703	295.485	2.539	2.471
		412.169	289.752	2.615	2.462
		413.823	283.048	2.617	2.452
		385.900	277.092	2.586	2.443
		516.348	273.194	2.713	2.436
		560.406	275.942	2.749	2.441
		549.030	283.269	2.740	2.452
		697.749	297.784	2.844	2.474
	S 4	87.632	105.195	1.943	2.022
		108.661	122.770	2.036	2.089
		138.309	125.381	2.141	2.098
		140.584	143.121	2.148	2.156
		124.244	190.193	2.094	2.279
		142.377	176.821	2.153	2.248
		229.733	229.350	2.361	2.360
		346.048	247.744	2.539	2.394
		419.339	247.651	2.623	2.394
		334.672	199.282	2.525	2.299
		455.881	254.125	2.659	2.405
		513.453	291.827	2.711	2.465
		514.832	278.122	2.712	2.444
		559.716	286.727	2.748	2.457
Equation in	power format	$MR = 11.715\theta^{0.5125}$			
	linear format	$\log(MR) = 0.5097*\log(\theta) + 1.075$			

Table D6. Batch's 2 data regression summary output.

Regular Scale

Regression Statistics	
Multiple R	0.88924386
R Square	0.790754643
Adjusted R Square	0.787083671
Standard Error	36.2052559
Observations	59

ANOVA

	df	*SS*	*MS*	*F*	*Significance F*
Regression	1	282360.5492	282360.5492	215.4074776	5.12674E-21
Residual	57	74716.77161	1310.820555		
Total	58	357077.3208			

	Coefficients	*Standard Error*	*t Stat*	*P-value*	*Lower 95%*	*Upper 95%*	*Lower 95.0%*	*Upper 95.0%*
Intercept	86.3231	9.7438	8.8593	0.0000	66.8114	105.8348	66.8114	105.8348
X Variable 1	0.3698	0.0252	14.6768	0.0000	0.3194	0.4203	0.3194	0.4203

Logarithmic Scale

Regression Statistics	
Multiple R	0.921837215
R Square	0.84978385
Adjusted R Square	0.847148479
Standard Error	0.069622125
Observations	59

ANOVA

	df	*SS*	*MS*	*F*	*Significance F*
Regression	1	1.5630	1.5630	322.4532	0.0000
Residual	57	0.2763	0.0048		
Total	58	1.8393			

	Coefficients	*Standard Error*	*t Stat*	*P-value*	*Lower 95%*	*Upper 95%*	*Lower 95.0%*	*Upper 95.0%*
Intercept	0.9853	0.0733	13.4340	0.0000	0.8384	1.1322	0.8384	1.1322
X Variable 1	0.5355	0.0298	17.9570	0.0000	0.4758	0.5952	0.4758	0.5952

APPENDIX E - UNIAXIAL COMPRESSIVE TESTS

UNCONFINED COMPRESSION

TEST REPORT

Sample: **B0S1** Test Date: 20/01/2023

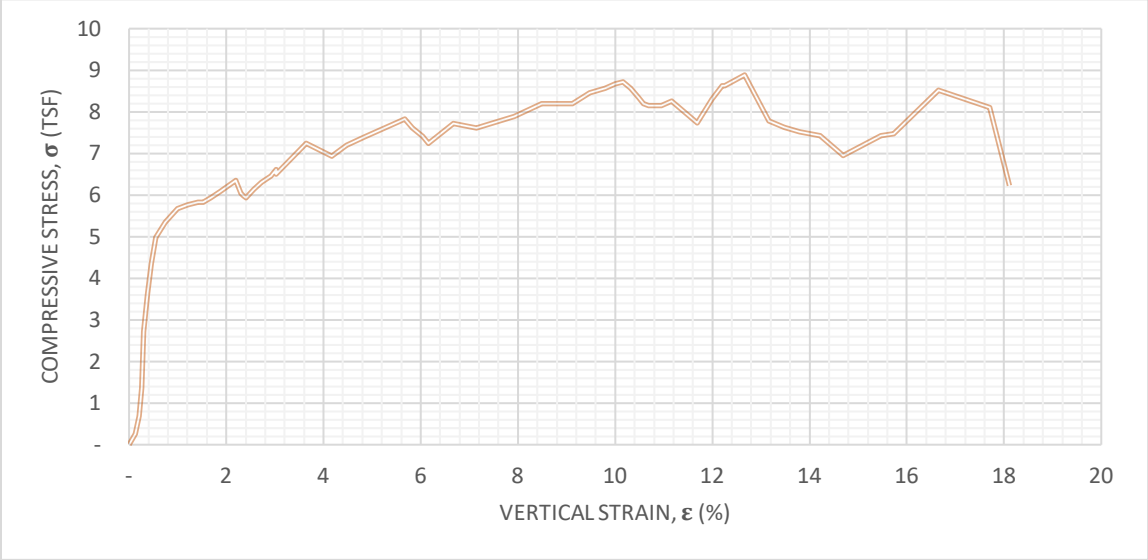

Initial	Diameter, in	2.97
	Height, in	5.67
	Water content, %	0.00
	Dry Density, pcf	23.22
	Saturation, %	0.00
	Void Ratio	6.26
Unconfined Compressive Strength, tsf		8.871
Undrained Shear Strength, tsf		4.435
Time to Failure, min		4.8825
Strain Rate, %/min		2.5
Estimated Specific Gravity		2.70

Unconfined compression test report of sample 1 of batch 0 (B0-S1)

UNCONFINED COMPRESSION

TEST REPORT

Sample: **B0S2** Test Date: 20/01/2023

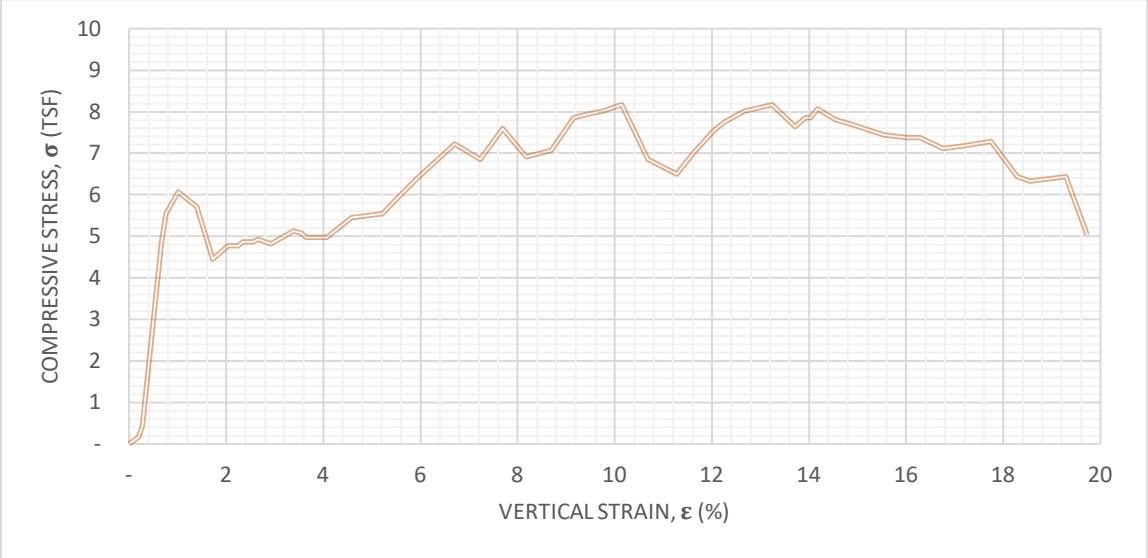

Initial	Diameter, in	2.96
	Height, in	5.67
	Water content, %	0.00
	Dry Density, pcf	23.3
	Saturation, %	0.00
	Void Ratio	6.23
Unconfined Compressive Strength, tsf		8.165
Undrained Shear Strength, tsf		4.083
Time to Failure, min		5.0644
Strain Rate, %/min		2.5
Estimated Specific Gravity		2.70

Unconfined compression test report of sample 2 of batch 0 (B0-S2)

UNCONFINED COMPRESSION

TEST REPORT

Sample: **B0S3** Test Date: 20/01/2023

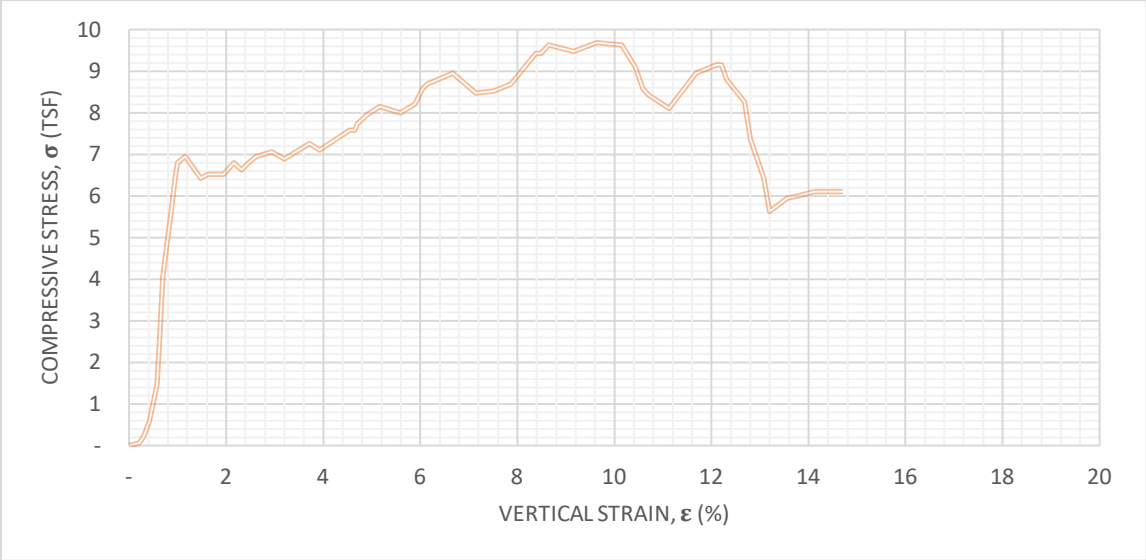

Initial	Diameter, in	2.97
	Height, in	5.73
	Water content, %	0.00
	Dry Density, pcf	23.23
	Saturation, %	0.00
	Void Ratio	6.26
Unconfined Compressive Strength, tsf		9.644
Undrained Shear Strength, tsf		4.822
Time to Failure, min		3.7502
Strain Rate, %/min		2.5
Estimated Specific Gravity		2.70

Unconfined compression test report of sample 3 of batch 0 (B0-S3)

UNCONFINED COMPRESSION

TEST REPORT

Sample: **B0S4** Test Date: 20/01/2023

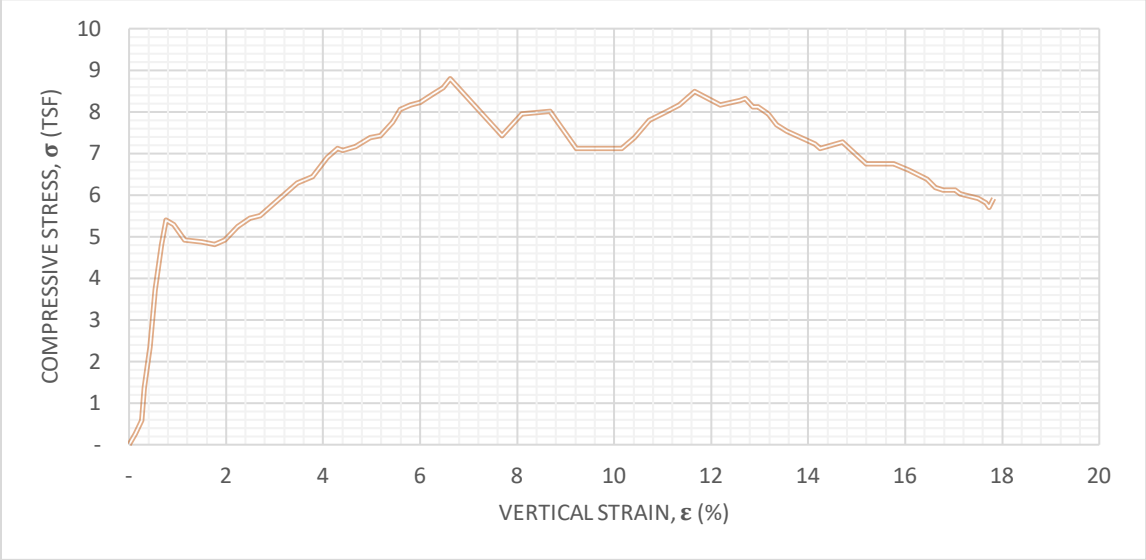

Initial	Diameter, in	2.97
	Height, in	5.65
	Water content, %	0.00
	Dry Density, pcf	23.15
	Saturation, %	0.00
	Void Ratio	6.28
Unconfined Compressive Strength, tsf		8.749
Undrained Shear Strength, tsf		4.375
Time to Failure, min		2.5814
Strain Rate, %/min		2.5
Estimated Specific Gravity		2.70

Unconfined compression test report of sample 4 of batch 0 (B0-S4)

UNCONFINED COMPRESSION

TEST REPORT

Sample: **B1S1** Test Date: 20/01/2023

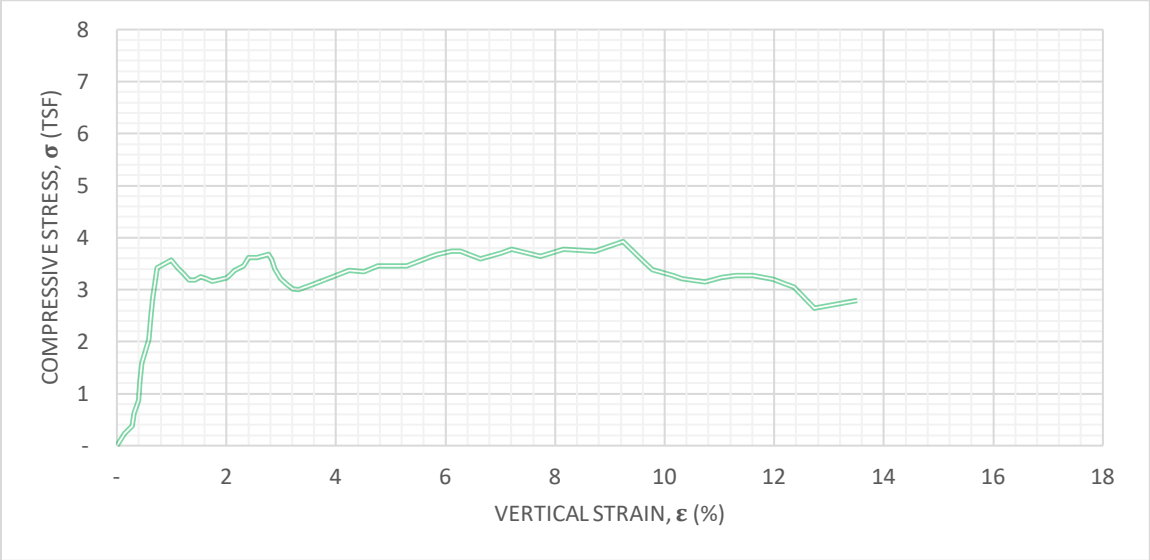

Initial	Diameter, in	3.01
	Height, in	5.27
	Water content, %	0.00
	Dry Density, pcf	19.89
	Saturation, %	0.00
	Void Ratio	7.47
Unconfined Compressive Strength, tsf		3.943
Undrained Shear Strength, tsf		1.972
Time to Failure, min		3.5872
Strain Rate, %/min		2.5
Estimated Specific Gravity		2.70

Unconfined compression test report of sample 1 of batch 1 (B1-S1)

UNCONFINED COMPRESSION

TEST REPORT

Sample: **B1S2** Test Date: 20/01/2023

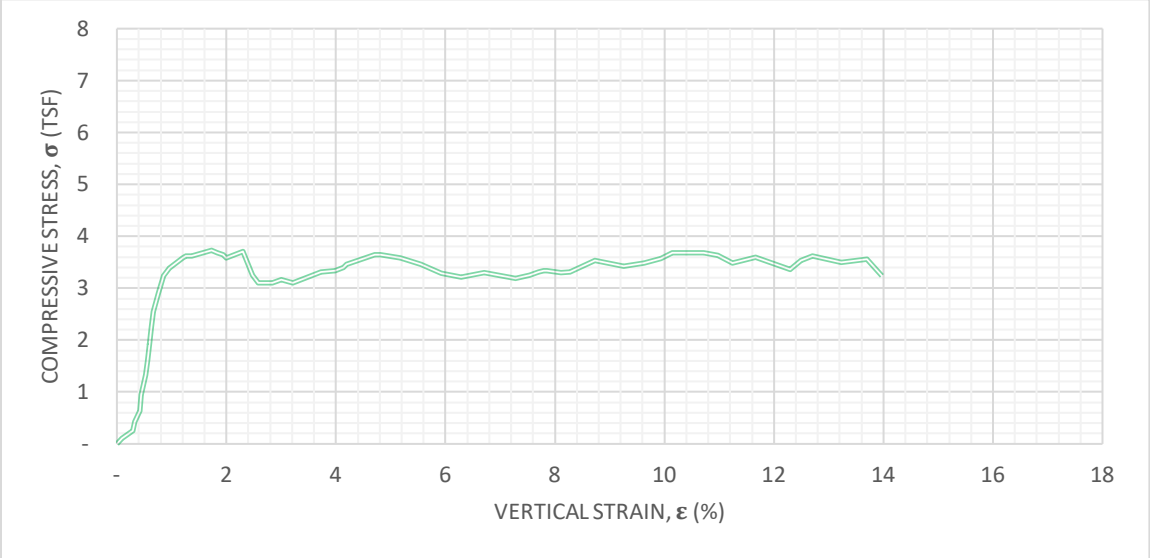

Initial	Diameter, in	3.01
	Height, in	5.33
	Water content, %	0.00
	Dry Density, pcf	19.84
	Saturation, %	0.00
	Void Ratio	7.5
Unconfined Compressive Strength, tsf		3.724
Undrained Shear Strength, tsf		1.862
Time to Failure, min		0.696
Strain Rate, %/min		2.5
Estimated Specific Gravity		2.70

Unconfined compression test report of sample 2 of batch 1 (B1-S2)

UNCONFINED COMPRESSION

TEST REPORT

Sample: **B1S4** Test Date: 20/01/2023

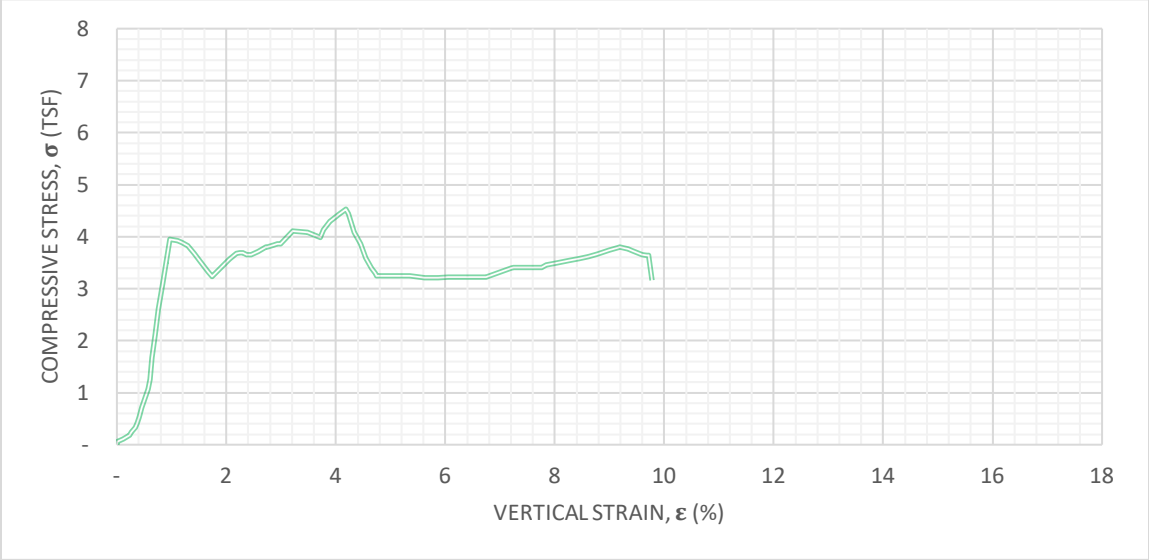

Initial	Diameter, in	3.01
	Height, in	5.01
	Water content, %	0.00
	Dry Density, pcf	19.81
	Saturation, %	0.00
	Void Ratio	7.51
Unconfined Compressive Strength, tsf		4.525
Undrained Shear Strength, tsf		2.263
Time to Failure, min		1.6422
Strain Rate, %/min		2.5
Estimated Specific Gravity		2.70

Unconfined compression test report of sample 4 of batch 1 (B1-S4)

UNCONFINED COMPRESSION

TEST REPORT

Sample: **B1S7** Test Date: 20/01/2023

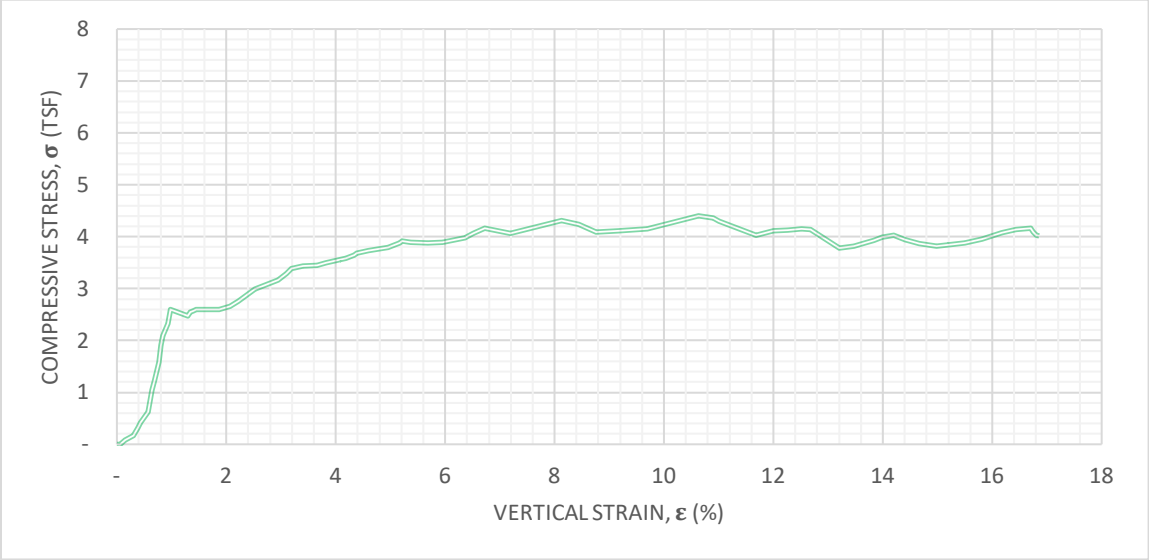

Initial	Diameter, in	3.01
	Height, in	5.25
	Water content, %	0.00
	Dry Density, pcf	20.78
	Saturation, %	0.00
	Void Ratio	7.11
Unconfined Compressive Strength, tsf		4.399
Undrained Shear Strength, tsf		2.199
Time to Failure, min		4.1573
Strain Rate, %/min		2.5
Estimated Specific Gravity		2.70

Unconfined compression test report of sample 7 of batch 1 (B1-S7)

UNCONFINED COMPRESSION

TEST REPORT

Sample: **B2S1** Test Date: 20/01/2023

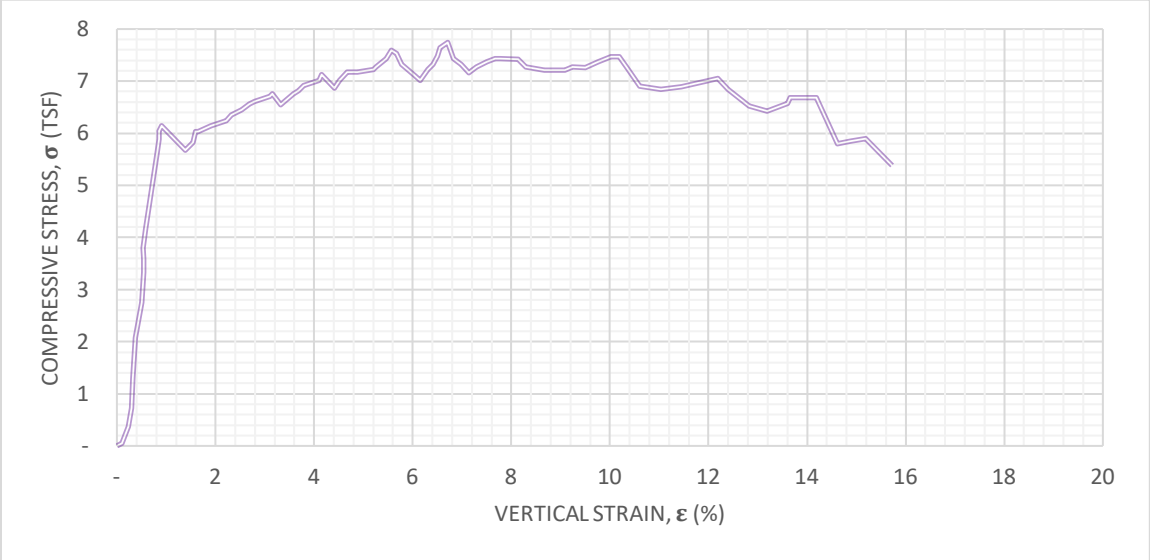

Initial	Diameter, in	3.01
	Height, in	5.03
	Water content, %	0.00
	Dry Density, pcf	21.35
	Saturation, %	0.00
	Void Ratio	6.59
Unconfined Compressive Strength, tsf		7.718
Undrained Shear Strength, tsf		3.859
Time to Failure, min		2.5996
Strain Rate, %/min		2.5
Estimated Specific Gravity		2.70

Unconfined compression test report of sample 1 of batch 2 (B2-S1)

UNCONFINED COMPRESSION

TEST REPORT

Sample: **B2S2** Test Date: 20/01/2023

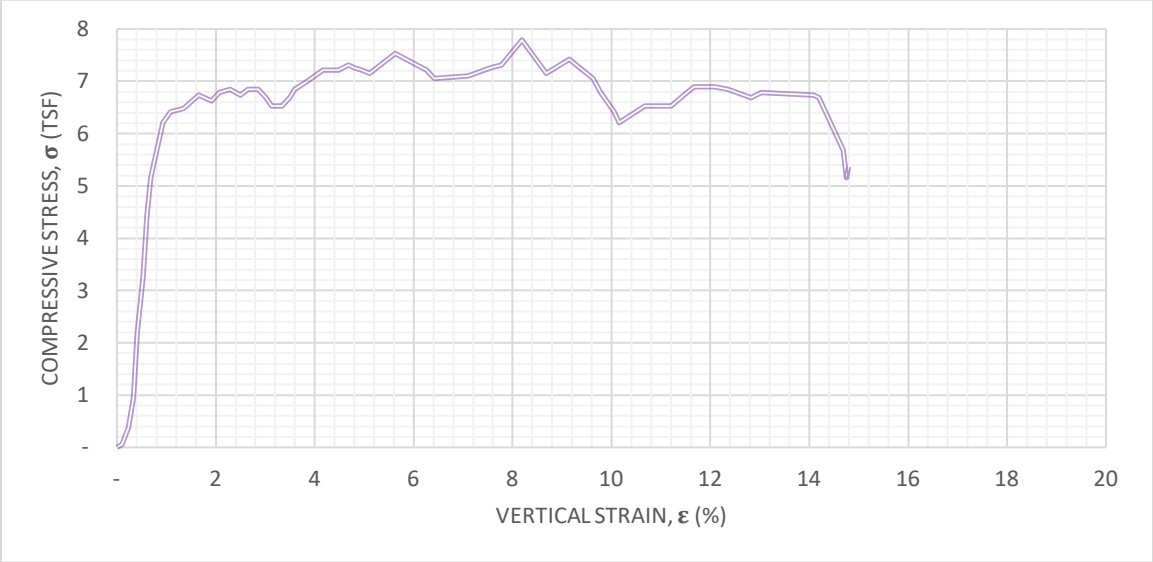

Initial	Diameter, in	3.01
	Height, in	5.08
	Water content, %	0.00
	Dry Density, pcf	20.91
	Saturation, %	0.00
	Void Ratio	7.06
Unconfined Compressive Strength, tsf		7.72
Undrained Shear Strength, tsf		3.86
Time to Failure, min		3.1671
Strain Rate, %/min		2.5
Estimated Specific Gravity		2.70

Unconfined compression test report of sample 2 of batch 2 (B2-S2)

UNCONFINED COMPRESSION

TEST REPORT

Sample: **B2S3** Test Date: 20/01/2023

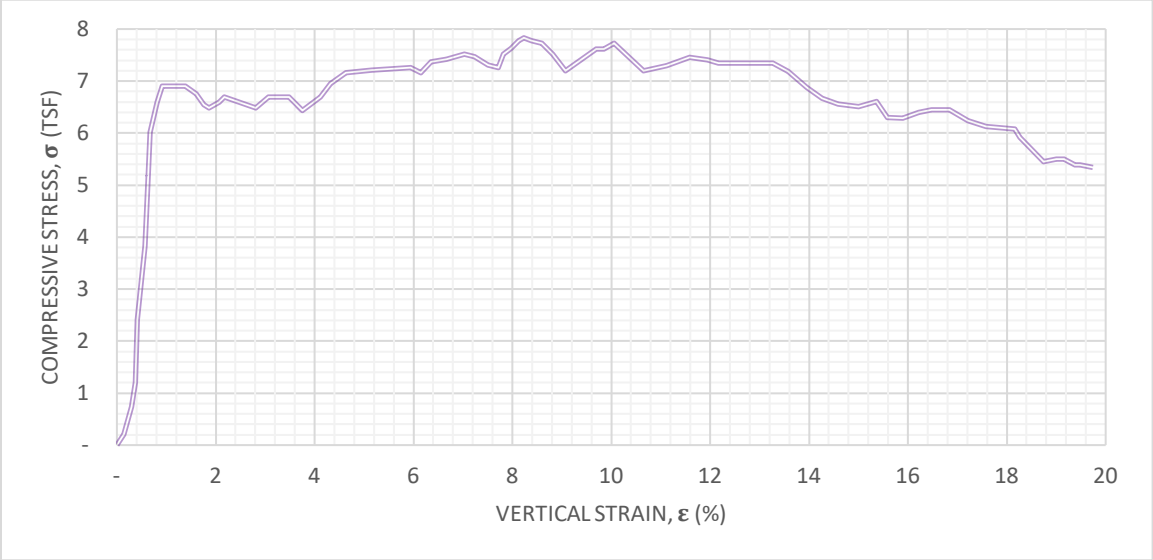

Initial	Diameter, in	3
	Height, in	5.06
	Water content, %	0.00
	Dry Density, pcf	21.16
	Saturation, %	0.00
	Void Ratio	6.97
Unconfined Compressive Strength, tsf		7.861
Undrained Shear Strength, tsf		3.93
Time to Failure, min		3.1705
Strain Rate, %/min		2.5
Estimated Specific Gravity		2.70

Unconfined compression test report of sample 3 of batch 2 (B2-S3)

UNCONFINED COMPRESSION

TEST REPORT

Sample: **B2S4** Test Date: 20/01/2023

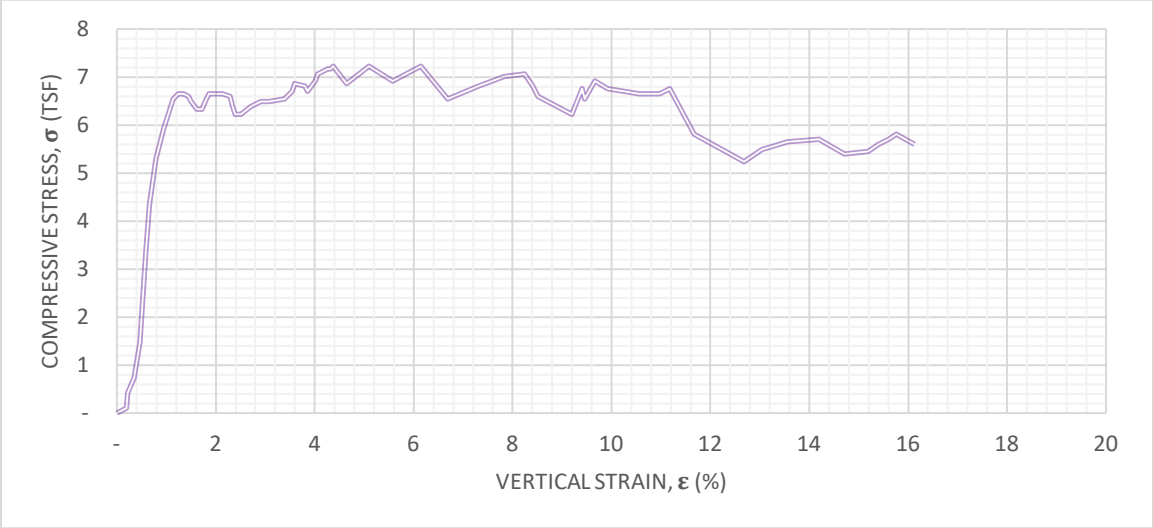

Initial	Diameter, in	3.01
	Height, in	5.15
	Water content, %	0.00
	Dry Density, pcf	21.14
	Saturation, %	0.00
	Void Ratio	6.97
Unconfined Compressive Strength, tsf		7.268
Undrained Shear Strength, tsf		3.634
Time to Failure, min		1.7248
Strain Rate, %/min		2.5
Estimated Specific Gravity		2.70

Unconfined compression test report of sample 4 of batch 2 (B2-S4)